

Money Creation in Decentralized Finance: A Dynamic Model of Stablecoin and Crypto Shadow Banking*

Ye Li[†] Simon Mayer[‡]

First Draft: Dec. 30, 2020; Current Version: Aug. 17, 2021

Abstract

Stablecoins rise to meet the demand for safe assets in decentralized finance. Stablecoin issuers transform risky reserve assets into tokens of stable values, deploying a variety of tactics. To address the questions on the viability of stablecoins, regulations, and the initiatives led by large platforms, we develop a dynamic model of optimal stablecoin management and characterize an instability trap. The system is bimodal: stability can last for a long time, but once stablecoins break the buck following negative shocks, volatility persists. Debasement triggers a vicious cycle but is unavoidable as it allows efficient risk sharing between the issuer and stablecoin users.

*We are grateful to helpful comments from Bruno Biais, Markus Brunnermeier, Jean-Édouard Colliard, Denis Gromb, Sebastian Gryglewicz, Zhiguo He, Konstantin Milbradt, Anil Kashyap, Alexei Ovtchinnikov, Jonathan Payne, Enrico Perotti, Alp Simsek, Quentin Vandeweyer, Ariel Zetlin-Jones, and conference participants at CESifo Macro Money & International Finance, China International Conference in Finance, Dublin DeFi & Digital Finance Workshop, Econometric Society, Stanford Institute for Theoretical Economics, UC Berkeley Decentralized Finance course. Ye acknowledges financial support from Dice Center of Financial Economics. This paper was previously circulated under the title “Managing Stablecoins: Optimal Strategies, Regulation, and Transaction Data as Productive Capital”.

[†]The Ohio State University Fisher College of Business. E-mail: li.8935@osu.edu

[‡]University of Chicago, Booth School of Business, and HEC Paris. E-mail: simon.mayer@chicagobooth.edu.

1 Introduction

More than a decade ago, Bitcoin heralded a new era of digital payments and decentralized finance. Cryptocurrencies challenge the bank-centric payment systems by offering round-the-clock settlement, anonymity, low-cost international remittances, and programmable money via smart contracting (Brunnermeier, James, and Landau, 2019; Duffie, 2019). However, the substantial volatility exhibited by the first-generation cryptocurrencies limits their utility as a means of payment. Stablecoins aim to maintain a stable price against a reference currency or a basket of currencies by pledging to hold fiat money or other assets against which stablecoin holdings can be redeemed.¹

This paper provides a dynamic model of stablecoins in continuous time that rationalizes a rich set of strategies that are common in practice (Bullmann, Klemm, and Pinna, 2019), such as open market operations, dynamic requirement of users’ collateral, transaction fees or subsidies, targeted price band, re-pegging, and the issuances of “secondary units” (or governance tokens) that function as equity shares of the stablecoin issuer.² Our model demonstrates a novel mechanism of instability and lends itself to an evaluation of regulatory proposals. It can also be applied to analyze the incentives behind the stablecoin initiatives led by large platforms (e.g., Facebook).

The creation of stablecoins resembles money creation in shadow banking—the unregulated creation of safe assets to meet agents’ transactional demand (Gorton and Pennacchi, 1990; Moreira and Savov, 2017). The issuer transforms risky assets, which are often cryptocurrencies in practice, into stablecoins with one-to-one convertibility to fiat currencies. The issuer usually requires stablecoin users to post collateral and imposes a margin requirement. This is similar to special purpose vehicles (SPVs) that over-collateralize their debts. In case the users’ collateral falls sharply in value, the issuer uses its own reserves (invested in risky assets) to support the stablecoin value. This is similar to the guarantee from banks that set up the SPVs (Acharya, Schnabl, and Suarez, 2013).

However, the creation of stablecoins differs from traditional shadow banking in one key aspect. The issuer can debase the stablecoins to avoid liquidation, while shadow banks have to honor the debt contracts or become insolvent. The debasement option allows the stablecoin issuer to avoid costly liquidation but induces an amplification mechanism that generates a bimodal distribution of states. In states of high reserves, the issuer maintains a fixed exchange rate, so the stablecoin demand is strong and transaction volume is high. Through open market operations and transaction fees, the issuer earns revenues that further grow its reserves. In states of low reserves, the issuer off-

¹Balvers and McDonald (2021) study stablecoins with stable purchasing power rather than stable exchange rates.

²An alternative to collateralization is to use algorithmic supply rules to stabilize price but success has been limited.

loads risk to users through debasement, which depresses the stablecoin demand and thus reduces the issuer’s revenues, so the issuer can only rebuild its reserves slowly and thus falls into an instability trap. Therefore, a fixed exchange rate can last for a long time, but once debasement happens, recovery is slow. Such ergodic instability resembles that in [Brunnermeier and Sannikov \(2014\)](#).³

Our paper addresses the key questions on the credibility and sustainability of a fixed exchange rate. Different from [Routledge and Zetlin-Jones \(2021\)](#) who study speculative attacks on under-collateralized stablecoins and coordination failure ([Morris and Shin, 1998](#); [Goldstein and Pauzner, 2005](#)), we characterize a novel mechanism of risk amplification and show that in line with evidence ([Lyons and Viswanath-Natraj, 2020](#)), even over-collateralized stablecoins can break the buck when the issuer’s reserves fall below a critical threshold. What drives debasement is the issuer’s trade-off between sustaining a stable value that stimulates demand and sharing risk with users to avoid liquidation. Our focus on fully collateralized stablecoins is motivated by the recent regulatory proposals and bank run events that have cast doubts on the viability of under-collateralized stablecoins.⁴

The stablecoin issuer’s reserve management is reminiscent of dynamic corporate cash management ([Bolton, Chen, and Wang, 2011](#); [Décamps, Mariotti, Rochet, and Villeneuve, 2011](#); [Hugonnier, Malamud, and Morellec, 2015](#); [Malamud and Zucchi, 2019](#)), but different from a corporation, the stablecoin issuer can depreciate its liabilities (the outstanding stablecoins) through debasement, akin to a country monetizing its debt through inflation. Stablecoins share similarities with contingent convertible bonds (CoCos) that automatically share risk between equity investors and debt holders ([Pennacchi, 2010](#); [Glasserman and Nouri, 2012](#); [Chen, Glasserman, Nouri, and Pelger, 2017](#); [Pennacchi and Tchisty, 2018, 2019](#)). But unlike CoCos, risk sharing is done through debasement rather than converting stablecoins into the issuer’s equity, and debasement happens under the discretion of the issuer and does not have pre-specified trigger events.⁵

Next, we provide more details on the basic model setup and our main results. The model is built

³The banking model of [Klimenko, Pfeil, Rochet, and Nicolo \(2016\)](#) generates ergodic instability under regulations unlike the laissez-faire economy in [Brunnermeier and Sannikov \(2014\)](#) and our paper. The commonality is that the financial-slack variable, which drives the equilibrium dynamics, can be trapped in a certain region by a large probability over the long run. The continuous-time approach allows a complete characterization of equilibrium dynamics. Ergodic instability is often ignored by the traditional approach of log-linearization near the steady state.

⁴In December 2020, three U.S. house representatives proposed the [Stablecoin Tethering and Bank Licensing Enforcement \(STABLE\) Act](#) that emphasized full collateralization. On June 16, 2021, a bank run happened to IRON, a partially collateralized token soft pegged to the U.S. dollar. This was the first large-scale bank run in the cryptocurrency market, and major cryptocurrency investors were calling for regulators’ attention ([Tiwari, 2021](#)).

⁵Our model is also related to the continuous-time models of exchange rate determination in small-open economies (e.g., [Penati and Pennacchi, 1989](#)) but differs in our endogenous process of money supply. The capital structure of a stablecoin issuer consists of stablecoins and governance tokens (equity) and is different from that of money market funds (full equity). Money market funds have a different fragility mechanism ([Kacperczyk and Schnabl, 2013](#); [Parlatore, 2016](#); [Schmidt, Timmermann, and Wermers, 2016](#); [La Spada, 2018](#); [Li, Li, Macchiavelli, and Zhou, 2021](#)).

to be technology-neutral so that it applies to stablecoins built on different blockchain protocols.⁶ In a continuous-time economy, a digital platform issues stablecoins (“tokens”) to a unit mass of representative users. A user’s token holdings deliver a flow utility that captures the transactional benefits. The network effect of tokens as means of payment is modelled by embedding the aggregate holdings in individuals’ flow utility (Cong, Li, and Wang, 2021).⁷ Following Moreira and Savov (2017), we assume that users’ demand for tokens declines in the volatility of token price. Such safety preference is motivated by the link between information sensitivity and asset illiquidity.⁸

Users can redeem token holdings for numeraire goods (“dollars”) and trade tokens amongst themselves. The issuer can continuously trade tokens against dollar reserves, directly influencing the token price. Thus, the token price is at any time optimal from the issuer’s perspective. On the issuer’s balance sheet, the liability side has tokens and equity. On the asset side, the platform holds dollar reserves that earn an interest rate and load on Brownian shocks. The shocks capture operational risk and unexpected fluctuations of reserve value.⁹ When the platform requires the stablecoin users to post collateral, the shocks originate from the fluctuation of users’ collateral value, and the size of the shock can be controlled through the margin requirement on the users.

The amount of excess reserves (equity) is the state variable in the issuer’s dynamic optimization program. The value function that solves the Hamilton-Jacobi-Bellman (HJB) equation delivers a state-contingent valuation of governance tokens (the issuer’s equity shares). The optimal payout to shareholders implies an endogenous upper bound on the state variable. Reserves are paid out when there are a sufficient amount as risk buffer. The issuer accumulates reserves through the interests earned on reserves, transaction fees charged to users, and open market operations. We specify the lower (liquidation) bound on the excess reserves to be zero to focus on over-collateralization.

Through the recursive formulation via the HJB equation, the platform’s choice of token price process boils down to choosing the local drift and diffusion, and the optimal process of token price can be achieved through open market operations (i.e., trading reserves against tokens). We show that the token-price drift, diffusion, and optimal transaction fees can be implemented through directly setting users’ token demand and token-price diffusion. The recovery of the implied equilib-

⁶At the current stage of stablecoin developments, policy makers take a technology-neutral approach that emphasizes economic insights over technological aspects of implementation ECB Crypto-Assets Task Force (2019).

⁷This money-in-utility approach follows the macroeconomics literature (Ljungqvist and Sargent, 2004). The modelling of network effect is in the tradition of social interaction (Glaeser, Sacerdote, and Scheinkman, 1996).

⁸To be liquid and circulate as a transaction medium, a security must be designed in a way that deters private information acquisition (e.g., via a safe payoff) and thus avoids asymmetric information between trade counterparties (Gorton and Pennacchi, 1990; DeMarzo and Duffie, 1999; Dang, Gorton, Holmström, and Ordoñez, 2014).

⁹Reserve assets are typically risky. Tether, one of the largest stablecoins by market value, are backed mainly by commercial papers of unknown quality. Stablecoin backed by safe assets is narrow banking (Pennacchi, 2012).

rium process of token price (and its drift) is a differential equation problem with the optimal token demand and token-price diffusion as inputs. The recovery also delivers the optimal transaction fees.

In spite of over-collateralization, the stablecoin issuer cannot always sustain one-to-one convertibility between tokens and dollars. To avoid costly liquidation, the platform opts for debasement whenever its excess reserves falls below a threshold. Debasement triggers a vicious cycle as the depressed token demand leads to a reduction in fee revenues, which causes a slow recovery of equity and persistent debasement. However, debasement is a valuable option, as it allows the platform to share risk with users. When negative shocks decrease equity, debasement causes token liabilities to shrink. Above the debasement threshold, the platform credibly sustains one-to-one convertibility. Then a strong token demand allows the platform to collect revenues to grow equity, which further strengthens the peg to dollar. This virtuous cycle implies persistent expansion of platform equity until it reaches the payout boundary. The stationary distribution of platform equity is thus bimodal with two peaks near zero (liquidation) and the payout boundary, respectively.¹⁰

Next, we allow the platform to raise equity. Under a fixed cost of issuance, the issuer first resorts to debasement when its excess reserves fall below the threshold and only raises equity when equity (excess reserves) falls to zero and when costly equity issuance leads to a higher shareholders' value than further debasement does. Once the issuance cost is paid, the platform raises equity to replenish excess reserves up to the payout boundary, where the marginal value of equity falls to one. The jump in reserves implies an immediate restoration of token-price stability and, accordingly, a jump in the aggregate token demand. To preclude a predictable jump in token price level (an arbitrage opportunity), the platform must expand token supply so that after the equity issuance, the token price remains at the pre-issuance level. Thus, the token is re-pegged at the pre-issuance price until future negative shocks deplete the reserves and trigger debasement and equity issuances.

We evaluate two types of stablecoin regulations. The first is a standard capital requirement that stipulates the minimal degree of excess reserves (equity). The capital requirement fails to eliminate debasement. As long as the threat of liquidation (or equity issuance costs) exists, whether it is due to reserve depletion or the violation of regulation, it is optimal for the stablecoin issuer and users to share risk through debasement. The second type of regulation, which enforces a fixed exchange rate, only hurts welfare by destroying the economic surplus from risk sharing. In practice, it is difficult for stablecoin issuers to commit against debasement, but even if such commitment is possible, we show

¹⁰We assume perfect liquidity for the reserve assets. When reserve assets are illiquid, the feedback effect is amplified as in [Chen, Goldstein, and Jiang \(2010\)](#): an increase (decrease) in the stablecoin demand brings reserve inflows (outflows), which, through the price impact, causes the existing reserve assets to appreciate (depreciate).

that it would not not optimal. In other words, the system does not feature dynamic inconsistency in the issuer’s choice of debasement. Admittedly, our model omits several elements and thus can underestimate the value of a perfectly stable token. For example, debasement invites speculation that in turn amplifies price fluctuation and triggers a vicious cycle (Mayer, 2020).

Stablecoins became the subject of heated debate after the technology giant Facebook and its partners announced their own stablecoin, Libra (now “Diem”), in June 2019.¹¹ Leveraging on their existing customer networks, global technology or financial firms are able to rapidly scale the reach of their stablecoins.¹² To understand the advantages of well-established networks in the stablecoin space, we compare platforms with different degrees of network effects. A stronger network effect is indeed associated with a lower frequency of debasement, because a stronger network effect allows the platform to accumulate fee revenues faster when its reserves run out, and, through a higher continuation value, it incentivizes the platform to maintain a larger level of equity to buffer risk.

Stablecoin initiatives sponsored by companies with global customer networks attract attention from regulators for not only its potential of wide adoption but also concerns over monopoly power. In our model, two counteracting forces determine the share of economic surplus seized by the platform. Under a stronger network effect, the platform can extract more rents from its users through fees or risk sharing, but it is also more eager to stimulate token demand by lowering fees and stabilizing tokens given that individual users do not internalize the positive network externalities. In equilibrium, these two forces balance each other out. As a result, the split of welfare between the stablecoin issuer and users is rather insensitive to the degree degree of network effects.

The enormous amount of transaction data brought by a payment system offers a strong incentive for digital platforms to develop their own stablecoins. Following Parlour, Rajan, and Zhu (2020), we model data as by-product of transactions. Under a constant money velocity, the value of users’ stablecoin holdings determines the transaction volume and the rate of data accumulation.¹³ Data helps the platform to improve its productivity that enters into the users’ flow utility from token holdings. A feedback loop emerges: transactions generate more data, which improves the platform and leads to a stronger token demand and even more transactions. As a result, data grows exponentially over time. The platform balances between data acquisition and reserves accumulation.

¹¹The announcement triggered a globally-coordinated response under the umbrella of the G7. From then on, the G20, the Financial Stability Board (FSB), and central banks around the world have also embarked on efforts to address the potential risks while harnessing the potential of technological innovation.

¹²Another example is JPM Coin, a blockchain-based digital coin for fast payment settlement that is being developed by JP Morgan Chase and was announced in February 2019.

¹³In the broader literature on the economics of data, Veldkamp (2005), Ordoñez (2013), Fajgelbaum, Schaal, and Taschereau-Dumouchel (2017), and Jones and Tonetti (2020) model data by-product of economic activities.

The former requires lower fees and a more stable token while the latter calls for higher fees and risk-sharing with users through debasement. A key result is that the ratio of excess reserves to data stock emerges as the new state variable that drives the platform’s trade-off. Moreover, data enters into the platform’s decisions through a sufficient statistic, the data marginal q , which is the marginal contribution of data to shareholders’ value in analogy to Tobin’s q of productive capital.

An increase of data productivity captures the revolutionary progress in big data technology.¹⁴ In response, the issuer maintains more reserves before payout because data allows shareholders’ equity to grow faster by improving platform productivity. However, more reserves do not lead to stabler tokens. The issuer becomes more aggressive in stimulating transactions for data acquisition. A larger transaction volume and a greater value of stablecoin liabilities amplifies the platform’s risk exposure, i.e., the shock loading of excess reserves (equity). As a result, debasement is more likely to happen. Therefore, a paradox exists — stablecoins built primarily for the acquisition and utilization of transaction data can become increasingly unstable precisely when data becomes more valuable.

2 Background: Crypto Shadow Banking in Decentralized Finance

Blockchain technology supports peer-to-peer transfer of assets on distributed ledgers, potentially eliminating the need to transact through intermediaries (Raskin and Yermack, 2016; Abadi and Brunnermeier, 2019; Brainard, 2019). Decentralization avoids sizable intermediation costs (Philippon, 2015). Depending on the blockchain protocols, decentralization can enhance operational resilience by eliminating single point of failure while still achieve scalability (John, Rivera, and Saleh, 2020).¹⁵ Decentralized finance (“DeFi”) offers blockchain-based alternatives to traditional financial services, such as banking, brokerage, and exchanges (Lehar and Parlour, 2021). It also builds on smart contracts (coded enforcement via programmable money (Timm, 2017; Cong and He, 2019; Goldstein, Gupta, and Sverchkov, 2019), a concept independent from blockchain (Halaburda, 2018).

¹⁴Alternative payment-service providers also benefit from regulatory initiatives that facilitate data sharing. A new European Union directive, PSD2, requires banks to provide non-bank service providers with data that would allow those providers to offer payment and other services to the banks’ customers (Duffie, 2019).

¹⁵Decentralized ledger technology is nascent and faces many challenges. The finality of settlement can be compromised when the nodes of a distributed network disagree (Biais, Bisiere, Bouvard, and Casamatta, 2019; Ebrahimi, Routledge, and Zetlin-Jones, 2020). Law of one price can fail in segmented markets (Makarov and Schoar, 2020). Proof-of-work protocol has innate limits on adoption (Hinzen, John, and Saleh (2019), system security risks (Budish, 2018; Pagnotta, 2021), and requires wasteful energy consumption that crowds out other users (Benetton, Compiani, and Morse, 2021). Researchers are active in studying alternative protocols, such as proof-of-stake (e.g., Saleh, 2020; Fanti, Kogan, and Viswanath, 2019). The cost of decentralization also depends on the market structure of decentralized ledger keepers (Huberman, Leshno, and Moallemi, 2019; Pagnotta and Buraschi, 2018; Easley, O’Hara, and Basu, 2019; Cong, He, and Li, 2020; John, Rivera, and Saleh, 2020; Lehar and Parlour, 2020; Prat and Walter, 2021).

This emerging financial architecture requires blockchain-based currencies. A viable means of payment should maintain a stable value at least within the settlement period (i.e., time needed for generating decentralized consensus on transactions (Chiu and Koepl, 2017)). However, most cryptocurrencies are highly volatile (Hu, Parlour, and Rajan, 2019; Stulz, 2019; Liu and Tsyvinski, 2020). They are platform-specific currencies (Catalini and Gans, 2018; Sockin and Xiong, 2018; Li and Mann, 2020; Bakos and Halaburda, 2019; Gryglewicz, Mayer, and Morellec, 2020; Cong, Li, and Wang, 2021; Danos, Marcassa, Oliva, and Prat, 2021) whose values are unbacked and fluctuate with the supply and demand dynamics native to the hosting platforms (Cong, Li, and Wang, 2019).¹⁶

Stablecoins are advertised as blockchain-based copies of fiat currencies. The total market value is above \$100 billion dollars. In May 2021 alone, \$766 billion worth of stablecoins were transferred.¹⁷ The issuer can be a corporate entity or a consortium (e.g., a consortium led by Facebook, the developer of Diem).¹⁸ It can also be an internet protocol (e.g., MakerDAO, the issuer of Dai) whose rules may be updated upon users' consensus.¹⁹ A stablecoin is backed by the issuer's portfolio of reserve assets. The stability of value is sustained by the issuer conducting open market operations (i.e., trading reserves against stablecoins) and meeting redemption requests (Bullmann, Klemm, and Pinna, 2019). The distributed ledger records the ownership and transfer of stablecoins but verifying reserves still relies on traditional auditing (Calle and Zalles, 2019).

Stablecoins are the link between decentralized finance and the real economy. The volatility of the first-generation cryptocurrencies, such as Bitcoin and Ether, limits their adoption in real-world transactions. Stablecoins, designed to have stable exchange rates with respect to the reference fiat currencies, have the potential to mediate blockchain-based transactions of goods, services, and real assets. Stablecoins are also important for the cryptocurrency community. Traders' activities heavily involve rebalancing between stablecoins and more volatile cryptocurrencies. Cryptocurrency has become an emerging asset class with the total market capitalization around \$1.5 trillion dollars (with roughly \$700 billion in Bitcoin).²⁰ It is estimated that 50 to 60% of Bitcoin trading volume is against USDT, the stablecoin issued by Tether (J.P. Morgan Global Research, 2021).

¹⁶Unbacked cryptocurrencies are exposed to platform-specific risks (Liu, Sheng, and Wang, 2020; Shams, 2020), issuers' moral hazard (Chod and Lyandres, 2019; Davydiuk, Gupta, and Rosen, 2019; Gan, Tsoukalas, and Netessine, 2021; Garratt and Van Oordt, 2019), and self-fulfilling and speculative beliefs (Garratt and Wallace, 2018; Benetton and Compiani, 2020). Their returns exhibit a factor structure like other risky assets (Liu, Tsyvinski, and Wu, 2019).

¹⁷See Rajpal and Marshall (2021), Op-ed: Stablecoin is the future of virtual payments. How wise regulation can foster its growth, *CNBC* July 13, 2021.

¹⁸Central banks digital currencies are alternatives to privately issued stablecoins (Bech and Garratt, 2017).

¹⁹It is technologically feasible to hard-code certain aspects of a protocol. Kim and Zetlin-Jones (2019) propose an ethical framework for developers to determine which aspects should be immutable and which should not.

²⁰Nearly half of millennial millionaires have at least 25% of their wealth in cryptocurrencies (CNBC Survey).

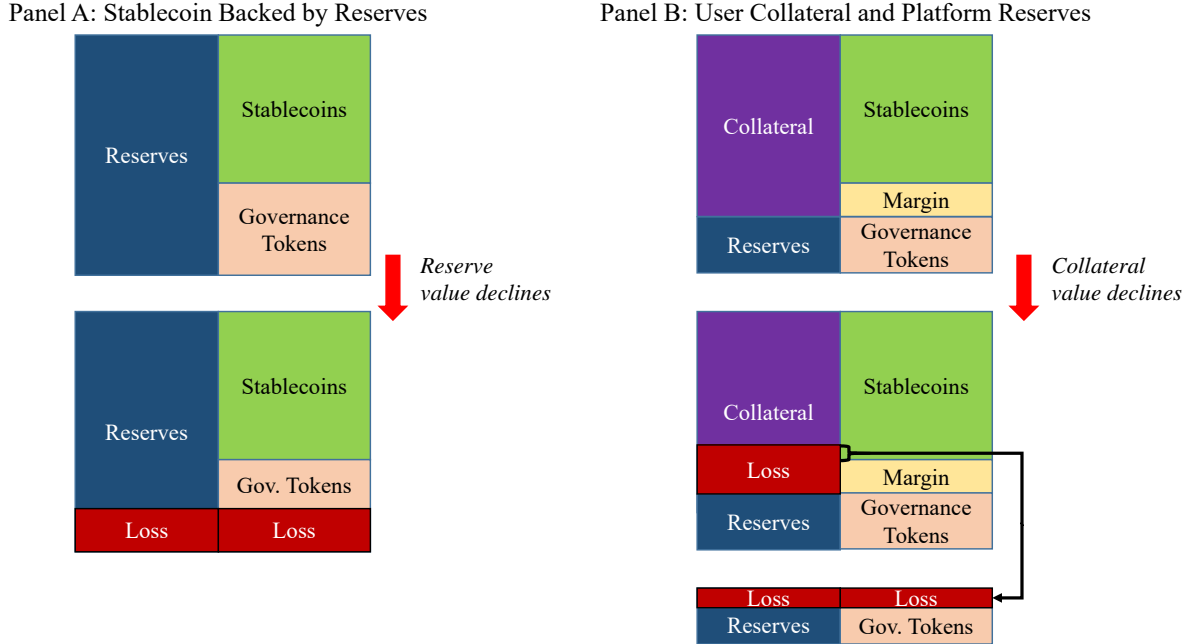


Figure 1: **Crypto Shadow Banking.** This illustrates the two structures of stablecoins. In Panel A, a platform issues stablecoins backed by its reserves. The excess reserves, i.e., the equity position, belong to the holders of governance tokens who have the control right (i.e., the control over platform policies). When reserves are invested in risky assets, a potential loss is absorbed by the equity position. As long as the stablecoins are over-collateralized, their value is intact. In Panel B, stablecoins are backed by both the user’s collateral and the platform’s reserves. When the collateral value declines and the user fails to meet the margin requirement, the platform liquidates the collateral and uses the proceeds (and its own reserves) to buy back stablecoins in the secondary market.

In spite of the importance of stablecoins, there does not exist clear legal and regulatory frameworks. Unlike depository institutions, a stablecoin issuer does not have any obligation to maintain redemption at par. Given that reserves are often invested in risky assets, many are concerned that a major stablecoin “breaks the buck”, triggering financial turmoil (Massad, 2021). The concern is motivated by the relatively recent episode of money market funds switching from stable to floating NAV (net asset value) during the global financial crisis of 2007-2008. Indeed, the creation of stablecoins is essentially a new form of shadow banking—unregulated safety transformation.²¹

The reserve assets are often risky.²² Panel A of Figure 1 illustrates stablecoin creation that features over-collateralization.²³ The issuer’s excess reserves (equity) buffers the fluctuation of reserve value. The equity shares are called governance tokens (or “secondary units”) that carry

²¹A stable value is essential for a transaction medium because it reduces asymmetric information between transaction counterparties (Gorton and Pennacchi, 1990; DeMarzo and Duffie, 1999; Dang, Gorton, Holmström, and Ordoñez, 2014). Without informational frictions, stability may not be necessary (Schilling and Uhlig, 2019).

²²According to De and Hochstein (2021), USDT, the largest stablecoin by market value, is backed by dollar cash, cash equivalents, and commercial papers (75.85%), secured loans (12.55%), corporate bonds, funds, and precious metals (9.96%), and other investments including digital tokens (1.64%).

²³Over-collateralization is a common practice among stablecoin issuers (Bullmann, Klemm, and Pinna, 2019).

the rights to vote on changes of protocols (i.e., control rights) and pay out cash flows generated by transaction fees charged on the stablecoin users. Governance tokens can be issued to replenish reserves, just as traditional corporations can raise cash by issuing equity.

A stablecoin issuer essentially takes a leveraged bet on the value of reserve assets. The issuer can increase its leverage by issuing new stablecoins to finance the purchase of reserve assets, just as banks finance their lending and security trading with newly issued deposits (i.e., inside money creation (Tobin, 1963; Bianchi and Bigio, 2014; Piazzesi and Schneider, 2016; Faure and Gersbach, 2017; Donaldson, Piacentino, and Thakor, 2018; Parlour, Rajan, and Walden, 2020)). Unlike banks that commit to redeem deposits at par, the stablecoin issuer can debase the stablecoins.

Panel B of Figure 1 illustrates a more complex structure that is similar to the one adopted by MakerDAO, the issuer of Dai and an early decentralized autonomous organizations.²⁴ A user pledges her holdings of cryptocurrencies and other assets as collateral for newly created stablecoins, subject to a haircut (margin requirement). The user may transfer the stablecoins, which then circulate in the market, but she must maintain the margin requirement. If the collateral value declines and the user cannot maintain the margin, she loses her collateral to the stablecoin issuer, who then liquidates the collateral and uses the proceeds to buy back (and burn) the stablecoins created for this user.²⁵ If the liquidation of collateral does not generate sufficient proceeds, the stablecoin issuer's reserves are used to supplement the expense of repurchasing the stablecoins.²⁶

The structure in Panel B of Figure 1 is common in traditional shadow banking: A bank sets up a conduit (special purpose vehicle) that tranches risky investments into debt and equity, and at the same time, extends a guarantee to the debt investors so that when the conduit becomes insolvent, the bank internalizes the loss (Acharya, Schnabl, and Suarez, 2013). The stablecoin is like the debt (senior) tranche of the conduit, and the stablecoin issuer and the user in Panel B of Figure 1 correspond to the bank and the conduit, respectively. The stablecoin issuer's commitment to buy back stablecoins potentially with her own reserves is analogous to the bank's guarantee.

In the language of traditional shadow banking, the difference between the two structures in Figure 1 is that from Panel A to Panel B, the stablecoin issuer off loads risk to off-balance-sheet entities (i.e., the users) so that the stablecoins will be backed by both users' collateral and the issuer's reserves. Relative to the simple structure in Panel A of Figure 1, such double collateraliza-

²⁴Decentralized autonomous organizations (DAOs) are organizations represented by rules encoded as computer programs and controlled by the organization members through various voting mechanisms on blockchains.

²⁵Burning is to send the stablecoins to an irretrievable digital address

²⁶While the repurchase (and burn) of stablecoins is recorded on the blockchain, the liquidation of non-cryptocurrency collateral and reserves happens off-chain and still requires the traditional financial and legal systems.

tion does not necessarily strengthen stability because both users’ collateral and the issuer’s reserve assets can be risky and highly correlated in value, especially when both are cryptocurrencies.

We set up our model in the next section following the structure in Panel A of Figure 1 and present the solution in Section 4, discussing the stablecoin issuer’s strategies, welfare, and optimal regulations. In Section 5, we show that our model can be easily extended to incorporate double collateralization in Panel B of Figure 1, and we analyze the optimal margin requirement.

3 A Model of Stablecoins

Consider a continuous-time economy where a continuum of agents (“users”) of unit measure conduct peer-to-peer transactions on a digital platform. The platform facilitates transactions by introducing a local currency (“token”). The generic consumption goods (“dollars”) are the numeraire in this economy. The platform sets the exchange rate between tokens and dollars.

Let P_t denote the token price in units of dollars. At time t , users can redeem their token holdings for dollars or buy more tokens from the platform at the dollar price P_t . They may also trade tokens amongst themselves in the secondary market at the same price P_t by no arbitrage. In equilibrium, the dollar price of token has a law of motion which the atomic users take as given:

$$\frac{dP_t}{P_t} = \mu_t^P dt + \sigma_t^P dZ_t, \quad (1)$$

where the standard Brownian shock, dZ_t , will be introduced below as a shock to the platform’s reserves. We will show how μ_t^P and σ_t^P depend on the platform’s optimal strategies. Next, we first introduce users and then set up the platform’s problem.

Users. We use $u_{i,t}$ to denote the dollar value of user i ’s holdings of tokens, so user i holds $k_{i,t} = u_{i,t}/P_t$ units of tokens. The aggregate dollar value of token holdings is $N_t \equiv \int_{i \in [0,1]} u_{i,t} dt$.

A representative user i derives a flow utility from token holdings

$$\frac{1}{\beta} N_t^\alpha u_{i,t}^\beta A^{(1-\alpha-\beta)} dt - \eta u_{i,t} |\sigma_t^P| dt, \quad (2)$$

where $\alpha, \beta \in (0,1)$ with $\alpha + \beta < 1$, $A > 0$, and $\eta > 0$. We model the utility from holding means of payment following the classic models of monetary economics (e.g., [Baumol, 1952](#); [Tobin, 1956](#); [Feenstra, 1986](#); [Freeman and Kydland, 2000](#)) and related empirical studies (e.g., [Poterba and](#)

Rotemberg, 1986; Lucas and Nicolini, 2015; Nagel, 2016). In this literature, agents derive utility from the real value of holdings, i.e., $u_{i,t}$.²⁷ Following Rochet and Tirole (2003), we introduce network effect via N_t^α . As in Cong, Li, and Wang (2021), it captures the fact that when tokens are more widely used as means of payment, each user’s utility is higher.²⁸ Later we conduct comparative statics analysis on α to show how network effects affect token price stability. The quality of the payment system is captured by parameter A which we will endogenize in Section 6.2. We define transaction utility from an ex ante perspective and do not model the ex post circulation of tokens in line with the aforementioned literature on money-in-utility and cash-in-advance constraint.

The user’s preference for stability is captured by the parameter $\eta (> 0)$, and is defined on the absolute value of σ_t^P to capture the fact that users are averse to token price fluctuation no matter whether the price moves with ($\sigma_t^P > 0$) or against ($\sigma_t^P < 0$) the platform’s reserve shock dZ_t . We motivate such preference for stability following Moreira and Savov (2017): to be liquid and circulate as a transaction medium, a security must be designed in a way that deters private information acquisition and thus avoids asymmetric information between trade counterparties (Gorton and Pennacchi, 1990; DeMarzo and Duffie, 1999; Dang, Gorton, Holmström, and Ordoñez, 2014).²⁹

User i pays a proportional fee on her token holdings, $u_{i,t}f_t dt$, where f_t is set by the platform. In practice, fees are often charged on transactions, in that f_t can be interpreted as the transaction fee per dollar transaction.³⁰ Note that as long as the money (token) velocity is constant within the small time interval (dt), transaction volume is proportional to token holdings. There exists a technical upper bound on the volume of transactions that the platform can handle per unit of time. Without loss of generality, we model the bound as follows:

$$N_t \leq \bar{N}. \tag{3}$$

Let $R_{i,t}$ denote user i ’s (undiscounted) *cumulative* payoff from platform activities. The instan-

²⁷We refer readers to the textbook treatments (e.g., Galí, 2015; Ljungqvist and Sargent, 2004; Walsh, 2003). For the nominal value (i.e., $k_{i,t}$) to affect agents’ decisions, additional frictions, such as nominal illusion (e.g., Shafir, Diamond, and Tversky, 1997) or sticky prices (e.g., Christiano, Eichenbaum, and Evans, 2005), have to be introduced.

²⁸For instance, when there are more people use tokens, it becomes easier to find a transaction counterparty that accepts tokens, so token holders expect more token usage of means of payment.

²⁹The disutility from token volatility can also be motivated by risk-averse preference or users’ aversion to exchange-rate shocks that cause losses of net worth when assets and liabilities are denominated in different currencies (tokens and dollars) (Doepke and Schneider, 2017; Gopinath, Boz, Casas, Díez, Gourinchas, and Plagborg-Møller, 2020).

³⁰Without loss of generality, we consider homogeneous users and the same fees applied to all users. In the presence of user heterogeneity as in Cong, Li, and Wang (2021), price discrimination in fees can be interesting but would still be difficult in practice as users can easily disperse their holdings into different addresses or wallets.

taneous payoff depends on user i 's choice of $u_{i,t} \geq 0$ and is given by

$$dR_{it} \equiv \left(\frac{1}{\beta} N_t^\alpha u_{i,t}^\beta A^{(1-\alpha-\beta)} - \eta u_{i,t} |\sigma_t^P| \right) dt + u_{i,t} \left(\frac{dP_t}{P_t} - r dt - f_t dt \right), \quad (4)$$

where the first term is the flow utility (2) and the second term includes the return from token price change net of the forgone interests and fees. A representative user i chooses $u_{i,t} \geq 0$ to maximize

$$\max_{u_{i,t} \geq 0} \mathbb{E}_t [dR_{it}] = \max_{u_{i,t}} \left[\frac{1}{\beta} N_t^\alpha u_{i,t}^\beta A^{(1-\alpha-\beta)} dt + u_{i,t} \left(\mu_t^P - r - f_t - \eta |\sigma_t^P| \right) dt \right]. \quad (5)$$

The Platform. Let S_t denote the total units of tokens outstanding (the token supply). The token market clearing condition is given by

$$S_t = \int_{i \in [0,1]} \frac{u_{i,t}}{P_t} dt, \quad (6)$$

or equivalently, in the numeraire (dollar) value:

$$S_t P_t = N_t = \int_{i \in [0,1]} u_{i,t} dt. \quad (7)$$

The platform decides on the fees and controls the dollar price of tokens, P_t , by adjusting the token supply. This is akin to central banks using open market operations to intervene in the foreign exchange markets (e.g., [Calvo and Reinhart, 2002](#)). When the platform issues more tokens ($dS_t > 0$), it collects dollar revenues as users buy tokens with dollars. When the platform retires tokens ($dS_t < 0$), it loses dollars to users.

Let M_t denote the platform's reserves (dollar holdings), which has a law of motion

$$dM_t = r M_t dt + (P_t + dP_t) dS_t + N_t f_t dt + N_t \sigma dZ_t - dDiv_t. \quad (8)$$

The first term is the interests earned on the reserves balance, and r is the constant interest rate. The second term is the revenues (losses) from issuing (buying back) tokens the secondary market. From t to $t + dt$, the quantity adjustment dS_t is multiplied by the end-of-period price $P_{t+dt} = P_t + dP_t$. The third term is the fee revenues. In the fourth term, Z_t is a standard Brownian motion, and its increment, dZ_t , captures the shocks to the reserve holdings, which can stem from unexpected operating expenses or risks in the reserve assets. This shock is the only source of uncertainty in the model. Let Div_t denote the *cumulative* dividend process. The platform's reserves decrease when

the platform pays its owners dividends, $dDiv_t$, which must be non-negative under limited liability.

The platform maximizes the expected discounted value of dividend payouts to its owners:

$$V_0 \equiv \max_{\{f_t, dS_t, dDiv_t\}} \mathbb{E} \left[\int_0^\infty e^{-\rho t} dDiv_t \right] \quad \text{subject to (8) and } dDiv_t \geq 0. \quad (9)$$

We assume that the platform’s shareholders are impatient relative to other investors, $\rho > r$.³¹

Liquidation. The policy literature emphasizes the fragility of stablecoins due to bank runs (Brainard, 2019; G7 Working Group on Stablecoins, 2019; ECB Crypto-Assets Task Force, 2019; Massad, 2021; Gorton and Zhang, 2021). To distinguish our analysis from the well-studied mechanism of bank runs, we assume that the platform is liquidated and its owners’ value falls permanently to zero once $M_t < S_t P_t$ (i.e., the reserves are insufficient to meet users’ redemption requests all at once). As we show below, the platform has a positive continuation value, so it optimally maintains $M_t \geq S_t P_t$ to avoid liquidation.³² Focusing on fully collateralized stablecoins also differentiates our paper from the earlier work of Routledge and Zetlin-Jones (2021) on the strategy of maintaining exchange rate stability for under-collateralized stablecoins.³³ The case of over-collateralization is likely to be increasingly relevant under recent regulatory proposals and dramatic failure of under-collateralized stablecoins.³⁴ The conventional wisdom is that breaking the buck (or debasement) will not happen under over-collateralization. Our analysis below challenges this notion.

4 Equilibrium

In this section, we characterize the analytical properties of the dynamic equilibrium and, to sharpen the economic intuition, we also provide graphical illustrations based on the numerical solutions.

³¹Impatience could be preference-based or due to shareholders outside investment opportunities. From a modeling perspective, impatience motivates the platform to pay out; otherwise, the expected return on M_t is greater than r (due to revenues from the fees and token issuance), which then implies that the platform never pays out dividends.

³²Our model features (small) diffusive shocks, so the platform can maintain $M_t \geq S_t P_t$ via continuous adjustments. If we do not assume liquidation upon $M_t < S_t P_t$, there is under-collateralization and equilibrium multiplicity. On one equilibrium path, users never withdraw en masse and continuously trade tokens at the dynamic price P_t . The other equilibrium paths feature runs (related to the dynamics in Donaldson and Piacentino (2020)). In the no-run equilibrium our analysis carries through as long as there exists a liquidation lower bound on C_t .

³³Routledge and Zetlin-Jones (2021) study the speculative attacks on under-collateralized stablecoins that are akin to those on currencies (Morris and Shin, 1998; Goldstein, Ozdenoren, and Yuan, 2011).

³⁴In December 2020, the U.S. house representatives proposed the *Stablecoin Tethering and Bank Licensing Enforcement (STABLE) Act* that emphasized full collateralization. On June 16, 2021, a bank run happened to IRON, a partially collateralized token. This was the first large-scale run in the cryptocurrency market (Tiwari, 2021).

4.1 Managing Stablecoin: Optimal Strategies

User Optimization. A representative user i solves a static problem in (5) and the solution is

$$u_{i,t} = \left(\frac{N_t^\alpha A^{(1-\alpha-\beta)}}{r + f_t - \mu_t^P + \eta|\sigma_t^P|} \right)^{\frac{1}{1-\beta}}. \quad (10)$$

Users' choices exhibit strategic complementarity as $u_{i,t}$ increases in the aggregate value N_t .³⁵ In equilibrium, $N_t = u_{i,t}$ under user homogeneity, which, through (10), implies

$$N_t = \frac{A}{(r + f_t - \mu_t^P + \eta|\sigma_t^P|)^{\frac{1}{1-\xi}}}. \quad (11)$$

To simplify the notations, we define $\xi \equiv \alpha + \beta (< 1)$. Aggregate token demand decreases in the fees, f_t , and depends on the token price dynamics, which the platform controls. This is the solution within the system throughput (i.e., $N_t < \bar{N}$); otherwise, we have $u_{i,t} = N_t = \bar{N}$.

Platform Optimization. To solve for the platform's optimal strategies, we first note that, given the token price dynamics (i.e., μ_t^P and σ_t^P), the platform can directly set N_t through the fees f_t . Rearranging (11), we can back out the fees implied by the platform's choice of N_t :

$$f_t = \left(\frac{A}{N_t} \right)^{1-\xi} - r + \mu_t^P - \eta|\sigma_t^P|. \quad (12)$$

Using (12), we substitute out f_t in the law of motion of reserves (8) and obtain

$$dM_t - (P_t + dP_t)dS_t = rM_t dt + N_t^\xi A^{1-\xi} dt - rN_t dt + N_t (\mu_t^P - \eta|\sigma_t^P|) dt + N_t \sigma dZ_t - dDiv_t. \quad (13)$$

Next, we show the state variable for the platform's dynamic optimization is the *excess reserves*,

$$C_t \equiv M_t - S_t P_t. \quad (14)$$

To derive the law of motion of C_t , we first note that

$$\begin{aligned} dC_t &= dM_t - d(S_t P_t) = dM_t - (P_t + dP_t)dS_t - S_t dP_t \\ &= dM_t - (P_t + dP_t)dS_t - N_t (\mu_t^P dt + \sigma_t^P dZ_t). \end{aligned} \quad (15)$$

³⁵There is a trivial equilibrium where $u_{i,t} = N_t = 0$. We focus on the Pareto-dominant equilibrium where $N_t > 0$.

The second equality uses $d(S_t P_t) = dS_t P_t + S_t dP_t + dS_t dP_t$ (by Itô's lemma) and the last equality uses (1) and $N_t = S_t P_t$. From a balance-sheet perspective, the reserves, M_t , are the platform's assets and the outstanding tokens, $S_t P_t$, are the liabilities. The excess reserves constitute the equity. Thus, equation (15) is essentially the differential form of the balance-sheet identity. Using (13) to substitute out $dM_t - (P_t + dP_t)dS_t$ in (15), we obtain the following law of motion of C_t :

$$dC_t = \left(rC_t + N_t^\xi A^{1-\xi} - N_t \eta |\sigma_t^P| \right) dt + N_t (\sigma - \sigma_t^P) dZ_t - dDiv_t, \quad (16)$$

with drift $\mu_C(C_t) \equiv rC_t + N_t^\xi A^{1-\xi} - N_t \eta |\sigma_t^P|$ and diffusion $\sigma_C(C_t) \equiv N_t (\sigma - \sigma_t^P)$. Note that $N_t \mu_t^P$ disappears. As shown in (13), the platform receives more fee revenues (see (12)) when users expect tokens to appreciate ($N_t \mu_t^P$), but such revenues do not increase the platform's equity (excess reserves) as they are cancelled out by the appreciation of token liabilities. Thus, the drift term, $rC_t + N_t^\xi A^{1-\xi} - N_t \eta |\sigma_t^P|$, is the expected appreciation of the platform's equity position.

The platform controls the law of motion of dC_t through dividend payouts, $dDiv_t$, aggregate token demand, N_t (or equivalently, transaction fees f_t), and token price volatility σ_t^P . We will show that once we solve for these optimal control variables, the equilibrium processes of token supply, S_t , and token price, P_t , can be obtained. We characterize a Markov equilibrium with the platform's excess reserves, C_t , as the only state variable. We solve for the platform's control variables, $dDiv_t$, σ_t^P , and N_t , as functions of C_t , and thereby, show that (16) is an autonomous law of motion of C_t .

The platform owners' value function at time t is given by

$$V_t = V(C_t) = \max_{\{N, \sigma^P, Div\}} \mathbb{E} \left[\int_{s=t}^{\infty} e^{-\rho(s-t)} dDiv_s \right]. \quad (17)$$

The platform pays dividends when the marginal value of excess reserves is equal to one, i.e., one dollar has the same value either held within the platform or paid out,

$$V'(\bar{C}) = 1. \quad (18)$$

The optimality of payouts at \bar{C} also requires the following super-contact condition (Dumas, 1991),

$$V''(\bar{C}) = 0. \quad (19)$$

The next proposition states that the value function is concave. The declining marginal value of

excess reserves implies that \bar{C} in (18) is an endogenous upper bound of the state variable C_t . At any $C_t \in (0, \bar{C})$, the platform does not pay dividends to its owners because the marginal value of excess reserve, $V'(\bar{C})$, is greater than one, i.e., the owners' value of dividend.

Proposition 1 (Value Function and Optimal Payout). *There exists $\bar{C} > 0$ such that $C_t \leq \bar{C}$. For $C_t < \bar{C}$, the value function is strictly concave, and $V'(C_t) > 1$. At $C_t = \bar{C}$, $V'(\bar{C}) = 1$ and the platform pays dividends when $dC_t > 0$ so that dividend payments cause C_t to reflect at \bar{C} .³⁶*

Before characterizing the solution as C_t approaches zero, we note that

$$\max_{\{N \in [0, \bar{N}]\}} \left\{ N^\xi A^{1-\xi} - \eta N \sigma \right\} > 0, \quad (20)$$

because $N^\xi A^{1-\xi} - \eta N \sigma = 0$ at $N = 0$ and, under $\xi = \alpha + \beta < 1$ as previous stated, the first derivative goes to infinity as N approaches zero, (i.e., $\lim_{N \rightarrow 0} \xi \left(\frac{A}{N}\right)^{1-\xi} - \eta \sigma = +\infty$).

As C_t approaches zero, the platform can only avoid liquidation by reducing the diffusion of C_t (i.e., the shock exposure $\sigma_C(C_t) = N_t(\sigma - \sigma_t^P)$) to zero, which requires

$$\lim_{C \rightarrow 0^+} \sigma^P(C) = \sigma, \quad (21)$$

and by keeping the drift of C_t (i.e., $\mu_C(C_t) = rC_t + N_t^\xi A^{1-\xi} - N_t \eta |\sigma_t^P|$) non-negative, which is already guaranteed by (20) under (21). It is optimal to do so and avoid liquidation because, as we show below, the value of platform as an ongoing concern is positive. In the region $C \in (0, \bar{C})$, we obtain the following Hamilton-Jacobi-Bellman (HJB) equation (with time subscripts suppressed):

$$\rho V(C) = \max_{\{N \in [0, \bar{N}], \sigma^P\}} \left\{ V'(C) \left(rC + N^\xi A^{1-\xi} - \eta N |\sigma_t^P| \right) + \frac{1}{2} V''(C) N^2 (\sigma - \sigma^P)^2 \right\}. \quad (22)$$

Setting $\sigma^P = \sigma$ is always feasible in the HJB equation, which implies:

$$\begin{aligned} V(C) &\geq \frac{V'(C)}{\rho} \left(rC + \max_{\{N \in [0, \bar{N}]\}} \left\{ N^\xi A^{1-\xi} - \eta N \sigma \right\} \right) \\ &\geq \frac{1}{\rho} \left(\max_{\{N \in [0, \bar{N}]\}} \left\{ N^\xi A^{1-\xi} - \eta N \sigma \right\} \right) > 0, \end{aligned} \quad (23)$$

where the second inequality uses $C \geq 0$ and $V'(C) \geq 1$ and the last inequality follows (20). By the continuity of the value function $V(C)$, a strictly positive lower bound of $V(C)$ on $(0, \bar{C})$ implies

³⁶When $dC_t > 0$ at $C_t = \bar{C}$, the dividend amount is equal to dC_t (i.e., exactly the amount needed to avoid $C_t > \bar{C}$).

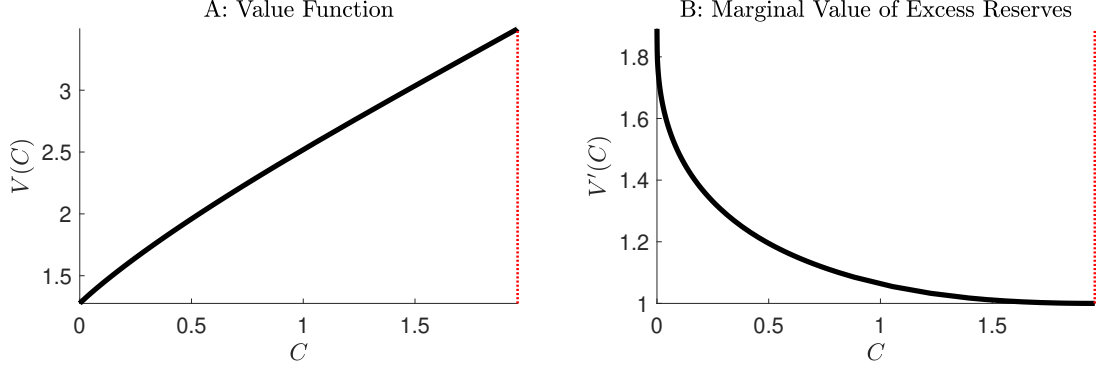


Figure 2: Value Function. This illustrates the level and first derivative of the platform's value function. The red dotted lines in both panels mark \bar{C} (defined in Proposition 1). The parameters are $r = 0.05$, $\rho = 0.06$, $\sigma = 0.1$, $\bar{N} = 5$, $\eta = 0.15$, $\alpha = 0.45$, $\beta = 0.05$, and $A = 0.0025$.

that $\lim_{C \rightarrow 0} V(C) > 0$. In sum, we have shown that it is optimal for the platform to implement (21) and thereby avoid liquidation because the value as an ongoing concern is positive as C_t approaches zero. Finally, (21) implies that, when taking the right-limit on both sides of (22), we obtain

$$\lim_{C \rightarrow 0^+} \frac{V(C)}{V'(C)} = \frac{1}{\rho} \max_{\{N \in [0, \bar{N}]\}} \{N^\xi A^{1-\xi} - \eta N \sigma\} = \frac{1}{\rho} \{ \underline{N}^\xi A^{1-\xi} - \eta \underline{N} \sigma \} > 0, \quad (24)$$

where the second equality follows from plugging in the optimal N_t given by

$$\underline{N} \equiv \lim_{C \rightarrow 0^+} N(C) = \arg \max_{N \in [0, \bar{N}]} \{N^\xi A^{1-\xi} - \eta N \sigma\} = A \left(\frac{\xi}{\eta \sigma} \right)^{\frac{1}{1-\xi}} \wedge \bar{N} > 0. \quad (25)$$

The condition (24) serves as a boundary condition for the HJB equation.

As an interim summary, the next proposition summarizes the value function solution as solution to an ordinary differential equation (ODE) problem with an endogenous boundary \bar{C} . Figure 2 plots the numerical solution of value function (Panel A) and the decreasing marginal value of excess reserves with the red dotted line marking the payout boundary \bar{C} .

Proposition 2 (Value Function). *The value function, $V(C)$, and the boundary \bar{C} solve the ODE (22) on $(0, \bar{C})$ subject to the boundary conditions (18), (19), and (24).*

Next, we fully characterize the platform's optimal choices of σ_t^P and N_t as functions of the state variable, C_t (via the derivatives of $V(C)$). First, we define the platform's *effective risk aversion*:

$$\gamma(C) \equiv -\frac{V''(C)}{V'(C)}. \quad (26)$$

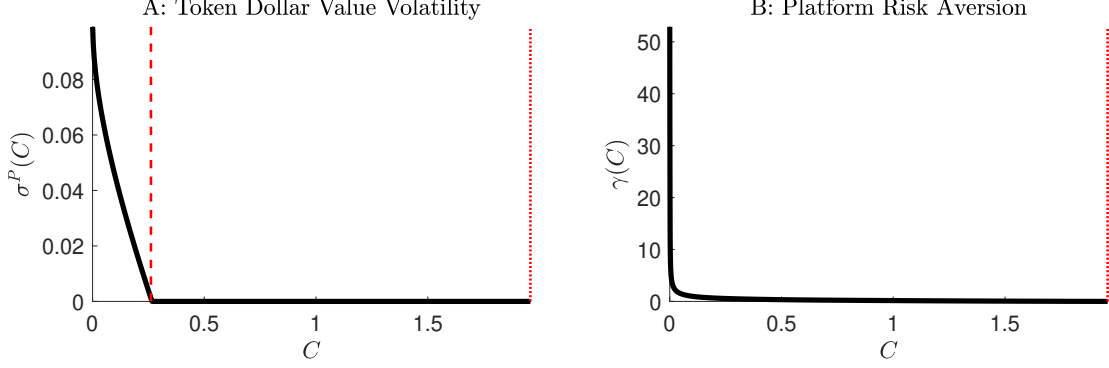


Figure 3: Token Volatility and Platform Risk Aversion. This figure plots token return volatility $\sigma^P(C)$ in Panel A and the effective risk aversion $\gamma(C)$ in Panel B. In Panel A, the red dashed line marks \tilde{C} (in Proposition 3). The red dotted lines in both panels mark \bar{C} (in Proposition 1). The parameterization follows Figure 2.

This definition is analogous to the classic measure of absolute risk aversion of consumers (Arrow, 1965; Pratt, 1964). From Proposition 1, $\gamma(C) \geq 0$ and, in $(0, \bar{C})$, $\gamma(C) > 0$. The next proposition states the monotonicity of $\gamma(C)$ in C and summarizes the optimal $\sigma_t^P = \sigma^P(C_t)$ and $N = N(C_t)$.

Proposition 3 (Risk Aversion, Token Volatility, and Transaction Volume). *The platform's effective risk aversion, $\gamma(C)$, strictly decreases in the level of reserve holdings, C . There exists $\tilde{C} \in (0, \bar{C})$ such that, at $C \in (0, \tilde{C})$, $N(C) = \underline{N}$ and $\sigma^P(C)$ strictly decreases in C , given by,*

$$\sigma^P(C) = \sigma - \frac{\eta}{\gamma(C)\underline{N}} \in (0, \sigma), \quad (27)$$

and at $C \in [\tilde{C}, \bar{C}]$, $\sigma^P(C) = 0$ and $N(C)$ increases in C , given by

$$N(C) = \min \left\{ \left(\frac{\xi A^{1-\xi}}{\gamma(C)\sigma^2} \right)^{\frac{1}{2-\xi}}, \bar{N} \right\}. \quad (28)$$

When the platform's reserves are low, i.e., $C \in (0, \tilde{C})$, it is the ratio of users' risk aversion to the platform's risk aversion that determines token volatility. Equation (27) shows that, in this region, when the platform accumulates more reserves and becomes less risk-averse, it absorbs risk from users by tuning down σ_t^P , and when the platform exhausts its reserves, it off-loads the risk in its dollar revenues to users.³⁷ The platform and its users engage actively in risk-sharing when $C \in (0, \tilde{C})$. This is illustrated by the numerical solution in Panel A of Figure 3 with \tilde{C} marked by the dashed line. In Panel B, we show that the platform's risk aversion declines in C . In this region

³⁷Equation (27) implies that the condition (24) is equivalent to $\gamma(C)$ (or $-V''(C)$) approaching infinity in the limit.

of low reserves, the transaction volume, which is simply the dollar value of users' token holdings under our assumption of constant velocity, is pinned to the lowest level given by \underline{N} in (25).

Once the platform's reserves surpass the critical threshold \tilde{C} , its risk aversion becomes sufficiently low and it optimally absorbs all the risk in its dollar revenues, setting $\sigma^P(C)$ to zero which also implies that in this region $\mu^P(C) = 0$.³⁸ As a result, the transaction volume on the platform starts to rise above the "hibernation level", \underline{N} , as illustrated by Panel A of Figure 4. Therefore, reserves are absolutely essential for stimulating economic activities on a stablecoin platform.

Interestingly, even though the platform shelters its users from risk at any $C > \tilde{C}$, its risk aversion still shows up in N_t given by (28). As shown in (12), the choice of N_t is implemented through fees. Therefore, the intuition can be more easily explained when we substitute (28), the optimal N_t , and the optimal $\sigma_t^P = 0$ (as well as $\mu_t^P = 0$) into (12) to solve f_t : when $\left(\frac{\xi A^{1-\xi}}{\gamma(C)\sigma^2}\right)^{\frac{1}{2-\xi}} < \bar{N}$,

$$f(C) = \left(\frac{A\gamma(C)\sigma^2}{\xi}\right)^{\frac{1-\xi}{2-\xi}} - r, \quad (29)$$

i.e., the platform charges higher fees to build up its reserves when its precautionary savings motive is strong ($\gamma(C)$ is higher); when $\left(\frac{\xi A^{1-\xi}}{\gamma(C)\sigma^2}\right)^{\frac{1}{2-\xi}} \geq \bar{N}$, i.e., C is sufficiently high such that $\gamma(C)$ falls below $\frac{\xi A^{1-\xi}}{\sigma^2 \bar{N}^{2-\xi}}$, the platform de-links the fees from its risk aversion,

$$f(C) = \left(\frac{A}{\bar{N}}\right)^{1-\xi} - r. \quad (30)$$

The platform faces a risk-return trade-off. The fees serve as a compensation for risk exposure but discourages users from participation. So when the platform's risk aversion rises, it charges users more per dollar of transaction at the expense of a smaller volume. When the platform's risk aversion declines, the fees per dollar of transaction decline while the total transaction volume increases. Once reserves are sufficiently high such that $\gamma(C) \leq \frac{\xi A^{1-\xi}}{\sigma^2 \bar{N}^{2-\xi}}$, the fees no longer decline with the platform's risk aversion, as the platform has maxed out its transaction capacity, i.e., $N_t = \bar{N}$, and it becomes impossible to further stimulate user participation. Likewise, when the platform's reserves are below \tilde{C} and $\sigma^P(C) > 0$, $N_t = \underline{N}$, and the fees are given by

$$f(C) = \left(\frac{A}{\underline{N}}\right)^{1-\xi} + \mu^P(C) - \eta\sigma^P(C) - r. \quad (31)$$

³⁸This result arises because we express the equilibrium token price as a function of C , in that $P_t = P(C_t)$. Thus, token volatility and token returns can be expressed as functions of C too, in that $\sigma_t^P = \sigma^P(C_t)$ and $\mu_t^P = \mu^P(C_t)$. Since $\sigma^P(C) = 0$ for $C > \tilde{C}$, $P'(C)$ must be zero by Itô's lemma (i.e., $P(C)$ is constant), implying $\mu^P(C) = 0$.

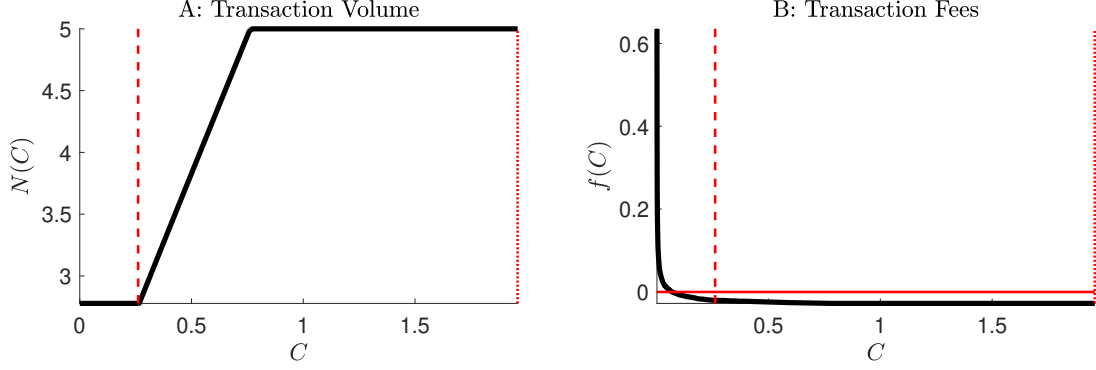


Figure 4: **Transaction Volume and Fees.** This figure plots transaction volume $N(C)$ in Panel A and fees per dollar of transaction $f(C)$ in Panel B. The red dotted line marks \bar{C} (in Proposition 1). In both panels, the red dashed line marks \tilde{C} (in Proposition 3). In Panel B, the red solid line marks zero. The parameterization follows Figure 2.

Even though the platform's risk aversion is high, it no longer sacrifices transaction volume for higher fees because user participation has already fallen to a very low level.

Panel B of Figure 4 plots the numerical solution of optimal fees that decrease in excess reserves. Depending on the parameters, fees can actually turn into user subsidies (i.e., fall below zero) when excess reserves are sufficiently high.³⁹ The next corollary summarizes the results on fees.

Corollary 1 (Optimal Transaction Fees). *Transaction fees, $f(C)$, decrease in excess reserves, C . At $C \in (0, \tilde{C})$, where \tilde{C} is defined in Proposition 3, transaction fees are given by (31). At $C \in [\tilde{C}, \tilde{C}')$, where \tilde{C}' is defined by $\gamma(\tilde{C}') = \frac{\xi A^{1-\xi}}{\sigma^2 \bar{N}^{2-\xi}}$, transaction fees are given by (29). At $C \in [\tilde{C}', \bar{C})$, where \bar{C} is defined in Proposition 1, transaction fees are given by (30).*

When C is below \tilde{C} , an interesting implication of (31) is that the platform charges (compensates) users the expected appreciation (depreciation) of tokens over risk-free rate (i.e., $\mu_t^P - r$ shows up in f_t). To fully solve the fees, we need to know both $\gamma(C_t)$ and the function $\mu_t^P = \mu^P(C_t)$. In fact, the platform's choice of $\sigma_t^P = \sigma^P(C_t)$ already pins down the function of token price, $P_t = P(C_t)$, so $\mu^P(C_t)$ can be obtained from Itô's lemma. Next, we solve $P_t = P(C_t)$ from the function $\sigma^P(C_t)$. By Itô's lemma,

$$\sigma^P(C) = \frac{P'(C)}{P(C)} N(C) (\sigma - \sigma^P(C)), \quad (32)$$

where $N(C) (\sigma - \sigma^P(C))$ is the diffusion of state variable C . Using Proposition 2, we solve the value function $V(C)$ and obtain $\gamma(C)$. Using Proposition 3, we obtain the functions $\sigma^P(C)$ and $N(C)$. Plugging $\sigma^P(C)$ and $N(C)$ into (32), we obtain a first-order ODE for the function $P(C)$.

³⁹Specifically, under the particular parameterization, the condition is for fees to turn into subsidies near \bar{C} is that $\frac{A^{1-\xi}}{\bar{N}^{1-\xi}} < r$ where we use (30) and the fact that $\mu^P(C) = 0$ for $C \in (\tilde{C}, \bar{C})$ (to be discussed later in this section).

To uniquely solve the function $P(C)$, we need to augment the ODE (32) with a boundary condition. In our model, both the platform and users are not concerned with the level of token price and only care about the expected token return, μ_t^P , and volatility, σ_t^P . Therefore, we have the liberty to impose the following boundary condition:

$$P(\bar{C}) = 1. \quad (33)$$

i.e., the platform sets an exchange rate of one dollar for one token when C_t reaches \bar{C} . The next corollary states the solution of token price as solution to a first-order ODE problem.

Corollary 2 (Solving Equilibrium Token Price). *Given the solutions of $V(C)$ (and $\gamma(C)$) from Proposition 2 and $\sigma^P(C)$ and $N(C)$ from Proposition 3, the equilibrium dollar price of token, $P(C)$, is a function of C that solves the ODE (32) under the boundary condition (33).*

Proposition 3 states that, once C crosses above the critical threshold \tilde{C} , $\sigma^P(C) = \mu^P(C) = 0$, which, by Itô's lemma, implies that $P'(C) = 0$. Therefore, if the platform's reserves are sufficiently high, it optimally fixes the dollar price (or the redemption value by no arbitrage) of token at $P(C) = 1$. When C falls below \tilde{C} , (32) implies that $P'(C) > 0$ (because $\sigma^P(C) \in (0, \sigma)$ in Proposition 3) so the token redemption value comoves with the platform's excess reserves.

The endogenous transition between redemption at par and redemption below par happens as the platform accumulates or depletes reserves through various activities laid out in (8) (and then in (16)), including the platform's issuance of new tokens ($dS_t > 0$), users' token redemption ($dS_t < 0$), fee revenues, and shocks to the dollar reserves. The platform's choice of token price is optimally chosen and thus credible in the sense that it the platform does not have any incentives to deviate.

Proposition 4 (Credible Redemption Value Regimes). *At $C \in [\tilde{C}, \bar{C}]$, where \tilde{C} is defined in Proposition 3, the platform credibly commits to redeem token at par, i.e., $P(C) = 1$. At $C \in (0, \tilde{C})$, the redemption value of token comoves with the platform's excess reserves (i.e., $P'(C) > 0$).*

Proposition 4 states that redemption at par is credible if and only if the platform holds a sufficiently large amount of *excess* reserves ($C > \tilde{C}$). When excess reserves fall below \tilde{C} , the platform optimally debases its tokens. By allowing the redemption value to comove with its excess reserves, the platform off-loads the risk in its dollar reserves to users and thereby prevents liquidation.

Figure 5 plots the numerical solutions of aggregate token value, $N(C) = S(C)P(C)$ (Panel A), the redemption value of one token optimally set by the platform $P(C)$ (Panel B), and the

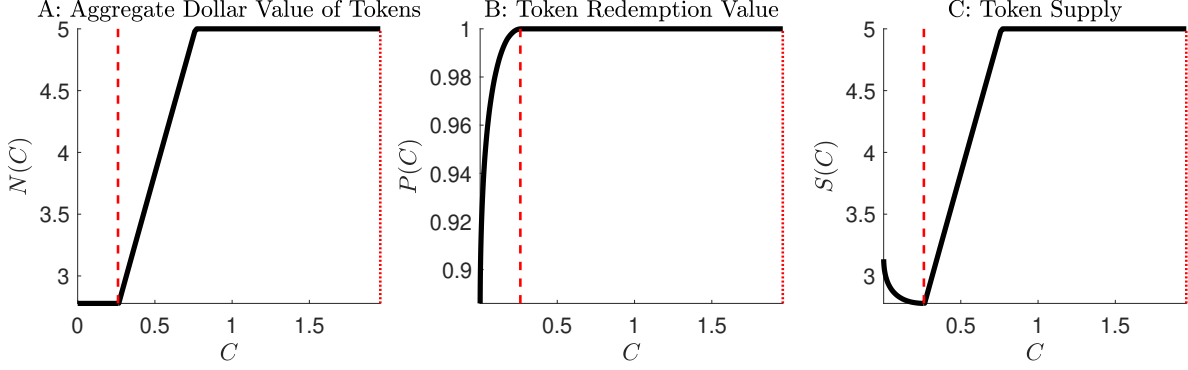


Figure 5: Token Price and Quantity Dynamics. This figure plots the aggregate dollar value of tokens $N(C)$ in Panel A, the token redemption value or dollar price $P(C)$ in Panel B, and token supply $S(C)$ in Panel C. The red dotted lines in all panels mark \bar{C} (defined in Proposition 1). The red dashed lines in all panels mark \tilde{C} (defined in Proposition 3). The parameterization follows Figure 2.

total quantity of tokens $S(C)$ implied by $N(C)$ and $P(C)$ (Panel C). The dashed line marks \tilde{C} . The platform implements the optimal token redemption value through the manipulation of token supply. When the platform has enough reserves to credibly sustain redemption at par (i.e., $C > \tilde{C}$), token supply comoves with demand so that $P(C)$ is fixed. Below \tilde{C} , a decrease of excess reserves triggers the platform to supply more tokens in exchange for dollars that replenishes reserves. The users respond to token debasement by reducing their token demand to \underline{N} , which in turn reinforces the debasement by reducing the platform's revenues from open market operations ($dS_t > 0$) and transaction fees. The system falls into an instability trap.

In practice, stablecoin platforms often claim commitment to redemption at par and substantiate this commitment by holding reserves that just cover their token liabilities. However, such a claim is only credible (and incentive-compatible) if the excess reserves are sufficiently high; otherwise, as shown in Proposition 4, it is in the platform's interest to debase its tokens.

Using the parameters in Figure 2 and the numerical solutions, we simulate in Figure 6 a path of excess reserves C_t (Panel A), token redemption value P_t (Panel B), token supply S_t (Panel C), and transaction volume N_t (Panel D). The horizontal axis records the number of years. In the first three years, in spite of the volatility in C_t , the platform manages to sustain redemption at par, and with the transaction volume (or token demand) at the full capacity at \bar{N} , a fixed dollar price of token implies a fixed token supply. Following a sequence of negative shocks between the third and fourth years, the platform raises fees. Users respond by reducing their token demand N_t , so the platform reduces token supply, maintaining redemption at par. The platform optimally trades off replenishing dollars reserves by raising fees and using dollar reserves in token buy-back. As

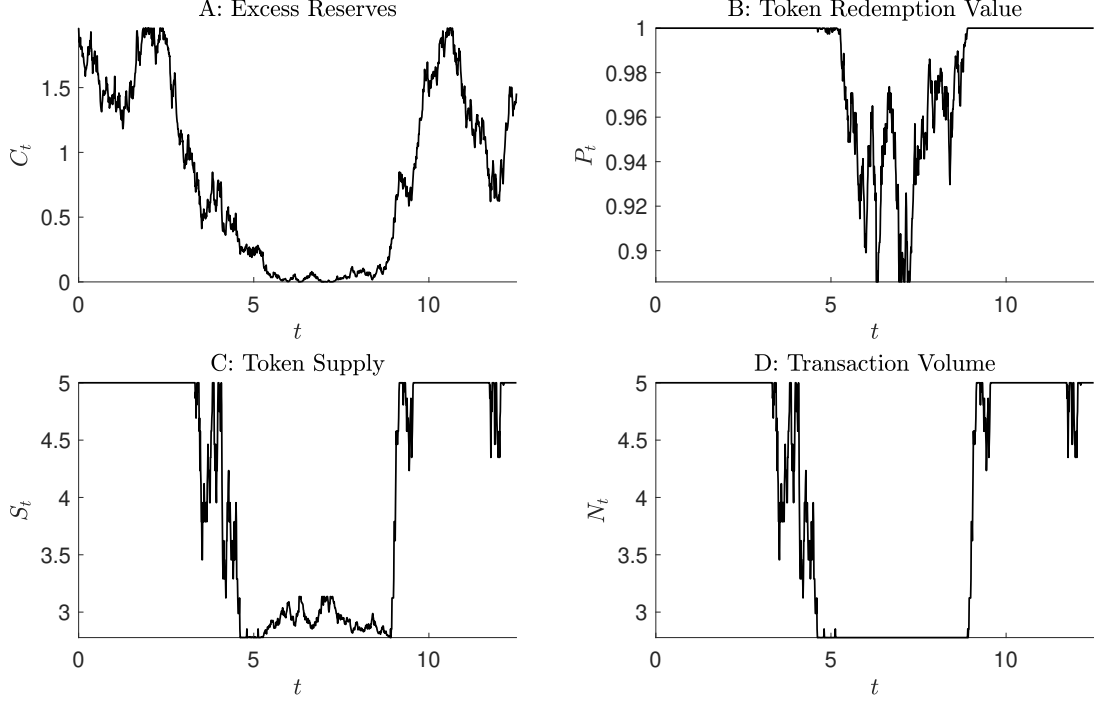


Figure 6: **The Instability Trap in Simulation.** Using the numerical solutions, we simulate a path of excess reserves (Panel A), token redemption value (Panel B), token supply (Panel C), and transaction volume on the platform (Panel D). The horizontal axis records the number of years. The parameterization follows Figure 2.

more negative shocks hit between the fourth and ninth years, the platform gives up the peg and off-loads risk to users through the fluctuation of token redemption price. Users' token demand hits \underline{N} , and the platform starts actively expanding token supply in exchange for dollar revenues. Then following a sequence of positive shocks, the recovery started in the ninth year, and by the tenth year, the platform finally restores token redemption at par.

We demonstrate the long-run dynamics of the model in Figure 7. Panel A plots the stationary probability density of excess reserves. It shows how much time over the long run the platform spends in different regions of C . The distribution is bimodal. The concentration of probability mass near $C = 0$ is due to the fact that, when the transaction volume (or token demand) gets stuck at the hibernation level \underline{N} , the platform can only grow out of this region very slowly by accumulating reserves through fee revenues and proceeds from expanding token supply. The platform also spends a lot of time near the payout boundary \bar{C} as this is a stable region where, given a sufficiently high level of reserve buffer, shocks' impact is limited. In Panel B, we show that, even though redemption at par seems to be the norm, the system exhibits significant risk of token debasement ($P(C) < 1$), so the stationary probability density of token price has a long left tail.

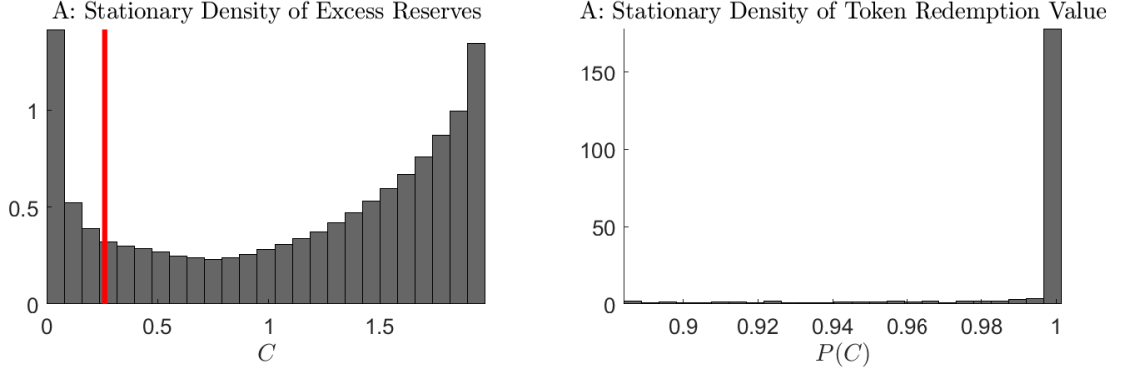


Figure 7: **Long-Run Dynamics and Stationary Density.** We plot stationary probability densities of excess reserves C (Panel A) and token value $P(C)$ (Panel B) in numerical solutions. The parameterization follows Figure 2.

4.2 The Optimal Issuance of Governance Tokens

In this subsection, we take an excursion to analyze the issuance of platform equity (or “governance tokens” in practice). So far, the platform recovers from the low- C region through the accumulation of internal funds. We now allow the platform to raise dollar funds by issuing equity shares subject to a fixed financing cost, χ .⁴⁰ To characterize the optimal issuance policy, we first note that when issuing equity, the platform raises enough funds so that C jumps to \bar{C} where $V'(\bar{C}) = 1$. Once the fixed cost χ is paid, raising one more dollar does not incur further costs, so as long as the marginal value of reserves, $V'(C)$, is greater than one, the platform keeps raising funds. In Appendix B.3, we extend the model to incorporate a proportional cost of equity issuance.

The platform raises external funds only when C falls to zero. First, it is not optimal to issue equity at the payout boundary, \bar{C} , because newly raised funds will be paid out immediately and thus the issuance cost is incurred without any benefits. Therefore, let \underline{C} denote the recapitalization boundary and we have $\underline{C} < \bar{C}$. Consider the *change* of existing shareholders’ value after equity issuance: $[V(\bar{C}) - (\bar{C} - \underline{C}) - \chi] - V(\underline{C})$. To obtain the post-issuance value of existing shareholders, we deduct the issuance cost, χ , and the competitive new investors’ equity value (equal to the funds they invested), $(\bar{C} - \underline{C})$, from the total platform value post-issuance, $V(\bar{C})$. To calculate the change, we subtract $V(\underline{C})$, the value without issuance. Taking the derivative with respect to \underline{C} , we

⁴⁰Firms face significant financing costs due to asymmetric information and incentive issues. A large literature has sought to measure these costs, in particular, the costs arising from the negative stock price reaction in response to the announcement of a new issue. Lee, Lochhead, Ritter, and Zhao (1996) document that for initial public offerings (IPOs) of equity, the direct costs (underwriting, management, legal, auditing and registration fees) average 11.0% of the proceeds, and for seasoned equity offerings (SEOs), the direct costs average 7.1%. IPOs also incur a substantial indirect cost due to short-run underpricing. An early study by Asquith and Mullins (1986) found that the average stock price reaction to the announcement of a common stock issue was -3% and the loss in equity value as a percentage of the size of the new equity issue was as high as -31% (see Eckbo, Masulis, and Norli, 2007, for a survey).

obtain $-V'(\underline{C}) + 1 < 0$ for $\underline{C} < \bar{C}$ because $V'(\underline{C}) > V'(\bar{C}) = 1$ under value function concavity.⁴¹ Therefore, the platform prefers \underline{C} to be as low as possible and thus optimally sets it to zero.

Finally, as in the baseline model, the platform can avoid liquidation by off-loading risk to users, as shown in (21), and obtain the value given by (24). Therefore, as C approaches zero, the platform only opts for recapitalization at $C = 0$ if recapitalization generates a higher value. Accordingly, the lower boundary condition (24) for the value function is modified to

$$\lim_{C \rightarrow 0^+} V(C) = \max \left\{ \lim_{C \rightarrow 0^+} \frac{V'(C)}{\rho} \left\{ \underline{N}^\xi A^{1-\xi} - \eta \underline{N} \sigma \right\}, V(\bar{C}) - \bar{C} - \chi \right\}, \quad (34)$$

The first term in the max operator is the value obtained from off-loading risk to users, given by (24). The second term is the post-issuance value for existing shareholders. The results in Proposition 1 to 2, 3 and Corollary 1 still hold except that the boundary condition (24) is replaced by (34).

Proposition 5 (Optimal Recapitalization). *The platform raises external funds through equity issuances only if $V(\bar{C}) - \bar{C} - \chi > \lim_{C \rightarrow 0^+} \frac{V'(C)}{\rho} \left\{ \underline{N}^\xi A^{1-\xi} - \eta \underline{N} \sigma \right\}$ (see (34)), where \bar{C} is given by Proposition 1, and only when excess reserves fall to zero. The amount of funds raised is \bar{C} .*

When recapitalization happens, C_t jumps from zero to \bar{C} , which then implies an upward jump in the aggregate token demand from $N(0)$ to $N(\bar{C})$ (for $N(0) < N(\bar{C})$, see Proposition 3). If the platform does not adjust the token supply, S_t , there will be an upward *predictable* jump in P_t , which implies an arbitrage opportunity. To preclude arbitrage, the platform must expand token supply simultaneously as it issues equity so that the token price stays at the pre-issuance level.⁴² Let us revisit the results on the token price level in Corollary 2 and Proposition 4. Let $P_j(C)$ denote the token price function after the j -th recapitalization. We have

$$P_j(\bar{C}) = P_{j-1}(0), \quad (35)$$

which replaces (33) as the boundary condition for the price-level ODE (32). Token price level before the first recapitalization, $P_0(C)$ is still solved under the boundary condition (33), i.e., $P_0(\bar{C}) = 1$.

Corollary 3 (Recapitalization and Token Price Level). *Token price after the j -th recapitalization is solved by the ODE (32) subject to the boundary condition (35).*

⁴¹To prove the concavity of value function stated in Proposition 1, we only need the HJB equation (22) and the upper boundary conditions (18) and (19), so recapitalization does not affect value function concavity.

⁴²Note that the expansion of token supply brings dollars of equal value into the reserve portfolio. This simultaneous expansion of assets and liabilities does not imply any variation in the excess reserves C_t at \bar{C} .

In the baseline model without recapitalization, the debasement of token is temporary: token price level falls below 1 when C falls below \tilde{C} due to negative shocks and it recovers back to 1 when the platform accumulates sufficient amount of dollar revenues so that C crosses above \tilde{C} (Proposition 4). When recapitalization happens, the debasement is permanent. After the j -th recapitalization, token price level starts anew at a lower peg, $P_j(\bar{C}) = P_{j-1}(0)$, and if negative shocks deplete the platform’s reserves and triggers another recapitalization, token price level declines along the process and, right after recapitalization, stabilizes at an even lower peg, $P_{j+1}(\bar{C}) = P_j(0)$.

Discussion: financial frictions. In our model, financial frictions play a key role. If costless recapitalization is possible, i.e., $\chi = 0$, then the platform will never allow the marginal value of reserves to exceed one because, when $V'(C) > 1$, it is profitable to raise funds from competitive investors that cost 1 per dollar and generates a value of $V'(C) > 1$ for the existing shareholders. The constant marginal value of C implies that the platform is no longer risk-averse, i.e., $\gamma(C) = 0$, and thus, will absorb all risk, setting σ_t^P to zero. Token price will be pegged at one.

4.3 Regulating Stablecoins

We apply our model to analyze two types of regulations. The first type, which is of our focus, stipulates a minimum level of excess reserves (“capital requirement”). The rationale behind is to generate a sufficient risk buffer so that the platform is unlikely to debase the tokens. The second type of regulation (“stability regulation”) is more direct. It requires the platform to keep the token price stable (i.e., $\sigma_t^P = 0$). Our conclusion is that capital requirement, if carefully designed, can achieve Pareto improvement for the platform and its users. Stability regulation, in contrast, destroys the economic surplus from risk-sharing and reduces welfare for the platform and its users.

Capital Requirement. The regulator requires $C \geq C_L$ and forces the platform to liquidate if the requirement is violated. Therefore, C_L replaces zero as the lower (liquidation) bound of excess reserves.⁴³ In Figure 8, we plot the payout boundary \bar{C} (Panel A), which is a measure of voluntary over-collateralization, and the welfare measures for different values of C_L . Not so surprisingly, when the capital requirement tightens, the whole region of excess reserves is pushed to the right, resulting in a higher payout boundary \bar{C} in Panel A. Because reserves earn an interest rate r that is below the shareholders’ discount rate ρ , the platform shareholders’ value, V_0 , declines in C_L , as shown in

⁴³Because the stablecoins are over-collateralized so that coordination failure (or run) does not happen, unlike Carletti, Goldstein, and Leonello (2019), our model does not feature a need to introduce a separate liquidity requirement.

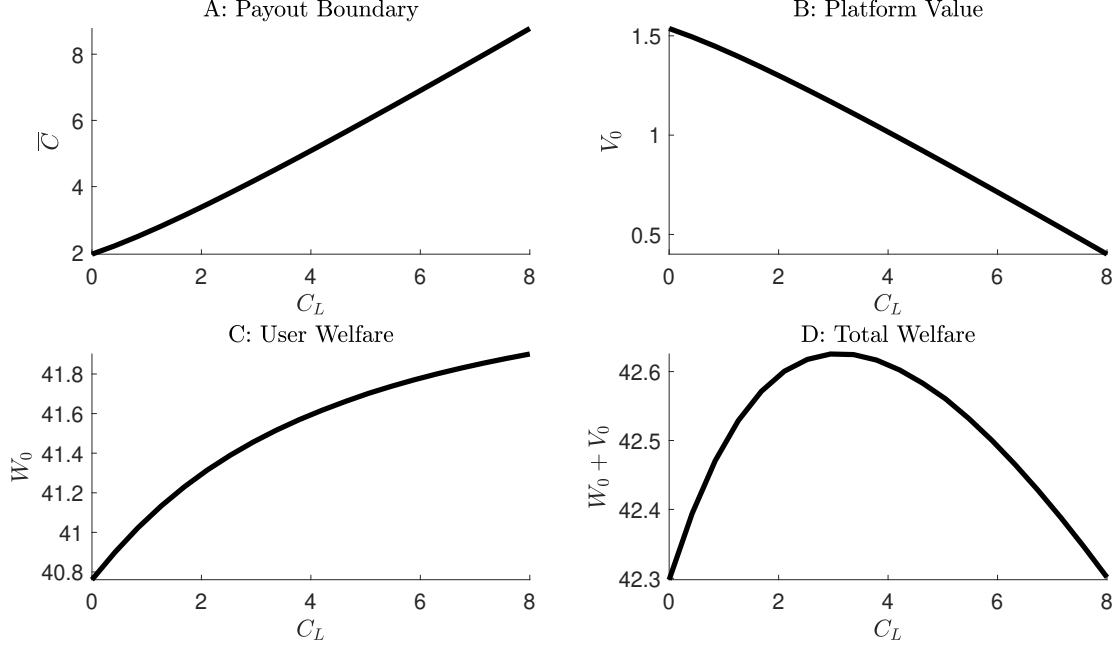


Figure 8: **Capital Requirement and Welfare.** We plot the numerical solutions of payout boundary \bar{C} (Panel A), the platform shareholders' value at $t = 0$, V_0 (Panel B), users' welfare at $t = 0$, W_0 (Panel C), and total welfare $W_0 + V_0$ (Panel D) over the regulatory minimum of excess reserves, C_L . The parameterization follows Figure 2.

Panel B. Panel C shows that users' welfare is improved by the capital requirement but there exists a significant degree of decreasing return as the regulator pushes up C_L . Appendix B.1 shows how we calculate user welfare, $W_0 = \mathbb{E} [\int_0^\infty e^{-rt} dR_{i,t}]$.

What is interesting is that, in Panel D of Figure 8, the total welfare is non-monotonic in C_L . When the regulator increases C_L from zero, the increase of users' welfare overwhelms the decrease of platform value, but as the capital requirement is tightened, the loss of platform value eventually dominates. This suggests the existence of an optimal level of C_L that maximizes the total welfare.

As long as the users' welfare increases faster than the platform value decreases, the regulator can administer a transfer from users to the platform, making the regulation Pareto-improving. For example, the regulator can allow the platform to charge users a membership fees, i.e., a fixed cost of access, and imposes a cap on such fees. This type of access fees is commonly seen in the literature on regulation of utility networks (Laffont and Tirole, 1994; Armstrong, Doyle, and Vickers, 1996).

In Figure 9, we further demonstrate the stabilization effects of capital requirement. In Panel A, we plot the ratio of $\bar{C} - \tilde{C}$ to $\bar{C} - C_L$ that measures the size of the stable subset of C where the platform maintains token redemption at par (i.e., $P(C) = 1$). As C_L increases, the stable region enlarges. In Panel B, we plot the probability of $C > \tilde{C}$ (i.e., $\sigma^P(C) = 0$) based on the stationary

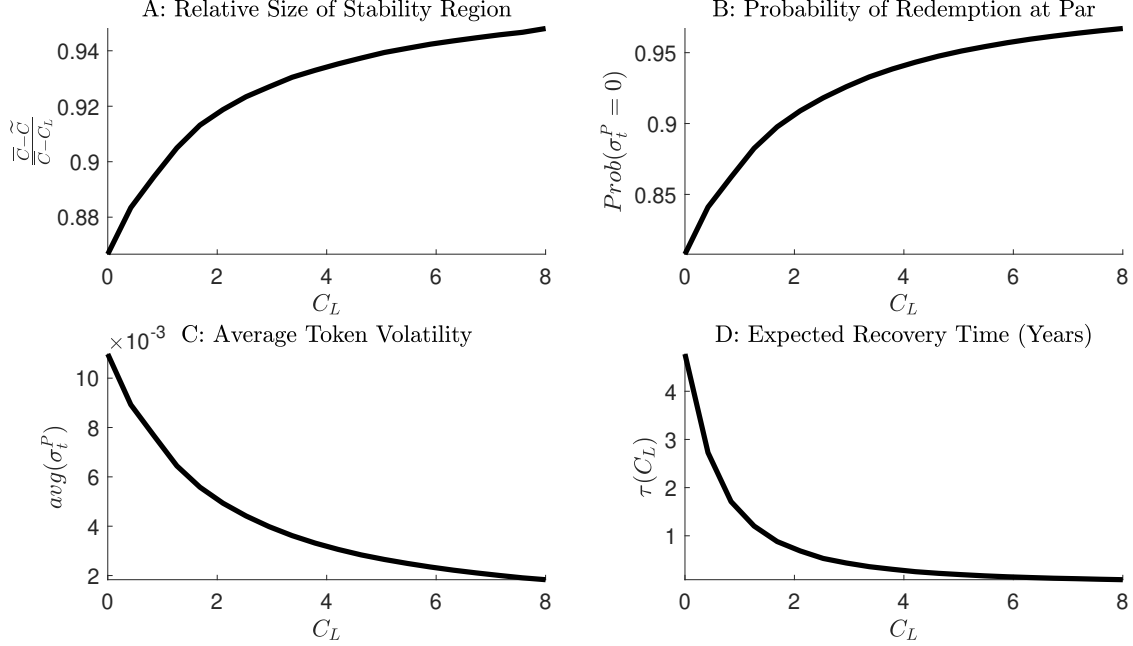


Figure 9: **Capital Requirement and Token Stability.** Using numeric solutions under different values of C_L , we plot the fraction of state space with redemption at par $\frac{\tilde{C}-C_L}{\tilde{C}-C_L}$ (Panel A), stationary probability of zero token volatility (Panel B), the long-run average (based on stationary probability density) of token volatility (Panel C), and the expected time to reach \tilde{C} from C_L (Panel D). The parameterization follows Figure 2.

distribution of C , which shows that over the long run the platform spends more time in the stable region when C_L increases. In Panel C, we plot the long-run average value of σ_t^P using the stationary probability distribution. A declining pattern emerges, indicating that capital requirement is indeed effective in reducing the token volatility. In Panel D, we plot the expected number of years it takes to reach \tilde{C} from C_L (denoted by $\tau(C_L)$ where Appendix B.2 demonstrates how to calculate $\tau(C_L)$). This recovery time decreases when the capital requirement is tightened. The intuition is that, as C_L increases, the platform near C_L still has abundant cash that self-accumulates over time by earning the interest rate r .

Stability Regulation. A key difference between stablecoins and bank deposits is that the issuers of stablecoins do not have any obligations to maintain redemption at par while a large portion of bank deposits offer redemption at par through the deposit insurance mechanism and various regulatory backstops. Should stablecoins be more like regulated deposits and be legally required to maintain a perfectly stable value? Our analysis below addresses this question.

In Panel A of Figure 10, we show that under the zero-volatility requirement (i.e., $\sigma_t^P = 0$), the platform maintains a higher level of excess reserves to reduce the likelihood of liquidation because

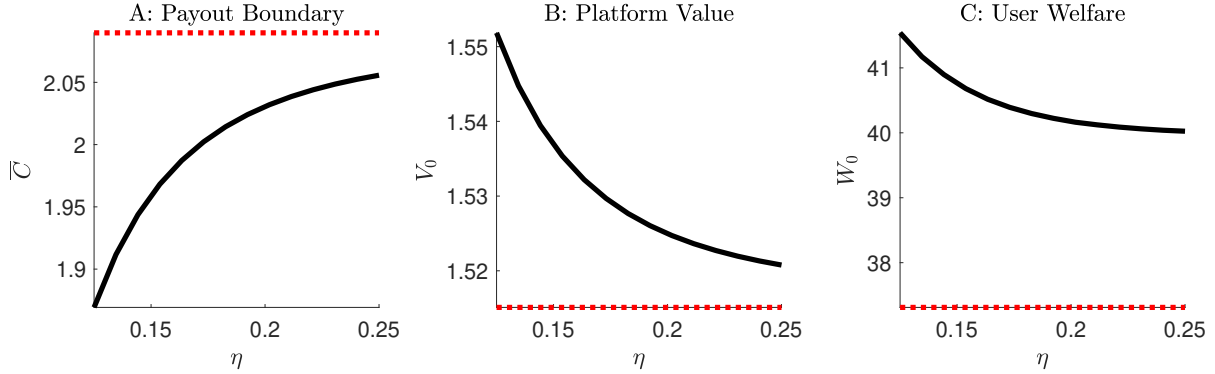


Figure 10: **Risk-Sharing, Stability Regulation, and Welfare.** Using the numerical solutions, we calculate the payout boundary \bar{C} (Panel A), the platform shareholders’ value at $t = 0$, V_0 (Panel B), users’ welfare at $t = 0$, W_0 (Panel C), and the long-run average fees based on stationary probability density (Panel D) over different values of users’ risk aversion η for both the baseline model (solid line) and the model under stability regulation (red dotted line). The parameterization follows Figure 2.

the option of off-loading risk to users is no longer available. Holding more reserves with an interest rate below the shareholders’ discount rate reduces the platform value (see Panel B of Figure 10).

An interesting finding is that imposing the stability regulation even decreases users’ welfare (Panel C of Figure 10) across all values of η . This seems to contradict the intuition that, by forcing the platform to maintain a perfectly stable token value, users will benefit, especially when they are more risk-averse. However, the argument ignores that, unable to off-load risk to users, the platform can compensate its risk exposure with higher fees. Stability regulation is counterproductive because it limits the risk-sharing between the platform and its users. When the platform is close to liquidation, its effective risk aversion can be higher than η , so there is economic surplus created from users’ absorbing risk from the platform. Stability regulation shuts down this insurance market. Our results on stability regulation also reveal the fact that a commitment to perfectly stable token does not improve welfare. In practice, stablecoin issuers cannot commit against debasement, but even when such commitment is available, doing so would not be optimal.

5 Crypto Shadow Banking with User Collateral

The double-collateralization structure in Panel B of Figure 1 behind many stablecoins (e.g., Dai issued by MakerDAO) fits into our analytical framework. By requiring users to post collateral, the platform gains an additional degree of freedom (margin requirement). When setting the margin requirement, the platform faces the trade-off between reducing risk exposure and user participation.

For each dollar of stablecoins, the platform requires a user to post m_t dollars worth of collat-

eral. In practice, many risky assets are eligible collateral, mainly cryptocurrencies such as Bitcoin and Ether, and thus are highly volatile. Let dZ_t denote a standard Brownian shock. Instead of interpreting it as a shock directly to reserves as in our baseline model, here we interpret the shock in the following way that is tied to the value of the user's collateral portfolio.

For simplicity, we do not model users' choice of collateral portfolio but rather assume that the collateral portfolio has a continuum of assets (indexed by a) and, from t to $t + dt$, a fraction, $2(\delta dt - \sigma dZ_t)$, of these assets incur a percentage loss, denoted by θ_a , which is drawn independently across assets a from a uniform distribution on $[0, 1]$.⁴⁴ At time t , the expected loss of the collateral portfolio is $\mathbb{E} \left[\frac{1}{2} \times 2(\delta dt - \sigma dZ_t) \right] = \delta dt$, where the expected loss per asset, $\frac{1}{2}$, is multiplied by the fraction of assets in losses. The collateral portfolio also generates an expected value appreciation, denoted by $\tilde{\mu}$. Therefore, for each dollar of stablecoins, a user posts m_t dollars worth of collateral, with an expected net return equal to $\tilde{\mu} - \delta - r$, where the last term represents the cost of giving up the outside option of return r by locking wealth in the collateral portfolio.⁴⁵

Under the collateral requirement, a representative user i 's problem of choosing the optimal dollar value of stablecoin holdings, $u_{i,t}$, given by (5) in the baseline model, is now described below

$$\max_{u_{i,t}} \left\{ \frac{1}{\beta} N_t^\alpha u_{i,t}^\beta A^{(1-\alpha-\beta)} dt + u_{i,t} (\mu_t^P - \eta |\sigma_t^P| - f_t) dt + u_{i,t} m_t (\tilde{\mu} - \delta - r) dt \right\}, \quad (36)$$

where the last term reflects the fact that the user's wealth is being locked in a risky collateral backing the stablecoins worth $u_{i,t}$. As in the baseline model, to solve the platform's optimal strategies, we first note that, given the token price dynamics (i.e., μ_t^P and σ_t^P), the platform can directly set N_t through the fees f_t . Under the collateral requirement, users' optimal choice of $u_{i,t}$ implies the following equation that connects N_t (i.e., the aggregated $u_{i,t}$) and f_t :

$$f_t = \left(\frac{A}{N_t} \right)^{1-\xi} - m_t (r + \delta - \tilde{\mu}) + \mu_t^P - \eta |\sigma_t^P|. \quad (37)$$

Clearly, when $m_t = 1$, $\delta = 0$, and $\tilde{\mu} = 0$ (i.e., the platform does not impose a haircut and the collateral does not have expected losses or gains), equation (37) reduces to (12), the corresponding

⁴⁴Klimenko, Pfeil, Rochet, and Nicolo (2016) show that $2(\delta dt - \sigma dZ_t)$ is the $\Delta \rightarrow 0$ limit of a random variable whose value is $2(\delta\Delta - \sigma\sqrt{\Delta})$ or $2(\delta\Delta + \sigma\sqrt{\Delta})$ with equal probabilities. Before taking the limit, the parameters, δ and σ , can be chosen so that the random fraction is well-defined within $[0, 1]$. The convergence is akin to that shown by Cox, Ross, and Rubinstein (1979) in their Binomial model of option pricing. In practice, the variation of a collateral asset (i.e., θ_a in our model) can be very large when the collateral is a cryptocurrency. What triggered the dramatic debasement of IRON was the almost 100% drop over two days of the collateral cryptocurrency, TITAN (Tiwari, 2021). The run on IRON in turn exacerbates the sell-off of TITAN.

⁴⁵This expression is analogous to the user's cost of capital (Jorgenson, 1963) with the additional $\tilde{\mu}$.

equation in the baseline model. Given f_t , a higher m_t leads to lower N_t according to (37), which reflects the fact that imposing a stricter collateral requirement leads to lower demand for stablecoins under the parameter restriction, $r + \delta - \tilde{\mu} > 0$ (i.e., it is costly for users to post collateral).

To derive the law of motion of the state variable C_t , the excess reserves, we first derive the platform's flow cost per dollar of stablecoins created:

$$\begin{aligned} & 2(\delta dt - \sigma dZ_t) \times \mathbb{P}(\{m_t(1 - \theta_a) < 1\}) \mathbb{E}[1 - m_t(1 - \theta_a) | m_t(1 - \theta_a) < 1] \\ &= 2(\delta dt - \sigma dZ_t) \times \left(\int_{1 - \frac{1}{m_t}}^1 (1 - m_t(1 - \theta_a)) d\theta_a \right) = \frac{1}{m_t} (\delta dt - \sigma dZ_t). \end{aligned} \quad (38)$$

In the first line, the fraction of users' collateral assets that incur losses is multiplied by the probability of a sufficiently large loss that leads to the violation of the margin requirement, and the last component is the platform's loss upon receiving and liquidating the collateral (with a remaining value of $m_t(1 - \theta_t)$) and repurchasing the one dollar worth of stablecoins out of circulation. Therefore, given N_t , the dollar value of all stablecoins issued, $-\frac{N_t}{m_t}(\delta dt - \sigma dZ_t)$ enters into the law of motion of reserves (8), replacing $N_t \sigma dZ_t$ (which is essentially the case where $m_t = 1$ and $\delta = 0$). This flow cost is essentially the consequence of the stablecoin issuer extending an guarantee of the stablecoins' value, which is a contingent liability akin to the guarantee that a bank extends to its off-balance-sheet conduits as discussed in Section 2.

Following the derivation in Section 4, we use (37) to substitute out f_t in the law of motion of reserves to obtain the law of motion of excess reserves, C_t :

$$dC_t = \left(rC_t - r(m_t - 1)N_t + m_t(\tilde{\mu} - \delta)N_t + N_t^\xi A^{1-\xi} - N_t \eta |\sigma_t^P| - \frac{N_t \delta}{m_t} \right) dt + N_t \left(\frac{\sigma}{m_t} - \sigma_t^P \right) dZ_t. \quad (39)$$

When $m_t = 1$, $\delta = 0$, and $\tilde{\mu} = 0$, equation (39) reduces to (16) in the baseline model. In Appendix B.4, we provide all omitted solution details and derive the HJB equation of the value function, $V(C_t)$ as well as the platform's optimal choices of fees (or equivalently, $N(C_t)$), token price dynamics (or equivalently, $\sigma^P(C_t)$), and the margin requirement $m(C_t)$. Figure 11 reports the numeric solutions.

In the model with user collateral, the shock to the platform's reserves, dZ_t , originates from the fluctuation of users' collateral value, and the platform's exposure is directly and inversely linked to the margin requirement, m_t , as shown in (39). Therefore, we expect the optimal margin requirement to be higher when the platform's excess reserves run down. This is shown in lower-left Panel of Figure 11. Introducing user collateral does not change the qualitative dynamics of the platform's

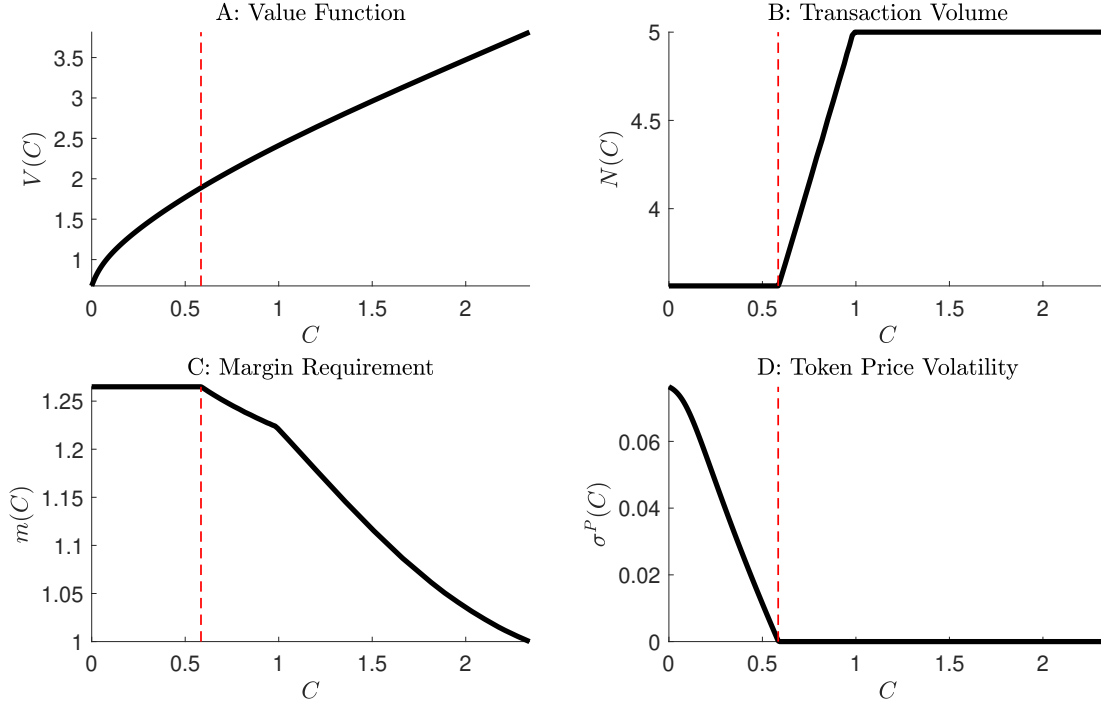


Figure 11: **Margin Requirement.** This figure plots the platform value function (Panel A), token demand or transaction volume (Panel B), optimal marginal requirement (Panel C), and token-price volatility (Panel D) as functions of excess reserves C . The parameterization follows Figure 2 with $\tilde{\mu} = 0.05$ and $\delta = 0.025$.

franchise value, $V(C)$, the transaction volume, $N(C)$, and the token price volatility, $\sigma^P(C)$.

Discussion: immediate liquidation of collateral. When users violate the margin requirement, the platform immediately liquidates users’ collateral and repurchase stablecoins out of circulation. A question naturally arises: instead of liquidating the collateral and repurchasing stablecoins right away, why not incorporate the collateral assets into the platform’s reserve portfolio? Doing so will create two types of stablecoins, one with the backing of both users’ collateral and reserves (users of these stablecoins have not yet violated the margin requirements) and the other only backed by the platform’s reserves (users of these stablecoins have violated the margin requirement). This is not done in practice, and analytically, it complicates the model by introducing a new stable variable, that is the fraction of stablecoins only backed by the platform’s reserves.

6 Stablecoins, Digital Platforms, and Big Data

The interest in stablecoins among practitioners and regulators skyrocketed after Facebook announced its stablecoin project Libra (recently renamed to Diem). Different from other stablecoin

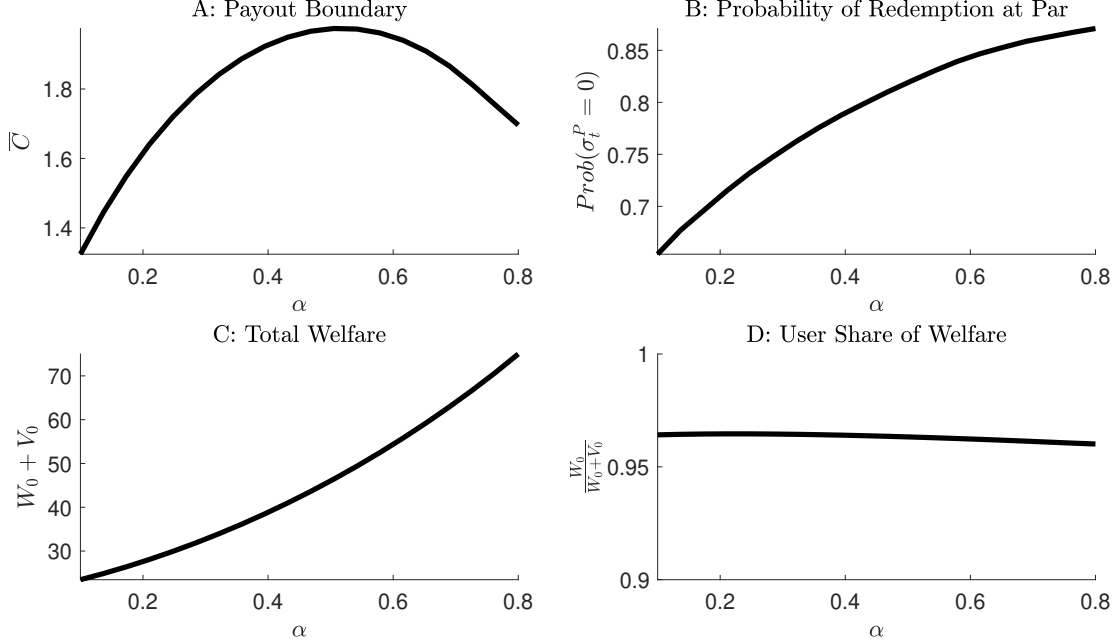


Figure 12: **Network Effects.** We plot the payout boundary (Panel A), the long-run probability of $C > \tilde{C}$ based on stationary distribution (Panel B), the sum of platform value and users’ welfare (Panel C), and users’ share of total welfare (Panel D) over different values of α (degree of network externality). The parameterization follows Figure 2.

issuers, Facebook has the unique advantage of strong network effects. Its comprehensive infrastructure covers social network, social media, and e-commerce (Facebook Shop). For individual users, the benefit of adopting Diem is enormous if other users on Facebook adopts Diem, because a great variety of activities can be enabled by a universal and global means of payment.

The stablecoin project of Facebook attracted enormous attention also because of the big data advantage of Facebook. Large platforms profit from user-generated data. A global payment system enabled by a stablecoin allows a platform to gather transaction data.

In this section, we analyze the role of network effects in stablecoin management and regulation. For simplicity, our analysis is based on the baseline model without users’ collateral. After analyzing the network effects, we extend the model to incorporate transaction data as a productive asset for the platform and explore how the incentive to accumulate transaction data affects a platform’s stablecoin strategies and the optimal regulations.

6.1 The Role of Network Effects

In our model, strong network effects are captured by a large value of α (see (2)). In Figure 12, we compare stablecoin platforms with different degrees of network effects. Panel A of Figure 12 plots

the payout boundary \bar{C} as a measure of voluntary over-collateralization over different values of α . On the one hand, stronger network effects make the platform more profitable, which stimulates more precautionary savings to protect the franchise value. On the other hand, stronger network effects imply a higher level of user activities near $C = 0$, i.e., \underline{N} in (25), which in turn implies a faster recovery out of the low- C region (through fee and token-issuance revenues) and thereby a weaker incentive to hold excess reserves. The two counteracting forces lead to the hump-shaped relationship between \bar{C} and α in Panel A of Figure 12.

In Panel B of Figure 12, we show the long-run probability of $C > \tilde{C}$ (based on stationary probability distribution of C) increases in α . Stronger network effects imply that, over the long run, the system spends more time in states with $P(C) = 1$. Under stronger network effects, recovery out of the low- C region is faster due to a higher level of user activities and the resultant faster replenishment of reserves via fees and token-issuance proceeds. Our paper sheds light on why stablecoins issued by Facebook and other technology giants with strong network infrastructure are regarded as more promising than those issued by start-up payment service providers. Stronger network effects lead to stabler tokens and a lower likelihood of token debasement.

Finally, we examine the impact of network effects on welfare. In Panel C of Figure 12, we show that total welfare of the platform and its users increases in the degree of network effects. This explains why it is particularly beneficial for technology giants with strong network infrastructure to introduce stablecoins as common means of payment among their customers. Network infrastructure is not limited to social network and e-commerce. Financial network is another example. JPMorgan Chase introduces JPM Coin to facilitate transactions among institutional clients.

Interestingly, as we gradually increase the degree of network effects in Panel D of Figure 12, the split of total welfare between the platform and its users is rather stable. Under stronger network effects, the monopolistic platform can extract more rents from its users through fees or off-loading risk in distress. However, precisely due to the network effects, individual users do not internalize the positive effect of their adoption on other users, so the platform has incentives to internalize the network externality by stimulating user activities through fee reductions (or subsidies) and token stability. These two counteracting forces imply that, as network effects become stronger, the platform's share of total surplus does not necessarily increase. This result alleviates the concern over technology giants abusing network effects in stablecoin projects.

Lastly, Figure 13 demonstrates how network effects, as captured by α , drive the optimal capital requirement. Panel A plots the capital requirement C_L^* that maximizes total welfare. Panel B plots

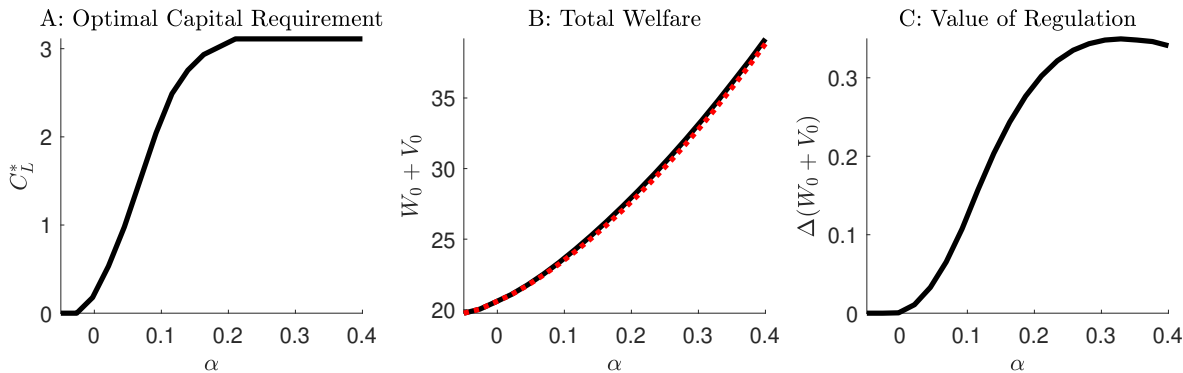


Figure 13: **Capital Requirement and Network Effects.** We calculate the optimal capital requirement C_L^* that maximizes total welfare (Panel A), total welfare both with capital requirement C_L^* (solid black line) and without capital requirement (dotted red line) (Panel B), and the welfare wedge between the optimally regulated equilibrium and the laissez-faire equilibrium (Panel C) over different values of α . Note that Panel C depicts the difference between the solid black line and the dotted red line from Panel B. The rest of parameterization follows Figure 2.

total welfare both with optimal capital requirements (solid line) and without capital requirements (dotted line). Panel C plots the welfare wedge between the optimally regulated equilibrium and laissez-faire equilibrium. Importantly, it is optimal to raise capital requirements as network effects strengthen. In fact, platforms with no network effects ($\alpha = 0$) do not benefit at all from the regulation. The key to this result is the positive externality of individual users' token holdings, which explains the deviation of laissez-faire equilibrium from social optimum. The platform internalizes such externality in its decision to preserve reserves and stabilize tokens, but the internalization is not perfect. As shown in Figure 12, the platform cannot seize the full surplus as its share of total welfare is rather stable in α and always below 100%. Therefore, as α increases, the total welfare increases together with the component that is not internalized by the platform. This calls for a tighter capital requirement that moves the overall level of reserves closer to social optimum.

6.2 Payment and Big Data

User-generated data is now a major asset of digital platforms. Social networks, such as Facebook and Twitter, utilize such data to target users for advertisement. Being able to utilize the enormous amount of transaction data has become a critical advantage of digital platforms relative to traditional payment service providers such as banks (Bank for International Settlements, 2019). Leading players, such as PayPal and Square, have become data centers and provide services beyond facilitating payments, for example, extending loans to consumers and businesses based on data-driven credit analysis. In this section, we follow Veldkamp (2005), Ordoñez (2013), Fajgelbaum, Schaal,

and [Taschereau-Dumouchel \(2017\)](#), [Parlour, Rajan, and Zhu \(2020\)](#), and [Jones and Tonetti \(2020\)](#) to model data as a by-product of user activities.⁴⁶ Our analysis focuses on how the impact of data on the optimal strategies of stablecoin issuers and the efficacy of regulations.

6.2.1 Big Data as a Productive Asset.

In the baseline model, the quality parameter A is constant. We now interpret A as a measure of effective data units that enhance platform productivity and assume the following law of motion:

$$dA_t = \kappa A_t^{1-\xi} N_t^\xi dt. \quad (40)$$

Users' transactions generate a flow of raw data, $\kappa N_t^\xi dt$, where the parameter κ captures the technological efficiency of data processing and storage. To what extent the raw data contributes to the effective data units depends on the current amount of effective data via $A_t^{1-\xi}$. The complementarity between the old and new data captures the fact that the value of new data increases in the quality of statistical algorithms, which in turn depends on the amount of existing data that are needed to train the algorithms.⁴⁷ The Cobb-Douglas form is chosen for analytical convenience.⁴⁸ To guarantee the convergence of the objective function, we impose the parametric restriction $\rho > \kappa \bar{n}^\xi$.

As platform productivity improves, we assume transaction capacity to increase accordingly, i.e., $\bar{N}_t = \bar{n}A_t$, where $\bar{n} > 0$ is constant. User optimization is static and follows the baseline model. As shown in (11), the dollar transaction volume (or token demand) $N_t \equiv n_t A_t$ where

$$n_t = \frac{1}{(r + f_t - \mu_t^P + \eta|\sigma_t^P|)^{\frac{1}{1-\xi}}} \wedge \bar{n}. \quad (41)$$

As in the baseline model, the platform sets n_t through the fees, f_t , and sets the dynamics of token redemption price through its choice of σ_t^P . The model now has three natural state variables, reserves M_t , token supply S_t , and data stock A_t . Similar to the baseline model, $C_t = M_t - S_t P_t$ and A_t summarize payoff-relevant information, driving the platform value, $V_t = V(C_t, A_t)$, and the dollar value of token, $P_t = P(C_t, A_t)$. To simplify the notations, we will suppress the time subscripts.

We conjecture that the system is homogeneous in A , and in particular, the platform's value function and dollar value of token are given by $V(C, A) = v(c)A$ and $P(C, A) = P(c)$, respectively,

⁴⁶[Veldkamp and Chung \(2019\)](#) provide an excellent survey of the literature of data and aggregate economy.

⁴⁷Related, in [Farboodi, Mihet, Philippon, and Veldkamp \(2019\)](#), data have increasing return to scale.

⁴⁸This data accumulation process is inspired by the specification of knowledge accumulation in [Weitzman \(1998\)](#).

where the excess reserves-to-data ratio is the key state variable for the platform's optimal strategies:

$$c \equiv \frac{C}{A}. \quad (42)$$

We will confirm the conjecture as we solve the platform's optimization problem in the following.

First, to derive the law of motion of c_t , we follow the derivation of the baseline model to obtain

$$dC_t = \left(rC_t + A_t n_t^\xi - \eta A_t n_t |\sigma_t^P| \right) dt + A_t n_t (\sigma - \sigma_t^P) dZ_t - dDiv_t. \quad (43)$$

Given (40) and (43), the law of motion of c_t reads

$$dc_t = \left(rc_t + n_t^\xi - \eta n_t |\sigma_t^P| - \kappa n_t^\xi c_t \right) dt + n_t (\sigma - \sigma_t^P) dZ_t - \frac{dDiv_t}{A_t}. \quad (44)$$

Under the value function conjecture, $V(C, A) = v(c)A$, and the laws of motion of A (40) and c (44), the HJB equation for $v(c)$ in the interior region (where $dDiv_t = 0$) is given by

$$\rho v(c) = \max_{n \in [0, \bar{n}], \sigma^P} \left\{ [v(c) - v'(c)c] \kappa n^\xi + v'(c) \left(rc + n^\xi - \eta n |\sigma^P| \right) + \frac{1}{2} v''(c) n^2 (\sigma - \sigma^P)^2 \right\}. \quad (45)$$

When the marginal value of reserves, $V_A(C, A) = v'(c)$, falls to one, the platform pays out dividends. We define the payout boundary as \bar{c} through $v'(\bar{c}) = 1$. The optimality of \bar{c} also implies $v''(\bar{c}) = 0$. Note that as in the baseline model, when C (or c) approaches zero, the platform can avoid liquidation by setting $\sigma^P(c) = \sigma$ to off-load risk to its users and gradually replenish reserves.⁴⁹ For simplicity, we do not consider recapitalization (equity issuance). In sum, the platform's excess reserves, C_t , move in $[0, \bar{c}A]$. As data grows, the platform accumulates more excess reserves.

Proposition 6 (Optimization under Data Growth). *The value function takes the form $v(c_t)A_t$, where $v(c_t)$ solves the HJB equation (45) subject to the conditions $v'(\bar{c}) = 1$, $v''(\bar{c}) = 0$, and $\lim_{c \rightarrow 0} \sigma^P(c) = \sigma$. The amount of excess reserves, C_t , stays below $\bar{c}A_t$ where the upper bound increases with A_t , the effective data units. At $C_t = \bar{c}A_t$, the platform pays dividends when $dC_t > 0$ so that dividend payments cause c_t to reflect at \bar{c} .⁵⁰*

The intuition behind Proposition 6 is that data growth provides another channel through which the continuation value appreciates, as shown on the right side of (45), which makes the platform

⁴⁹The boundary condition for $v(c)$ is that as c approaches zero, $-v''(c)$ approaches infinity (see footnote 37).

⁵⁰When $dC_t > 0$ at $C_t = \bar{c}A_t$, the dividend amount is equal to dC_t (i.e., exactly the amount needed to avoid $C_t > \bar{c}A_t$).

more patient in distributing excess reserves to shareholders. The first term on the right side contains the marginal value of data (which we call “data q”)

$$q(c) = \frac{\partial V(C, A)}{\partial A} = v(c) - v'(c)c. \quad (46)$$

Retaining more reserves allows the platform to sustain a wider region of c with credible token redemption at par. A more stable token in turn stimulates transactions and thereby allows the platform to accumulate more data and earn the data q, $q(c)$. Data as a productive asset and by-product of user activities enhances the platform’s incentive to accumulate reserves for tokens.

Next, we characterize the optimal transaction volume and token volatility. Following our analysis of the baseline model, we define the effective risk aversion based on $v(c)$:

$$\Gamma(c) = -\frac{v''(c)}{v'(c)}. \quad (47)$$

The following proposition summarizes the optimal choices of $n(c)$ and $\sigma^P(c)$.

Proposition 7 (Data q, Token Volatility, and Transaction Volume). *At c where the platform maintains the redemption of token at par, i.e., $\sigma^P(c) = 0$, the optimal transaction volume is*

$$N = n(c)A = \left[\frac{\xi}{\Gamma(c)\sigma^2} \left(1 + \frac{\kappa q(c)}{v'(c)} \right) \right]^{\frac{1}{2-\xi}} A \wedge \bar{n}A; \quad (48)$$

otherwise, the optimal token volatility is

$$\sigma^P(c) = \sigma - \frac{\eta}{\Gamma(c)n(c)} \in (0, \sigma), \quad (49)$$

and the optimal transaction volume is

$$N = n(c)A = \left[\frac{\xi}{\eta\sigma} \left(1 + \frac{\kappa q(c)}{v'(c)} \right) \right]^{\frac{1}{1-\xi}} A \wedge \bar{n}A. \quad (50)$$

The optimal transaction volume is proportional to A , the effective data units. Therefore, as data grows following (40), the transaction volume grows too. With data as a productive asset, the platform faces a new trade-off. It can accumulate more reserves through higher fee revenues or, by reducing fees, boost the transaction volume to accumulate more data. Therefore, the ratio of marginal value of data (the data q) and marginal value of reserves, $q(c)/v'(c)$, emerges in both

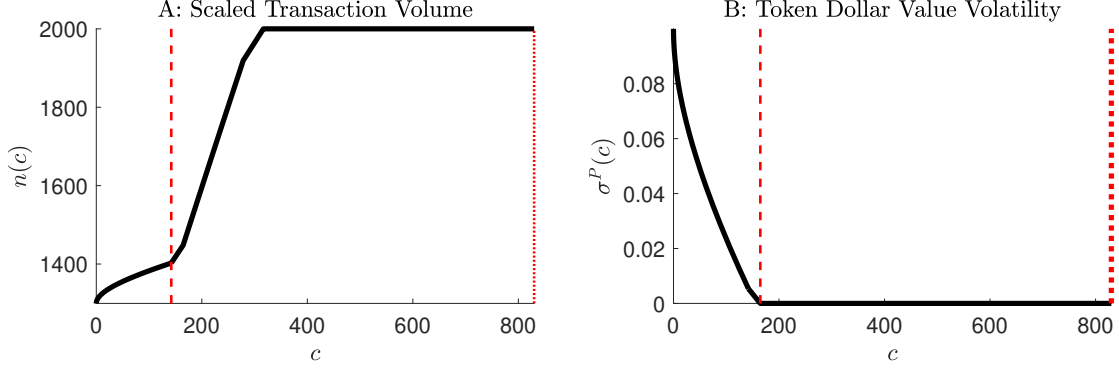


Figure 14: Transaction Volume and Token Volatility. This figure plots the A_t -scaled transaction volume $n(c)$ in Panel A and token return volatility $\sigma^P(c)$ in Panel B. In both panels, the red dotted lines mark the payout boundary \bar{c} , and the red dashed line marks \tilde{c} , the threshold that separates the regions of volatile and constant token prices. The parameterization follows Figure 2 with the additional parameters $\bar{n} = 2000$ and $\kappa = 0.00025$. Note that $\bar{n} = 2000$ implies that for $A_0 = 0.0025$, $\bar{N}_t = \bar{n}A_t = 5$ as under the parameterization in the baseline (see Figure 2).

(48) and (50). When the data q is high relative to the marginal value of reserves, the platform implements a high transaction volume through low fees. Note that given the token price dynamics, the monotonic relationship between transaction volume and fees is given by (41).

The optimal choice of token volatility resembles that of the baseline model. In the region where $\sigma^P(c) > 0$, it is the ratio of users' risk aversion to the platform's risk aversion that drives $\sigma^P(c)$. And in this region, the optimal transaction volume in (50), even scaled by A , is no longer the constant as in the baseline model but depends on $q(c)/v'(c)$ instead, showing the trade-off between investing in data and accumulating reserves. Moreover, the optimal transaction volume depends on users' risk aversion η as η determines the cost of obtaining insurance from users (losing transaction volume after off-loading risk to users). When the platform absorbs all risk (i.e., $\sigma^P(c) = 0$), the optimal transaction volume varies with its own risk aversion $\Gamma(c)$ (48) because $\Gamma(c)$ drives the required risk compensation through higher fees that causes the transaction volume to decline.

Panel A of Figure 14 reports the optimal transaction volume. In contrast to Panel A of Figure 4 where the transaction volume is constant in the region where $\sigma^P(c) > 0$, the A -scaled transaction volume now increases in c . The intuition is that as reserves become more abundant relative to data, the platform is more willing to lower fees, so it acquires more data through more active transactions at the expense of lower dollar revenues added to the reserve buffer. Panel B of Figure 14 shows a similar token volatility dynamics as Panel A of Figure 3 from the baseline model.

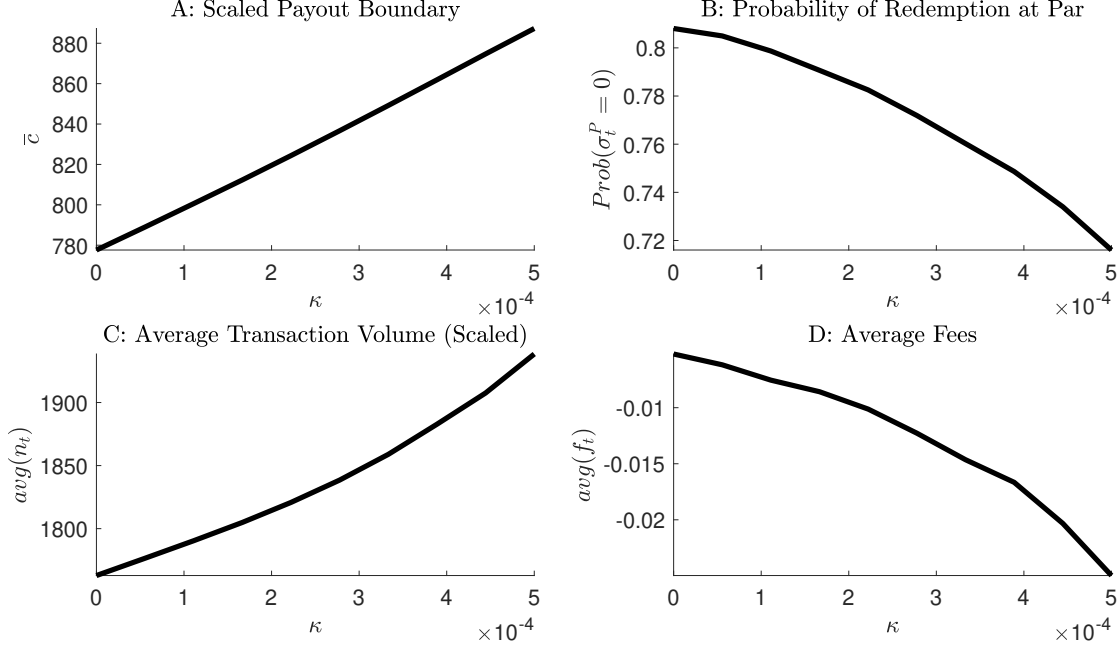


Figure 15: **Data Technology Progress and Platform Operation.** We plot the A -scaled payout boundary (Panel A), the probability of token redemption at par (Panel B), the average transaction volume (Panel C), and the average fees per dollar of transactions (Panel D) over κ (the efficiency of data technology). The moments in Panel B, C, and D are based on the stationary distribution of c . The parameterization follows Figure 2 with $\bar{n} = 2000$.

6.2.2 Data Technology Revolution and Stablecoin Platform Strategies

The last few decades have witnessed enormous progress in data science. In our model, such technological advance can be captured by an increase of the parameter κ . In Figure 15, we examine the impact of big data technology on the operation of stablecoin platforms. In Panel A, we show that in response to an increase in κ , the platform optimally raises the (A -scaled) payout boundary, \bar{c} , which suggests a greater degree of over-collateralization. The intuition of such response can be understood jointly with the platform’s decision on token volatility and fees.

To accumulate transaction data, the platform would like to increase the transaction volume. This can be achieved through lower fees. As shown in Panel C and D of Figure 15, the average fees (calculated from the stationary distribution of c) decline and the transaction volume increases in κ . The average fees per dollar of transaction even dips into the negative territory, becoming subsidies to users. This prediction is consistent with the practice that large digital platforms offer subsidies and fee services to retain and grow their customer base (Rochet and Tirole, 2006; Rysman, 2009).

However, a higher n implies a large exposure to operation risk as shown in (44). The platform responds by delaying payout, i.e., raising the boundary \bar{c} , to increase the reserve buffer, which

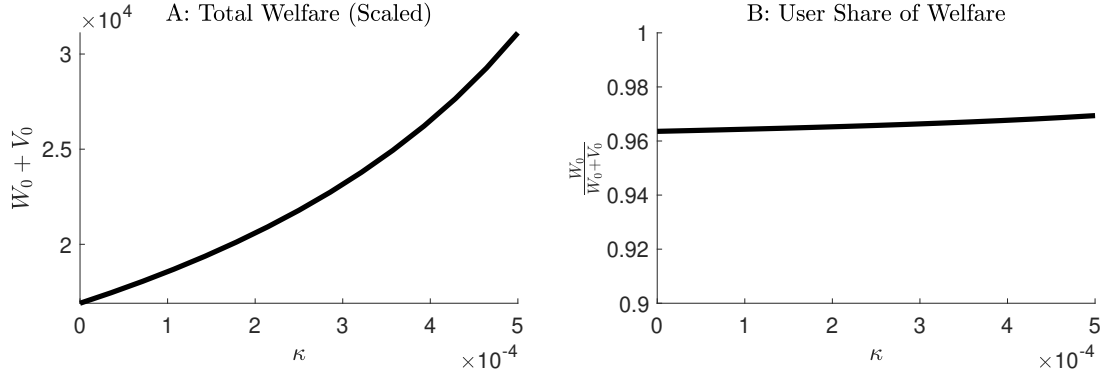


Figure 16: **Data Technology Progress and Welfare.** We plot the sum of platform value and users’ welfare (Panel A), and users’ share of total welfare (Panel B) against κ (the efficiency of data technology). The parameterization follows Figure 2 with $\bar{n} = 2000$ and all quantities are scaled by data units A .

explains why the payout boundary \bar{c} increases in κ in Panel A of Figure 15. The platform can also respond by off-loading more risk to users. As shown in Panel B, the stationary distribution of c implies a smaller probability of $\sigma^P(c) = 0$ and a higher average $\sigma^P(c)$ when κ increases. Therefore, a paradox exists — stablecoins built primarily for the acquisition and utilization of transaction data can become increasingly unstable precisely when data becomes more valuable.

In sum, when transaction data can be better utilized, the platform becomes more aggressive in raising transaction volume through fee reduction (or subsidy). Accordingly, the platform maintains more reserves to buffer the resultant increase in operation risk. Part of the increased risk is shared with users through token price fluctuations.⁵¹ In Figure 16, we show that the improving efficiency of data technology increases the total welfare (Panel A) while the platform’s share is rather stable and always below 100%. Therefore, even though the platform has monopolistic power as a unique marketplace where users transact with each other using tokens, the platform cannot possess the full economic surplus created by big data technology. Data originates from user activities, so to obtain data, the platform must share the economic surplus with users. These outcomes also suggest that regulations targeting and limiting the use of transaction data undermine the platform’s incentives to accumulate liquidity reserves and are detrimental for both user and total welfare.

6.2.3 Data Technology Revolution and Stablecoin Regulation

Because the transaction volume is proportional to A , equation (40) implies an exponential growth of effective data units that scales up the platform value and users’ welfare. The improving efficiency of

⁵¹Appendix B.1 demonstrates how to calculate (scaled) user welfare under this model specification.

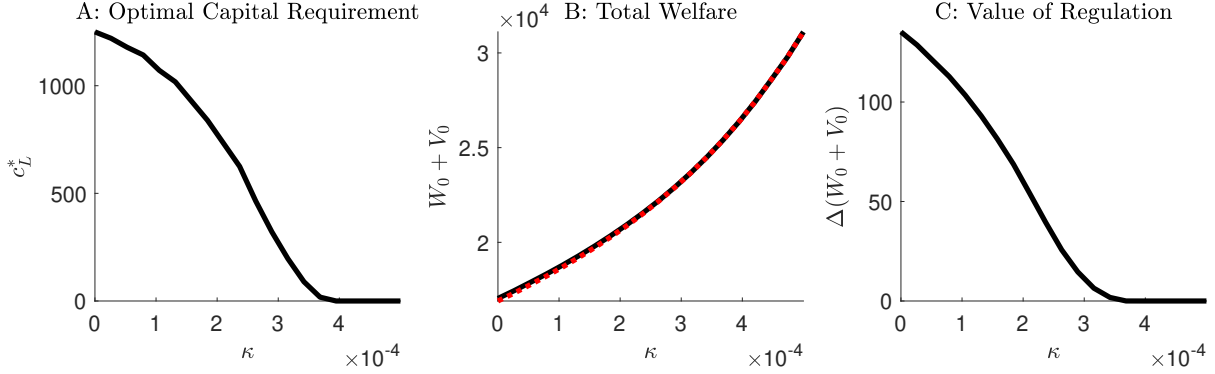


Figure 17: Data Technology Progress and Capital Requirements. We calculate the optimal scaled capital requirement $c_L^* \equiv C_L^*/A$ that maximizes total welfare (Panel A), scaled total welfare both with scaled capital requirement c_L^* (solid black line) and without capital requirement (dotted red line) (Panel B), and the welfare wedge between the optimally regulated equilibrium and laissez-faire equilibrium (Panel C) over different values of κ . Note that Panel C depicts the difference between the solid black line and the dotted red line from Panel B. The parameterization follows Figure 2 with $\bar{n} = 2000$ and all quantities are scaled by data units A .

data technology causes the exponential growth to be increasingly steeper. In such an environment, how should the optimal capital requirement adjust? In this subsection, we address this question.

As previously discussed, a larger transaction volume N amplifies the shock exposure of reserves, and to achieve a larger transaction volume, the platform has to lower fees, sacrificing the growth of dollar reserves. Therefore, there exists tension between precautionary management of reserves and data acquisition through users' transactions. Capital requirement favors preserving reserves over stimulating transaction volume for data acquisition. Therefore, as data becomes more productive (i.e., κ increases), capital requirement becomes more burdensome.

Panel A of Figure 17 confirms the intuition. The optimal requirement of excess reserves (scaled by A) declines in κ . We study the scaled capital requirement to preserve the homogeneity property of the system and keep the solution in one-dimensional space of $c = C/A$. Indeed, tightening capital requirement causes the platform to build up reserves at the expense of data acquisition. However, given the self-reinforcing growth of data in (40), such regulatory measure hurts the long-run exponential growth of both platform value and users' welfare. In Panel B of Figure 17, we compare the total welfare under *optimal* capital requirement with that from the laissez-faire equilibrium, and in Panel C we plot the wedge. The increase of welfare in κ is not surprising. What is interesting is that the benefit of capital requirement dwindles as κ increases in Panel C.

Moreover, as we show in Figure 15, data as a self-accumulating productive asset offers a new opportunity for shareholders' equity to grow over time. This effectively makes the platform more patient in paying out dividends. Therefore, the voluntary build-up of reserves is strengthened as

κ increases. As a result, capital requirement is less needed for the internalization of user-network effects. In sum, as data becomes more productive, the role of capital requirement weakens.

7 Conclusion

The first-generation cryptocurrencies, such as Bitcoin and Ethereum, were built to serve as transaction medium, but the price volatility compromises such functionality. As decentralized finance develops rapidly, various stablecoin initiatives arise to meet the demand for stable means of payment that are based on blockchains. Stablecoins are issued by private entities who promise to maintain price stability by holding collateral assets against which stablecoin holdings can be redeemed. However, as these issuers maximize their own payoffs rather than the total welfare, conflicts of interests between the issuers and stablecoin users naturally arise, making room for welfare-enhancing regulations. Moreover, well-established network companies (e.g., Facebook) plan to introduce their own stablecoins. Behind such initiatives, the incentives are even more complex, especially given the fact that operating a payment system allows the platform to gather and profit from transaction data.

In spite of the enormous attention from both regulators and practitioners, to this date, there has not been a unified framework to address these issues. In this paper, we fill this gap and develop a dynamic model of optimal stablecoin management. The equilibrium features two regimes. When the issuer's reserves are sufficiently high, the stablecoin price is fixed. When the reserves fall below a critical threshold, the stablecoin price comoves with the issuer's reserves, allowing the issuer to share risk with the stablecoin users and thus avoid costly liquidation. The distribution of states is bimodal. Above the debasement threshold, the issuer credibly sustains a fixed token price, which induces a strong token demand that allows the issuer to collect fee revenues and further grow reserve holdings. This virtuous cycle turns into a vicious cycle when negative shocks deplete the issuer's reserves below the debasement threshold. As the token price becomes volatile, the users' token demand declines, so the issuer's fee revenues and revenues from selling tokens in open market operations decline, which then slows down the rebuild of reserves, generating an instability trap. The vicious cycle can be broken by issuing equity (governance tokens) to replenish reserves. Equity issuance must be done with an simultaneous expansion of token supply to eliminate arbitrage.

Our model provides a framework to evaluate regulatory proposals. We show that capital requirement can potentially improve the total welfare, but imposing a legally binding commitment to perfect price stability destroys welfare. Our framework can also be applied to analyze the in-

centives behind the stablecoin initiatives led by the well-established platform companies. We show that strong network effects can indeed lead to stability of token value, which makes these platform companies natural issuers of stablecoins. Moreover, a stablecoin may be introduced to stimulate transactions and the transaction data can be used to improve the platform's profitability. However, an increase in the productivity of data destabilizes the stablecoin, as the platform becomes more eager to stimulate transactions, issuing more stablecoins per unit of reserves.

References

- Abadi, J. and M. K. Brunnermeier (2019). Blockchain economics. Working paper, Princeton University.
- Acharya, V. V., P. Schnabl, and G. Suarez (2013). Securitization without risk transfer. *Journal of Financial Economics* 107(3), 515–536.
- Armstrong, M., C. Doyle, and J. Vickers (1996). The access pricing problem: A synthesis. *The Journal of Industrial Economics* 44(2), 131–150.
- Arrow, K. J. (1965). *Aspects of the Theory of Risk Bearing*. Helsinki: Yrjo Jahnssoonin Saatio.
- Asquith, P. and D. W. Mullins (1986). Signalling with dividends, stock repurchases, and equity issues. *Financial Management* 15(3), 27–44.
- Bakos, Y. and H. Halaburda (2019). The role of cryptographic tokens and icos in fostering platform adoption. *Working Paper*.
- Balvers, R. J. and B. McDonald (2021). Designing a global digital currency. *Journal of International Money and Finance* 111, 102317.
- Bank for International Settlements (2019). Chapter 3. Big tech in finance: opportunities and risks. Technical report, Bank for International Settlements.
- Baumol, W. J. (1952). The transactions demand for cash: An inventory theoretic approach. *The Quarterly Journal of Economics* 66(4), 545–556.
- Bech, M. L. and R. Garratt (2017). Central bank cryptocurrencies. Bis quarterly review, Bank for International Settlements.
- Benetton, M. and G. Compiani (2020). Investors’ beliefs and asset prices: A structural model of cryptocurrency demand. working paper, University of Chicago and University of California at Berkeley.
- Benetton, M., G. Compiani, and A. Morse (2021). When cryptomining comes to town: High electricity-use spillovers to the local economy. working paper, University of Chicago and University of California at Berkeley.

- Biais, B., C. Bisiere, M. Bouvard, and C. Casamatta (2019). The blockchain folk theorem. *The Review of Financial Studies* 32(5), 1662–1715.
- Bianchi, J. and S. Bigio (2014). Banks, liquidity management and monetary policy. Working Paper Series 20490, National Bureau of Economic Research.
- Bolton, P., H. Chen, and N. Wang (2011). A unified theory of tobin’s q, corporate investment, financing, and risk management. *The Journal of Finance* 66(5), 1545–1578.
- Brainard, L. (2019, October). Digital currencies, stablecoins, and the evolving payments landscape. Speech by Governor Lael Brainard at The Future of Money in the Digital Age, Sponsored by the Peterson Institute for International Economics and Princeton University’s Bendheim Center for Finance, Washington, D.C.
- Brunnermeier, M. K., H. James, and J.-P. Landau (2019, September). The digitalization of money. Working Paper 26300, National Bureau of Economic Research.
- Brunnermeier, M. K. and Y. Sannikov (2014). A macroeconomic model with a financial sector. *American Economic Review* 104(2), 379–421.
- Budish, E. (2018, June). The economic limits of bitcoin and the blockchain. Working Paper 24717, National Bureau of Economic Research.
- Bullmann, D., J. Klemm, and A. Pinna (2019). In search for stability in crypto-assets: are stablecoins the solution? Occasional Paper Series 230, European Central Bank.
- Calle, G. and D. B. Zalles (2019). Will businesses ever use stablecoins? white paper, R3 Reports.
- Calvo, G. A. and C. M. Reinhart (2002). Fear of floating. *The Quarterly Journal of Economics* 117(2), 379–408.
- Carletti, E., I. Goldstein, and A. Leonello (2019). The interdependence of bank capital and liquidity. BAFFI CAREFIN Working Papers 19128, BAFFI CAREFIN, Centre for Applied Research on International Markets Banking Finance and Regulation, Università Bocconi, Milano, Italy.
- Catalini, C. and J. S. Gans (2018). Initial coin offerings and the value of crypto tokens. *Working Paper*.

- Chen, N., P. Glasserman, B. Nouri, and M. Pelger (2017). Contingent capital, tail risk, and debt-induced collapse. *The Review of Financial Studies* 30(11), 3921–3969.
- Chen, Q., I. Goldstein, and W. Jiang (2010). Payoff complementarities and financial fragility: Evidence from mutual fund outflows. *Journal of Financial Economics* 97(2), 239–262.
- Chiu, J. and T. V. Koepl (2017). The economics of cryptocurrencies—Bitcoin and beyond.
- Chod, J. and E. Lyandres (2019). A theory of ICOs: Diversification, agency, and information asymmetry. *Management Science* (forthcoming).
- Christiano, L. J., M. Eichenbaum, and C. L. Evans (2005). Nominal rigidities and the dynamic effects of a shock to monetary policy. *Journal of Political Economy* 113(1), 1–45.
- Cong, L. W. and Z. He (2019). Blockchain disruption and smart contracts. *The Review of Financial Studies* 32(5), 1754–1797.
- Cong, L. W., Z. He, and J. Li (2020, 04). Decentralized Mining in Centralized Pools. *The Review of Financial Studies* 34(3), 1191–1235.
- Cong, L. W., Y. Li, and N. Wang (2019). Token-based platform finance. Charles A. Dice Center Working Paper 2019-28, The Ohio State University Fisher College of Business.
- Cong, L. W., Y. Li, and N. Wang (2021). Tokenomics: Dynamic adoption and valuation. *The Review of Financial Studies* 34(3), 1105–1155.
- Cox, J. C., S. A. Ross, and M. Rubinstein (1979, September). Option pricing: A simplified approach. *Journal of Financial Economics* 7(3), 229–263.
- Dang, T. V., G. Gorton, B. Holmström, and G. Ordoñez (2014). Banks as secret keepers. Working Paper 20255, National Bureau of Economic Research.
- Danos, V., S. Marcassa, M. Oliva, and J. Prat (2021). Fundamental pricing of utility tokens. *Working Paper*.
- Davydiuk, T., D. Gupta, and S. Rosen (2019). De-crypto-ing signals in initial coin offerings: Evidence of rational token retention. Working paper, Carnegie Mellon University and Temple University.

- Décamps, J.-P., T. Mariotti, J.-C. Rochet, and S. Villeneuve (2011). Free cash flow, issuance costs, and stock prices. *The Journal of Finance* 66(5), 1501–1544.
- DeMarzo, P. M. and D. Duffie (1999). A liquidity-based model of security design. *Econometrica* 67(1), 65–99.
- Doepke, M. and M. Schneider (2017). Money as a unit of account. *Econometrica* 85(5), 1537–1574.
- Donaldson, J. R. and G. Piacentino (2020). Money runs. *Journal of Monetary Economics* forthcoming.
- Donaldson, J. R., G. Piacentino, and A. Thakor (2018). Warehouse banking. *Journal of Financial Economics* 129(2), 250 – 267.
- Duffie, D. (2019). Digital currencies and fast payment systems: Disruption is coming. working paper, Stanford University Graduate School of Business.
- Dumas, B. (1991). Super contact and related optimality conditions. *Journal of Economic Dynamics and Control* 15(4), 675 – 685.
- Easley, D., M. O’Hara, and S. Basu (2019). From mining to markets: The evolution of bitcoin transaction fees. *Journal of Financial Economics*.
- Ebrahimi, Z., B. Routledge, and A. Zetlin-Jones (2020). Getting blockchain incentives right. Working paper, Carnegie Mellon University Tepper School of Business.
- ECB Crypto-Assets Task Force (2019). Stablecoins: Implications for monetary policy, financial stability, market infrastructure and payments, and banking supervision in the euro area. Occasional Paper Series 247, European Central Bank.
- Eckbo, B. E., R. W. Masulis, and O. Norli (2007). Chapter 6 – security offerings. In B. E. Eckbo (Ed.), *Handbook of Corporate Finance: Empirical Corporate Finance*, Volume 1 of *Handbook of Finance Series*, pp. 233–373. Elsevier/North-Holland.
- Fajgelbaum, P. D., E. Schaal, and M. Taschereau-Dumouchel (2017, 05). Uncertainty Traps*. *The Quarterly Journal of Economics* 132(4), 1641–1692.
- Fanti, G., L. Kogan, and P. Viswanath (2019). Economics of proof-of-stake payment systems. Working paper.

- Farboodi, M., R. Mihet, T. Philippon, and L. Veldkamp (2019, January). Big data and firm dynamics. Working Paper 25515, National Bureau of Economic Research.
- Faure, S. and H. Gersbach (2017). Money creation and destruction. Working Paper 6565, CESifo.
- Feenstra, R. C. (1986). Functional equivalence between liquidity costs and the utility of money. *Journal of Monetary Economics* 17(2), 271 – 291.
- Freeman, S. and F. E. Kydland (2000, December). Monetary aggregates and output. *American Economic Review* 90(5), 1125–1135.
- G7 Working Group on Stablecoins (2019). Investigating the impact of global stablecoins. Technical report, Committee on Payments and Market Infrastructures, Bank for International Settlements.
- Galí, J. (2015). *Monetary Policy, Inflation, and the Business Cycle: An Introduction to the New Keynesian Framework and Its Applications Second edition*. Number 10495 in Economics Books. Princeton University Press.
- Gan, J. R., G. Tsoukalas, and S. Netessine (2021). Initial coin offerings, speculation, and asset tokenization. *Management Science* 67(2), 914–931.
- Garratt, R. and M. R. Van Oordt (2019). Entrepreneurial incentives and the role of initial coin offerings. working paper, University of California at Santa Barbara and Bank of Canada.
- Garratt, R. and N. Wallace (2018). Bitcoin 1, bitcoin 2,: An experiment in privately issued outside monies. *Economic Inquiry* 56(3), 1887–1897.
- Glaeser, E. L., B. Sacerdote, and J. A. Scheinkman (1996, 05). Crime and Social Interactions*. *The Quarterly Journal of Economics* 111(2), 507–548.
- Glasserman, P. and B. Nouri (2012). Contingent capital with a capital-ratio trigger. *Management Science* 58(10), 1816–1833.
- Goldstein, I., D. Gupta, and R. Sverchkov (2019). Initial coin offerings as a commitment to competition. Technical report, Carnegie Mellon University and University of Pennsylvania The Wharton School.
- Goldstein, I., E. Ozdenoren, and K. Yuan (2011, 01). Learning and Complementarities in Speculative Attacks. *The Review of Economic Studies* 78(1), 263–292.

- Goldstein, I. and A. Pauzner (2005). Demand–deposit contracts and the probability of bank runs. *The Journal of Finance* 60(3), 1293–1327.
- Gopinath, G., E. Boz, C. Casas, F. J. Díez, P.-O. Gourinchas, and M. Plagborg-Møller (2020, March). Dominant currency paradigm. *American Economic Review* 110(3), 677–719.
- Gorton, G. and G. Pennacchi (1990). Financial intermediaries and liquidity creation. *The Journal of Finance* 45(1), 49–71.
- Gorton, G. B. and J. Zhang (2021). Taming wildcat stablecoins. working paper, Federal Reserve Board and Yale University.
- Gryglewicz, S., S. Mayer, and E. Morellec (2020). Optimal financing with tokens. *Working Paper*.
- Halaburda, H. (2018, June). Blockchain revolution without the blockchain? *Commun. ACM* 61(7), 27–29.
- Hinzen, F. J., K. John, and F. Saleh (2019). Bitcoin’s fatal flaw: The limited adoption problem. *NYU Stern School of Business*.
- Hu, A. S., C. A. Parlour, and U. Rajan (2019). Cryptocurrencies: Stylized facts on a new investible instrument. *Financial Management* 48(4), 1049–1068.
- Huberman, G., J. D. Leshno, and C. C. Moallemi (2019). An economic analysis of the Bitcoin payment system.
- Hugonnier, J., S. Malamud, and E. Morellec (2015). Capital supply uncertainty, cash holdings, and investment. *The Review of Financial Studies* 28(2), 391–445.
- John, K., T. J. Rivera, and F. Saleh (2020). Economic implications of scaling blockchains: Why the consensus protocol matters. Working paper, New York University, McGill University, and Wake Forest University.
- Jones, C. I. and C. Tonetti (2020, September). Nonrivalry and the economics of data. *American Economic Review* 110(9), 2819–58.
- Jorgenson, D. W. (1963). Capital theory and investment behavior. *The American Economic Review* 53(2), 247–259.

- J.P. Morgan Global Research (2021, February). Digital transformation and the rise of fintech: blockchain, bitcoin, and digital finance 2021.
- Kacperczyk, M. and P. Schnabl (2013, 07). How Safe Are Money Market Funds?*. *The Quarterly Journal of Economics* 128(3), 1073–1122.
- Kim, T. W. and A. Zetlin-Jones (2019). The ethics of contentious hard forks in blockchain networks with fixed features. *Frontiers in Blockchain* 2, 9.
- Klimenko, N., S. Pfeil, J.-C. Rochet, and G. D. Nicolo (2016). Aggregate bank capital and credit dynamics. Swiss Finance Institute Research Paper Series 16-42.
- La Spada, G. (2018). Competition, reach for yield, and money market funds. *Journal of Financial Economics* 129(1), 87–110.
- Laffont, J.-J. and J. Tirole (1994). Access pricing and competition. *European Economic Review* 38(9), 1673 – 1710.
- Lee, I., S. Lochhead, J. Ritter, and Q. Zhao (1996). The costs of raising capital. *Journal of Financial Research* 19(1), 59–74.
- Lehar, A. and C. A. Parlour (2020). Miner collusion and the bitcoin protocol. Working paper, University of Calgary and University of California Berkeley.
- Lehar, A. and C. A. Parlour (2021). Decentralized exchanges. working paper, University of Calgary and University of California, Berkeley.
- Li, J. and W. Mann (2020). Digital tokens and platform building. *Working Paper*.
- Li, L., Y. Li, M. Macchiavelli, and X. Zhou (2021). Liquidity restrictions, runs, and central bank interventions: Evidence from money market funds. *Review of Financial Studies forthcoming*.
- Liu, Y., J. Sheng, and W. Wang (2020). Do cryptocurrencies have fundamental values? *Working paper*.
- Liu, Y. and A. Tsyvinski (2020, 09). Risks and Returns of Cryptocurrency. *The Review of Financial Studies* 34(6), 2689–2727.
- Liu, Y., A. Tsyvinski, and X. Wu (2019, May). Common risk factors in cryptocurrency. Working Paper 25882, National Bureau of Economic Research.

- Ljungqvist, L. and T. J. Sargent (2004). *Recursive Macroeconomic Theory, 2nd Edition*, Volume 1 of *MIT Press Books*. The MIT Press.
- Lucas, R. E. and J. P. Nicolini (2015). On the stability of money demand. *Journal of Monetary Economics* 73, 48 – 65.
- Lyons, R. K. and G. Viswanath-Natraj (2020, May). What keeps stablecoins stable? Working Paper 27136, National Bureau of Economic Research.
- Makarov, I. and A. Schoar (2020). Trading and arbitrage in cryptocurrency markets. *Journal of Financial Economics* 135(2), 293–319.
- Malamud, S. and F. Zucchi (2019). Liquidity, innovation, and endogenous growth. *Journal of Financial Economics* 132(2), 519–541.
- Massad, T. (2021, May). Can a cryptocurrency break the buck?
- Mayer, S. (2020). Token-based platforms and speculators. *Available at SSRN 3471977*.
- Moreira, A. and A. Savov (2017). The macroeconomics of shadow banking. *The Journal of Finance* 72(6), 2381–2432.
- Morris, S. and H. S. Shin (1998). Unique equilibrium in a model of self-fulfilling currency attacks. *The American Economic Review* 88(3), 587–597.
- Nagel, S. (2016, 07). The Liquidity Premium of Near-Money Assets. *The Quarterly Journal of Economics* 131(4), 1927–1971.
- Ordoñez, G. (2013). The asymmetric effects of financial frictions. *Journal of Political Economy* 121(5), 844–895.
- Pagnotta, E. and A. Buraschi (2018). An equilibrium valuation of Bitcoin and decentralized network assets. Working paper, Imperial College.
- Pagnotta, E. S. (2021, 01). Decentralizing Money: Bitcoin Prices and Blockchain Security. *The Review of Financial Studies*. hhaa149.
- Parlatore, C. (2016). Fragility in money market funds: Sponsor support and regulation. *Journal of Financial Economics* 121(3), 595–623.

- Parlour, C. A., U. Rajan, and J. Walden (2020). Payment system externalities and the role of central bank digital currency. *Journal of Finance* forthcoming.
- Parlour, C. A., U. Rajan, and H. Zhu (2020). When fintech competes for payment flows. Working paper, Massachusetts Institute of Technology, University of California (Berkeley), and University of Michigan.
- Penati, A. and G. Pennacchi (1989). Optimal portfolio choice and the collapse of a fixed-exchange rate regime. *Journal of International Economics* 27(1), 1–24.
- Pennacchi, G. (2010). A structural model of contingent bank capital. Working Papers (Old Series) 1004, Federal Reserve Bank of Cleveland.
- Pennacchi, G. (2012). Narrow banking. *Annual Review of Financial Economics* 4(1), 141–159.
- Pennacchi, G. and A. Tchisty (2018, 08). Contingent Convertibles with Stock Price Triggers: The Case of Perpetuities. *The Review of Financial Studies* 32(6), 2302–2340.
- Pennacchi, G. and A. Tchisty (2019). On equilibrium when contingent capital has a market trigger: A correction to sundaresan and wang journal of finance (2015). *The Journal of Finance* 74(3), 1559–1576.
- Philippon, T. (2015). Has the us finance industry become less efficient? on the theory and measurement of financial intermediation. *The American Economic Review* 105(4), 1408–1438.
- Piazzesi, M. and M. Schneider (2016). Payments, credit and asset prices. Working paper, Stanford University.
- Poterba, J. M. and J. J. Rotemberg (1986, 1986). Money in the utility function: An empirical implementation. Working Paper 1796, National Bureau of Economic Research.
- Prat, J. and B. Walter (2021). An equilibrium model of the market for bitcoin mining. *Journal of Political Economy* 129(8).
- Pratt, J. W. (1964). Risk aversion in the small and in the large. *Econometrica* 32(1/2), 122–136.
- Raskin, M. and D. Yermack (2016, May). Digital currencies, decentralized ledgers, and the future of central banking. Working Paper 22238, National Bureau of Economic Research.

- Rochet, J.-C. and J. Tirole (2003). Platform competition in two-sided markets. *Journal of the European Economic Association* 1(4), 990–1029.
- Rochet, J.-C. and J. Tirole (2006). Two-sided markets: A progress report. *The RAND Journal of Economics* 37(3), 645–667.
- Routledge, B. and A. Zetlin-Jones (2021). Currency stability using blockchain technology. *Journal of Economic Dynamics and Control*, 104155.
- Rysman, M. (2009). The economics of two-sided markets. *The Journal of Economic Perspectives* 23(3), 125–143.
- Saleh, F. (2020, 07). Blockchain without Waste: Proof-of-Stake. *The Review of Financial Studies* 34(3), 1156–1190.
- Schilling, L. and H. Uhlig (2019). Some simple bitcoin economics. *Journal of Monetary Economics* 106, 16–26. SPECIAL CONFERENCE ISSUE: “Money Creation and Currency Competition” October 19-20, 2018 Sponsored by the Study Center Gerzensee and Swiss National Bank.
- Schmidt, L., A. Timmermann, and R. Wermers (2016, September). Runs on money market mutual funds. *American Economic Review* 106(9), 2625–57.
- Shafir, E., P. Diamond, and A. Tversky (1997, 05). Money Illusion. *The Quarterly Journal of Economics* 112(2), 341–374.
- Shams, A. (2020). The structure of cryptocurrency returns. Charles A. Dice Center Working Paper 2020-11, The Ohio State University Fisher College of Business.
- Sockin, M. and W. Xiong (2018). A model of cryptocurrencies. Working paper, Princeton University and University of Texas at Austin.
- Stulz, R. M. (2019). Fintech, bigtech, and the future of banks. *Journal of Applied Corporate Finance* 31(4), 86–97.
- Tinn, K. (2017). Smart contracts and external financing. working paper, McGill University.
- Tobin, J. (1956). The interest-elasticity of transactions demand for cash. *The Review of Economics and Statistics* 38(3), 241–247.

- Tobin, J. (1963). Commercial banks as creators of “money”. Cowles Foundation Discussion Papers 159, Cowles Foundation for Research in Economics, Yale University.
- Veldkamp, L. and C. Chung (2019). Data and the aggregate economy. Working paper, Columbia University.
- Veldkamp, L. L. (2005). Slow boom, sudden crash. *Journal of Economic Theory* 124(2), 230 – 257. Learning and Bounded Rationality.
- Walsh, C. E. (2003). *Monetary Theory and Policy, 2nd Edition* (2 ed.). The MIT Press.
- Weitzman, M. L. (1998, 05). Recombinant Growth. *The Quarterly Journal of Economics* 113(2), 331–360.

A Proofs

A.1 Proof of Propositions 1 and 2

The proof of Propositions 1 and 2 is split in three parts. Part I derives the HJB equation and its boundary conditions. Part II establishes the concavity of the value function. Part III shows that there is no liquidation.

Part I — HJB equation and dividend payouts

Recall that the platform chooses dividends $\{dDiv_t\}$, transaction volume $\{N_t\}$ (or equivalently transaction fees $\{f_t\}$), and token price volatility $\{\sigma_t^P\}$ (which implicitly pins down token price and the choice of token supply via the market clearing condition $N_t = S_t P_t$) to maximize the future expected discounted value of dividends. By the dynamic programming principle, the platform solves (17) subject to $dDiv_t \geq 0$ and the law of motion (16). As such, platform value $V(C) = V(C_t)$ satisfies the following HJB equation (in differential form):

$$\rho V(C)dt = \max_{N \in [0, \bar{N}], \sigma^P, dDiv \geq 0} \{dDiv + \mathbb{E}[dV(C)]\}.$$

Using Ito's Lemma and expanding the right-hand-side, we obtain

$$\rho V(C)dt = \max_{\{N \in [0, \bar{N}], \sigma^P, dDiv \geq 0\}} \left\{ (1 - V'(C))dDiv + V'(C) \left(rC + N^\xi A^{1-\xi} - \eta N |\sigma_t^P| \right) dt \right. \quad (\text{A.1})$$

$$\left. + \frac{1}{2} V''(C) N^2 (\sigma - \sigma^P)^2 dt \right\}. \quad (\text{A.2})$$

It follows that dividend payouts are optimal if and only if $V'(C) \geq 1$. As in Bolton et al. (2011), the optimal dividend policy therefore follows a barrier strategy, so that (in optimum) dividend payouts $dDiv$ cause C_t to reflect at \bar{C} , i.e., $dDiv_t = \max\{C_t - \bar{C}, 0\}$. And, the threshold \bar{C} satisfies smooth pasting and super contact conditions (for details, see, e.g., Dumas (1991)), i.e.,

$$V'(\bar{C}) - 1 = V''(\bar{C}) = 0.$$

Given this dividend policy, the HJB equation (A.1) simplifies to (22) whenever $C_t \leq \bar{C}$, as stated in Proposition 2. In addition, the optimal dividend policy also implies $C_t \leq \bar{C}$ for all $t \geq 0$.

Part II — Value function concavity

We prove the concavity of value function in Proposition 1. Recall the HJB equation (22), that is,

$$\rho V(C) = \max_{\{N \in [0, \bar{N}], \sigma^P\}} \left\{ V'(C) \left(rC + N^\xi A^{1-\xi} - \eta N |\sigma^P| \right) + \frac{1}{2} V''(C) N^2 (\sigma - \sigma^P)^2 \right\}.$$

Using the envelope theorem, we differentiate both sides of the HJB equation (evaluated under the optimal controls N and σ^P) with respect to C to obtain

$$\rho V'(C) = rV'(C) + V''(C) \left(rC + N^\xi A^{1-\xi} - \eta N |\sigma_t^P| \right) + \frac{1}{2} V'''(C) N^2 (\sigma - \sigma^P)^2.$$

We can solve for

$$V'''(C) = \frac{2}{N^2 (\sigma - \sigma^P)^2} \left[(\rho - r) V'(C) - V''(C) \left(rC + N^\xi A^{1-\xi} - \eta N |\sigma^P| \right) \right]$$

Using the smooth pasting condition, $V'(\bar{C}) = 1$, and the super-contact condition, $V''(\bar{C}) = 0$, we obtain $V'''(\bar{C}) > 0$. As $V''(\bar{C}) = 0$, it follows that $V''(C) < 0$ in a left-neighbourhood of \bar{C} , in that there exists $\varepsilon > 0$ so that $V''(C) < 0$ for $C \in (\bar{C} - \varepsilon, \bar{C})$.

We show now that $V''(C) < 0$ for all $C \in [0, \bar{C})$. Suppose to the contrary that there exists $\hat{C} < \bar{C}$ with $V''(\hat{C}) \geq 0$ and set without loss of generality

$$\hat{C} = \sup\{C \in (0, \bar{C} - \varepsilon) : V''(C) \geq 0\}. \quad (\text{A.3})$$

As $V''(C) < 0$ on the interval $(\bar{C} - \varepsilon, \bar{C})$ and the value function is twice continuously differentiable, it follows that $V''(\hat{C}) = 0$ and therefore the optimization in the HJB equation (22) implies $\sigma^P(\hat{C}) < \sigma$. In addition, $V'(\hat{C}) \geq 1$, so that $V'''(\hat{C}) > 0$. Thus, there exists $C' > \hat{C}$ with $V''(C') \geq 0$, a contradiction. Therefore, the value function is strictly concave on $[0, \bar{C})$.

Part III — There is no liquidation

Consider that C_t approaches zero, i.e., $C_t \rightarrow 0$. If the volatility of dC_t , $\sigma_C(C_t) = N_t(\sigma - \sigma^P(C_t))$ does not tend to zero as C_t approaches zero, C_t drops below zero and the platform is liquidated with probability one in which case the platform owners' value becomes zero. To prevent liquidation as C_t approaches zero, it must be that i) the volatility of dC_t , $\sigma_C(C_t) = N_t(\sigma - \sigma_t^P)$, tends to zero and ii) the drift of dC_t , $\mu_C(C_t) = rC_t + N_t^\xi A^{1-\xi} - N_t \eta |\sigma_t^P|$, remains positive positive. Formally,

$$\lim_{C \rightarrow 0^+} \mu_C(C) > 0 = \lim_{C \rightarrow 0^+} \sigma_C(C), \quad (\text{A.4})$$

must hold.

Thus, if the platform prevents liquidation, then — by the law of motion (16) — it must be $\lim_{C \rightarrow 0^+} \sigma^P(C) = \sigma$. As $V(C)$ is concave with $V'(\bar{C}) = 1$, it follows that $V'(C) > 0$ for all $C \in [0, \bar{C}]$. As such, when $\sigma^P(C) \rightarrow \sigma$, then

$$V(C) \rightarrow \frac{1}{\rho} V'(C) \mu_C(C).$$

Therefore, when $\lim_{C \rightarrow 0^+} \sigma^P(C) \rightarrow 0$, the equivalence

$$\lim_{C \rightarrow 0^+} V(C) > 0 \iff \lim_{C \rightarrow 0^+} \mu_C(C) > 0$$

holds.

Next, using the HJB equation (22), we obtain

$$\begin{aligned} V(C) &\geq \frac{V'(C)}{\rho} \left(rC + \max_{\{N \in [0, \bar{N}]\}} \{N^\xi A^{1-\xi} - \eta N \sigma\} \right) \\ &\geq \frac{1}{\rho} \left(\max_{\{N \in [0, \bar{N}]\}} \{N^\xi A^{1-\xi} - \eta N \sigma\} \right) > 0. \end{aligned}$$

The first inequality uses that setting $\sigma^P = \sigma$ is always possible (but not necessarily optimal) and the second inequality uses $C \geq 0$ and $V'(C) \geq 1$. As such, the platform obtains strictly positive value from continuation, implying that liquidation is not optimal and the platform optimally prevents liquidation. Thus, liquidation never occurs, and (A.4) holds.

A.2 Proof of Proposition 3

The proof of Proposition 3 is split in three parts. Part I characterizes the optimal controls $N(C)$ and $\sigma^P(C)$. Part II shows that platform risk-aversion $\gamma(C)$ decreases with C . Part III demonstrates that there exists \tilde{C} so that for $C < \tilde{C}$ ($C \geq \tilde{C}$), $\sigma^P(C) > 0$ ($\sigma^P(C) = 0$).

Part I — Optimal control variables

We characterize the optimization in (22) and solve for the optimal control variables $N = N(C)$ and $\sigma^P = \sigma^P(C)$ in Proposition 3. To start with, we define

$$\underline{N} = \arg \max_{N \leq \bar{N}} \{N^\xi A^{1-\xi} - \eta N \sigma\}, \quad (\text{A.5})$$

which yields

$$\underline{N} = \min \left\{ \left(\frac{\xi A^{1-\xi}}{\eta \sigma} \right)^{\frac{1}{1-\xi}}, \bar{N} \right\}.$$

Now, we first optimize the HJB equation (22) over σ^P or equivalently over $N \sigma^P$.

If interior (i.e., $\sigma^P > 0$), the choice of σ^P satisfies the first order optimality condition

$$\frac{\partial V(C)}{\partial \sigma^P} = 0 \iff -\eta V'(C) - V''(C)(N \sigma - N \sigma^P) = 0.$$

We can rearrange the above first order condition to derive

$$N \sigma^P = \frac{-\eta V'(C) - N \sigma V''(C)}{-V''(C)}. \quad (\text{A.6})$$

It is clear from the maximization in the HJB equation (22) that setting $\sigma^P < 0$ is never optimal. As such, to obtain the optimal choice of σ^P we truncate the expression in (A.6) from below by zero and obtain

$$N\sigma^P = \max \left\{ 0, \frac{-\eta V'(C) - N\sigma V''(C)}{-V''(C)} \right\} = \max \left\{ 0, -\frac{\eta V'(C)}{-V''(C)} + N\sigma \right\}. \quad (\text{A.7})$$

Note that by (11), users' aggregate token holdings are always positive (i.e., $N_t > 0$ at all times $t \geq 0$) so that $\sigma^P > 0 \iff N\sigma^P > 0$ and $\sigma^P = 0 \iff N\sigma^P = 0$. We distinguish between two different cases: 1) $\sigma^P = 0$ and 2) $\sigma^P > 0$.

1. First, consider $\sigma^P > 0$. Then, we can insert the relation (A.6) (or (A.7) noting that $N\sigma^P > 0$) into (22) to get

$$\rho V(C) = \max_{N \in [0, \bar{N}]} \left\{ V'(C) \left[rC + N^\xi A^{1-\xi} - \eta N\sigma - \frac{\eta^2 V'(C)}{V''(C)} \right] + \frac{1}{V''(C)} \left[\frac{(\eta V'(C))^2}{2} \right] \right\}.$$

Thus, by (A.5), $N = \underline{N} > 0$ is the optimal choice of N , so that by means of (A.7):

$$\sigma^P = \max \left\{ 0, -\frac{\eta V'(C)}{-V''(C)\underline{N}} + \sigma \right\} = \max \left\{ 0, \sigma - \frac{\eta}{\gamma(C)\underline{N}} \right\}, \quad (\text{A.8})$$

where the last equality uses the definition $\gamma(C) = -\frac{V''(C)}{V'(C)}$.

2. Second, consider $\sigma^P = 0$. Inserting $\sigma^P = 0$ into (22), the HJB equation becomes

$$\rho V(C) = \max_{N \in [0, \bar{N}]} \left\{ V'(C)[rC + N^\xi A^{1-\xi}] + V''(C) \left[\frac{N^2 \sigma^2}{2} \right] \right\}. \quad (\text{A.9})$$

If interior (i.e., $N(C) < \bar{N}$), the optimal choice of $N = N(C)$ must solve the first order condition

$$V'(C)\xi N^{\xi-1} A^{1-\xi} + V''(C)N\sigma^2 = 0 \iff V'(C)\xi N^{\xi-2} A^{1-\xi} + V''(C)\sigma^2 = 0.$$

Thus, optimal $N = N(C)$ reads

$$N(C) = \min \left\{ \left(\frac{A^{1-\xi} \xi V'(C)}{-V''(C)\sigma^2} \right)^{\frac{1}{2-\xi}}, \bar{N} \right\}, \quad (\text{A.10})$$

where we truncate above by \bar{N} .

Overall, note that $\sigma^P(C)$ (partially) decreases with $\gamma(C)$, the platform's risk-aversion, in that $\frac{\partial \sigma^P(C)}{\partial \gamma(C)} \leq 0$. When $\sigma^P(C) > 0$, this follows from (A.8), and, when $\sigma^P = 0$, this trivially holds.

Part II — Effective risk-aversion

We prove $\gamma'(C) < 0$, i.e., $\frac{d(-V''(C)/V'(C))}{dC} < 0$, in Proposition 3. To do so, we consider the following two cases, 1) $\sigma^P = 0$ and 2) $\sigma^P = 0$:

1. Consider $\sigma^P > 0$ so that $N = \underline{N}$. Then, the HJB equation (22) can be simplified to

$$\rho \frac{V(C)}{V'(C)} = rC + \underline{N}^\xi A^{1-\xi} - \eta \underline{N} \sigma - \frac{\eta^2}{2} \frac{V'(C)}{V''(C)}. \quad (\text{A.11})$$

Differentiating the equation above with respect to C , we obtain

$$\rho \left(1 - \frac{V''(C)V(C)}{V'(C)^2} \right) = r - \frac{\eta^2}{2} \frac{d(V'(C)/V''(C))}{dC},$$

which can be rewritten as

$$\frac{d(V'(C)/V''(C))}{dC} = \frac{2}{\eta^2} \left[(r - \rho) + \rho \left(\frac{V''(C)V(C)}{V'(C)^2} \right) \right].$$

Note that because $\rho > r$ and $V''(C) < 0$, it follows that implies $\frac{d(V'(C)/V''(C))}{dC} < 0$, i.e., $\frac{d(-V''(C)/V'(C))}{dC} = \gamma'(C) < 0$.

2. Consider $\sigma^P = 0$, so the HJB (22) simplifies to

$$\rho V(C) = \max_{N \in [0, \bar{N}]} \left\{ V'(C)[rC + N^\xi A^{1-\xi}] + V''(C) \left[\frac{N^2 \sigma^2}{2} \right] \right\}, \quad (\text{A.12})$$

In this case, we further consider two cases, a) $N = N(C) < \bar{N}$ and b) $N = N(C) = \bar{N}$:

- a) $N(C) < \bar{N}$ and $N = \left(\frac{A^{1-\xi} \xi V'(C)}{-V''(C) \sigma^2} \right)^{\frac{1}{2-\xi}}$. In this case, the HJB can be simplified to

$$\rho \frac{V(C)}{V'(C)} = rC + \frac{1}{2} \left(\frac{\xi A^{1-\xi}}{\sigma^\xi} \right)^{\frac{2}{2-\xi}} \left(\frac{2-\xi}{\xi} \right) \left(\frac{V'(C)}{-V''(C)} \right)^{\frac{\xi}{2-\xi}}. \quad (\text{A.13})$$

Differentiating the equation above with respect to C , we obtain

$$\rho \left(1 - \frac{V''(C)V(C)}{V'(C)^2} \right) = r - \frac{1}{2} \left(\frac{\xi A^{1-\xi}}{\sigma^\xi} \right)^{\frac{2}{2-\xi}} \left(\frac{V'(C)}{-V''(C)} \right)^{\frac{2\xi-2}{2-\xi}} \frac{d(-V'(C)/V''(C))}{dC}, \quad (\text{A.14})$$

implying $\frac{d(V'(C)/V''(C))}{dC} < 0$ (because $V''(C) < 0$ and $\rho > r$), that is, $\frac{d(-V''(C)/V'(C))}{dC} = \gamma'(C) < 0$.

- b) $N(C) = \bar{N}$. In this case, the HJB can be simplified to

$$\rho \frac{V(C)}{V'(C)} = rC + \bar{N}^\xi A^{1-\xi} + \frac{\bar{N}^2 \sigma^2}{2} \frac{V''(C)}{V'(C)}. \quad (\text{A.15})$$

Differentiating the equation above with respect to C , we obtain

$$\rho \left(1 - \frac{V''(C)V(C)}{V'(C)^2} \right) = r - \frac{\bar{N}^2 \sigma^2}{2} \frac{d(-V''(C)/V'(C))}{dC}, \quad (\text{A.16})$$

which implies $\frac{d(-V''(C)/V'(C))}{dC} = \gamma'(C) < 0$ (because $V''(C) < 0$ and $\rho > r$).

Part III — Existence of threshold \tilde{C}

In Part I, we have shown that $\sigma^P(C)$ increases with $\gamma(C)$ and, in Part II, we have shown that $\gamma(C)$ decreases with C with $\gamma(\bar{C}) = 0$. Therefore, $\sigma^P(C)$ decreases with C . As $\gamma(\bar{C}) = 0$, it must be that $\sigma^P(C) = 0$ in a left-neighbourhood of \bar{C} . Because there is no liquidation, it holds that $\lim_{C \rightarrow 0^+} \sigma^P(C) = \sigma$ and thus — by continuity — $\sigma^P(C) > 0$ in a right-neighbourhood of $C = 0$. As $\sigma^P(C)$ is continuous and decreases with C on $[0, \bar{C}]$, there exists unique $\tilde{C} \in (0, \bar{C})$ so that $\sigma^P(C) > 0$ for $C < \tilde{C}$ and $\sigma^P(C) = 0$ for $C \geq \tilde{C}$ (while $C \in [0, \bar{C}]$). The threshold \tilde{C} solves

$$\sigma - \frac{\eta}{\gamma(\tilde{C})\underline{N}} = 0,$$

which implicitly defines \tilde{C} (see (A.8)). This concludes the argument.

A.3 Proof of Corollary 1

First, consider that $C < \tilde{C}$, so $\sigma^P(C) > 0$ and $N(C) = \underline{N}$. Using (12), we obtain

$$f(C) = \left(\frac{A}{\underline{N}} \right)^{1-\xi} - r + \mu^P(C) - \eta |\sigma^P(C)|. \quad (\text{A.17})$$

Second, consider that $C \geq \tilde{C}$ and $N(C) < \bar{N}$. Then, $\sigma^P(C) = \mu^P(C) = 0$ and

$$N(C) = \left(\frac{\xi A^{1-\xi}}{\gamma(C)\sigma^2} \right)^{\frac{1}{2-\xi}}.$$

Using (12) and simplifying, we obtain

$$f(C) = \left(\frac{A\gamma(C)\sigma^2}{\xi} \right)^{\frac{1-\xi}{2-\xi}} - r.$$

Third, consider $C \geq \tilde{C}$ and $N(C) = \bar{N}$ so that $\mu^P(C) = \sigma^P(C) = 0$. Using (12), we obtain

$$f(C) = \left(\frac{A}{\bar{N}} \right)^{1-\xi} - r.$$

Finally, note that because $\gamma(C)$ decreases with C , $N(C)$ increases with C for $C \geq \tilde{C}$ with $N(\bar{C}) = \bar{N}$. Therefore, there exists $\tilde{C}' \geq \tilde{C}$ so that $N(C) = \bar{N}$ if $C \in [\tilde{C}', \bar{C}]$.

A.4 Proof of Corollary 2 and Proposition 4

The relevant arguments are already presented in the main text. In a Markov equilibrium with state variable C , token price $P(C)$ and $\sigma^P(C)$ are functions of C only. Ito's Lemma implies

$$\sigma^P(C) = \frac{P'(C)}{P(C)}N(C)(\sigma - \sigma^P(C)),$$

as desired. We normalize $P(\bar{C}) = 1$. For $C \geq \tilde{C}$, it holds that $\sigma^P(C) = 0$ and thus $P'(C) = P''(C) = 0$, so $\mu^P(C) = 0$. For $C < \tilde{C}$, it holds that $\sigma^P(C) > 0$ and so $P'(C) > 0$.

A.5 Proof of Proposition 5

Follows from the arguments presented in the main text.

A.6 Proof of Corollary 3

Follows from the arguments presented in the main text.

A.7 Proof of Proposition 6

To start with, recall the law of motion of the state variables C_t (see (43)),

$$dC_t = \left(rC_t + A_t n_t^\xi - \eta A_t n_t |\sigma_t^P| \right) dt + A_t n_t (\sigma - \sigma_t^P) dZ_t - dDiv_t, \quad (\text{A.18})$$

and A_t ,

$$\frac{dA_t}{A_t} = \kappa n_t^\xi dt.$$

Define $n_t = N_t/A_t$. Using Ito's Lemma, we can calculate

$$dc_t = \left(rc_t + n_t^\xi - \eta n_t |\sigma_t^P| - \kappa n_t^\xi c_t \right) dt + n_t (\sigma - \sigma_t^P) dZ_t - \frac{dDiv_t}{A_t}, \quad (\text{A.19})$$

with drift $\mu_c(c_t) \equiv rc_t + n_t^\xi - \eta n_t |\sigma_t^P| - \kappa n_t^\xi c_t$ and volatility $\sigma_c(c_t) = n_t (\sigma - \sigma_t^P)$.

By the dynamic programming principle, the platform's value function $V(C, A)$ solves the following HJB equation (in differential form):

$$\rho V(C, A) dt = \max_{\sigma^P, N \in [0, \bar{N}], dDiv \geq 0} \{ dDiv + \mathbb{E}[dV(C, A)] \}.$$

We can use Ito's Lemma to expand the right-hand-side of the HJB equation:

$$\begin{aligned} \rho V(C, A) dt = \max_{\sigma^P, N \in [0, \bar{N}], dDiv \geq 0} & \left\{ dDiv(1 - V_C(C, A)) + V_C(C, A) \left(rC + An^\xi - \eta An |\sigma^P| \right) dt \right. \\ & \left. + V_A(C, A) A \kappa n^\xi dt + \frac{V_{CC}(C, A) N^2 (\sigma - \sigma^P)^2}{2} dt \right\}, \quad (\text{A.20}) \end{aligned}$$

where a subscript denotes the partial derivative (e.g., $V_C(C, A) = \frac{\partial V(C, A)}{\partial C}$). As such, dividend payouts $dDiv > 0$ are optimal if and only if $V_C(C, A) \leq 1$; otherwise, $dDiv = 0$. Using the conjecture $V(C, A) = Av(c)$, we obtain

$$V_C(C, A) = v'(c), \quad V_A(C, A) = v(c) - v'(c)c, \quad \text{and} \quad V_{CC}(C, A) = \frac{v''(c)}{A}. \quad (\text{A.21})$$

As is standard (see, e.g., [Bolton et al. \(2011\)](#)), optimal dividend payouts cause c_t to reflect at \bar{c} , where the payout threshold \bar{c} satisfies $v'(\bar{c}) - 1 = v''(\bar{c}) = 0$. That is, $dDiv = A \max\{c - \bar{c}, 0\}$, and $c_t \leq \bar{c}$ at all times $t \geq 0$.

When there are no dividend payouts, the HJB equation [\(A.20\)](#) therefore becomes (using [\(A.21\)](#), dividing both sides by dt and A , and simplifying):

$$\rho v(c) = \max_{n \in [0, \bar{n}], \sigma^P} \left\{ [v(c) - v'(c)c] \kappa n^\xi + v'(c) (rc + n^\xi - \eta n |\sigma^P|) + \frac{1}{2} v''(c) n^2 (\sigma - \sigma^P)^2 \right\}, \quad (\text{A.22})$$

which is [\(45\)](#).

As c approaches zero, the platform can either liquidate (yielding $v(0) = 0$) or prevent liquidation by i) setting $\sigma^P(c) \rightarrow \sigma$ and ii) ensuring that the drift of dc , $\mu_c(c)$, remains positive. Formally, to prevent liquidation as $c \rightarrow 0$,

$$\lim_{c \rightarrow 0^+} \mu_c(c) > 0 = \lim_{c \rightarrow 0^+} \sigma_c(c) \quad (\text{A.23})$$

must hold. Setting $\sigma^P(c) \rightarrow \sigma$ as $c \rightarrow 0$ yields

$$\lim_{c \rightarrow 0^+} \rho v(c) = \max_{n \in [0, \bar{n}]} \lim_{c \rightarrow 0^+} \left(v(c) \kappa n^\xi + v'(c) (n^\xi - \eta n \sigma) \right) > 0.$$

Note that because $\kappa \bar{n}^\xi < \rho$ and $v'(c) \geq 1$, $\lim_{c \rightarrow 0^+} v(c) > 0$ implies $\lim_{c \rightarrow 0^+} \mu_c(c) > 0$, as (under the optimal controls)

$$\lim_{c \rightarrow 0^+} (\rho - \kappa n(c)^\xi) v(c) = \lim_{c \rightarrow 0^+} v'(c) \max_{n \in [0, \bar{n}]} \mu_c(c).$$

As $v'(c) \geq 1$ for all $c \leq \bar{c}$ and so

$$\lim_{c \rightarrow 0^+} \max_{n \in [0, \bar{n}]} v'(c) \mu_c(c) \geq \max_{n \in [0, \bar{n}]} (n^\xi - \eta n \sigma) > 0, \quad (\text{A.24})$$

it follows that $\lim_{c \rightarrow 0^+} v(c) > 0$, and the platform is better off averting liquidation. In optimum, liquidation never occurs and [\(A.23\)](#) holds, implying $\lim_{c \rightarrow 0^+} \sigma^P(c) = 0$.

A.8 Proof of Proposition 7

The optimal control variables, $n = n(c)$ and $\sigma^P = \sigma^P(c)$, are determined by the optimization in the HJB equation (45), that is,

$$\rho v(c) = \max_{n \in [0, \bar{n}], \sigma^P} \left\{ [v(c) - v'(c)c] \kappa n^\xi + v'(c) \left(rc + n^\xi - \eta n |\sigma^P| \right) + \frac{1}{2} v''(c) n^2 (\sigma - \sigma^P)^2 \right\}. \quad (\text{A.25})$$

We consider the following two cases, 1) $\sigma^P > 0$ and 2) $\sigma^P = 0$.

1. If $\sigma^P > 0$, then the first order condition

$$\frac{\partial v(c)}{\partial \sigma^P} = 0 \iff -v'(c)\eta n(c) - v''(c)n(c)^2(\sigma - \sigma^P(c)) = 0$$

must hold. We can solve for

$$\sigma^P(c) = \sigma - \frac{\eta v'(c)}{v''(c)n(c)} = \sigma - \frac{\eta}{\Gamma(c)n(c)} \in (0, \sigma),$$

where

$$\Gamma(c) = -\frac{v''(c)}{v'(c)}.$$

Inserting the optimal choice of $\sigma^P(c)$ back into (45), we obtain

$$\rho v(c) = \max_{n \in [0, \bar{n}], \sigma^P} \left\{ [v(c) - v'(c)c] \kappa n^\xi + v'(c) \left(rc + n^\xi - \eta \sigma n + \frac{\eta}{\Gamma(c)} \right) + \frac{1}{2} v''(c) \left(\frac{\eta}{\Gamma(c)} \right)^2 \right\}.$$

If interior (i.e., $n(c) < \bar{n}$), the optimal choice of $n = n(c)$ solves the first order condition

$$\kappa \xi [v(c) - v'(c)c] n(c)^{\xi-1} + v'(c) (\xi n(c)^{\xi-1} - \eta \sigma) = 0.$$

We define

$$q(c) = v(c) - v'(c)c$$

and solve for

$$n(c)^{\xi-1} = \frac{v'(c)\eta\sigma}{\kappa\xi q(c) + \xi v'(c)} \iff n(c) = \left(\frac{\xi(v'(c) + \kappa q(c))}{\eta\sigma v'(c)} \right)^{\frac{1}{1-\xi}}.$$

Thus,

$$n(c) = \left[\frac{\xi}{\eta\sigma} \left(1 + \frac{\kappa q(c)}{v'(c)} \right) \right]^{\frac{1}{1-\xi}} \wedge \bar{n},$$

as desired.

2. Consider $\sigma^P(c) = 0$. If interior (i.e., $n(c) \in (0, \bar{n})$), optimal $n = n(c)$ must solve the first

order condition

$$\xi[\kappa q(c) + v'(c)]n(c)^{\xi-1} + v''(c)n(c)\sigma^2 = 0.$$

Dividing both sides through $n(c) > 0$, we obtain

$$\xi[\kappa q(c) + v'(c)]n(c)^{\xi-2} + v''(c)\sigma^2 = 0 \iff n(c)^{\xi-2} = \frac{-v''(c)\sigma^2}{\xi(\kappa q(c) + v'(c))}$$

We can solve for

$$n(c) = \left(\frac{\xi(\kappa q(c) + v'(c))}{-v''(c)\sigma^2} \right)^{\frac{1}{2-\xi}}.$$

Thus,

$$n(c) = \left[\frac{\xi}{\Gamma(c)\sigma^2} \left(1 + \frac{\kappa q(c)}{v'(c)} \right) \right]^{\frac{1}{2-\xi}} \wedge \bar{n},$$

which was to show.

Finally, note that analogous to the baseline, there exist three regions and two thresholds \tilde{c} and \tilde{c}' such that i) $\sigma^P(c) > 0$ if and only if $c < \tilde{c}$ (otherwise, $\sigma^P(c) = 0$) and ii) $n(c) = \bar{n}$ if and only if $c \geq \tilde{c}'$ (otherwise, $n(c) < \bar{n}$).

B Derivations

B.1 Calculating User Welfare

B.1.1 Baseline

To start with, recall that any users' utility flow is

$$dR_{it} \equiv N_t^\alpha A^{1-\xi} \frac{u_{it}^\beta}{\beta} dt + u_{it} \left(\frac{dP_t}{P_t} - r dt - f_t dt - \eta |\sigma_t^P| dt \right)$$

As such,

$$\mathbb{E}[dR_{it}] = N_t^\alpha A^{1-\xi} \frac{u_{it}^\beta}{\beta} dt + u_{it} \left(\mu_t^P dt - r dt - f_t dt - \eta |\sigma_t^P| dt \right).$$

Inserting $u_{it} = N_t$ and (12) and using $\xi = \alpha + \beta$ yields

$$\begin{aligned} \mathbb{E}[dR_{it}] &= \frac{N_t^\xi A^{1-\xi}}{\beta} dt + N_t \left(\mu_t^P dt - r dt - (N_t^{\xi-1} A^{1-\xi} + \mu_t^P - r - \eta |\sigma_t^P|) dt - \eta |\sigma_t^P| dt \right) \\ &= \frac{N_t^\xi A^{1-\xi}}{\beta} dt - N_t^\xi A^{1-\xi} dt = \frac{(1-\beta)A^{1-\xi}}{\beta} N_t^\xi dt. \end{aligned} \tag{B.26}$$

As a next step, define the user welfare from time t onward, i.e.,

$$W_t := \mathbb{E} \left[\int_t^\infty e^{-r(s-t)} dR_{is} \right]. \tag{B.27}$$

As C is the payoff-relevant state variable, we can express user welfare as function of C , in that $W_t = W(C_t)$. The dynamic programming principle implies that user welfare solves on $[0, \bar{C}]$ the ODE

$$rW(C_t)dt = \mathbb{E}[dR_{it}] + \mathbb{E}[dW(C_t)].$$

We can rewrite the ODE as

$$rW(C) = \frac{(1-\beta)A^{1-\xi}}{\beta}N(C)^\xi + W'(C)\mu_C(C) + \frac{W''(C)\sigma_C(C)^2}{2}, \quad (\text{B.28})$$

whereby

$$\begin{aligned} \mu_C(C) &= rC + N(C)^\xi A^{1-\xi} - \eta N(C)|\sigma^P(C)| \\ \sigma_C(C) &= N(C)(\sigma - \sigma^P(C)) \end{aligned}$$

are drift and volatility of net liquidity C respectively.

The ODE (B.28) is solved subject to the boundary conditions

$$W'(\bar{C}) = 0$$

and

$$\lim_{C \rightarrow 0^+} W(C) = \frac{1}{r} \lim_{C \rightarrow 0^+} \left(\frac{(1-\beta)A^{1-\xi}}{\beta}N(C)^\xi + W'(C)\mu_C(C) \right).$$

B.1.2 Model extension with Big Data as a Productive Asset

In the model extension with big data as a productive asset, user welfare is a function $W(C, A)$, that is, $W_t = W(C_t, A_t)$. We conjecture and verify that $W(C, A)$ scales with A , i.e., $W(C, A) = Aw(c)$ with $c = C/A$. First, we recall (B.26), that is,

$$\mathbb{E}[dR_{it}] = \frac{(1-\beta)A^{1-\xi}}{\beta}N_t^\xi dt = \frac{(1-\beta)A}{\beta}n_t^\xi dt,$$

and note that $n_t = N_t/A_t$ is a function of $c_t = C_t/A_t$ only, i.e., $n_t = n(c_t)$. Second, the dynamic programming principle implies that user welfare solves the ODE

$$rW(C_t, A_t)dt = \mathbb{E}[dR_{it}] + \mathbb{E}[dW(C_t, A_t)]. \quad (\text{B.29})$$

Using the conjecture $W(C, A) = Aw(c)$, we obtain

$$W_C(C, A) = w'(c), \quad W_A(C, A) = w(c) - w'(c)c, \quad \text{and} \quad W_{CC}(C, A) = \frac{w''(c)}{A}. \quad (\text{B.30})$$

Expanding the right hand side of (B.29), using (B.30) and $W(C, A) = Aw(c)$, simplifying and dividing both sides of (B.29) by dt , one derives

$$(r - \kappa n(c)^\xi)w(c) = w'(c)\mu_c(c) + \frac{w''(c)\sigma_c(c)^2}{2}, \quad (\text{B.31})$$

with drift $\mu_c(c) \equiv rc + n(c)^\xi - \eta n(c)|\sigma^P(c)| - \kappa n(c)^\xi c$ and volatility $\sigma_c(c) = n(c)(\sigma - \sigma^P(c))$. The ODE (B.31) is solved subject to the boundary conditions $w'(\bar{c}) = 0$ and

$$\lim_{c \rightarrow 0^+} (r - \kappa n(c)^\xi)w(c) = \lim_{c \rightarrow 0^+} w'(c)\mu_c(c).$$

B.2 Calculating the Expected Recovery Time

Note that there exists $\tilde{C} \in (0, \bar{C})$ such that $\sigma^P(C) = 0$. Given $C_t = C$ at time t , we define

$$\tau(C_t) = \mathbb{E}[\tau^* - t | C_t = C] \quad \text{with} \quad \tau^* = \inf\{s \geq t : C_s \geq \tilde{C}\},$$

which is the expected time until net liquidity reaches \tilde{C} and token price volatility vanishes.

We can rewrite $\tau(C_t)$ as

$$\tau(C_t) = \mathbb{E}_t \left[\int_t^{\tau^*} 1 dt \right]. \quad (\text{B.32})$$

By definition, it holds that when $C_t = C \geq \tilde{C}$, then $\tau^* = t$ and

$$\tau(C_t) = \tau(C) = 0.$$

By the integral expression (B.32) and the dynamic programming principle, it follows that For $C \leq \tau(C)$, the function $\tau(C)$ solves the ODE

$$0 = 1 + \tau'(C)\mu_C(C) + \frac{\sigma_C(C)^2 \tau''(C)}{2}, \quad (\text{B.33})$$

where

$$\begin{aligned} \mu_C(C) &= rC + N(C)^\xi A^{1-\xi} - \eta N(C)|\sigma^P(C)| \\ \sigma_C(C) &= N(C)(\sigma - \sigma^P(C)) \end{aligned}$$

are drift and volatility of net liquidity C respectively. The ODE (B.33) is solved subject to the boundary condition

$$\tau(\tilde{C}) = 0 \quad (\text{B.34})$$

at $C = \tilde{C}$. At $C = C_L$ (possibly $C_L = 0$), the lower boundary of the state space, the boundary

condition

$$\lim_{C \rightarrow \underline{C}_L} [1 + \tau'(C)\mu_C(C)] = 0$$

applies.

B.3 Proportional recapitalization costs

Suppose that upon refinancing/recapitalization, the platform incurs proportional costs as follows (while there are no fixed refinancing/recapitalization costs). The platform must issue $1 + \omega$ dollars of equity (governance tokens/secondary units) to raise one dollar of liquidity reserves. That is, recapitalization entails proportional costs ω . Also observe that the platform finds it only optimal to recapitalize if $V'(C) \geq 1 + \omega$. Note that in this specification, the platform's value function solves the HJB equation (22) whenever there is no refinancing event. As in Section 4.2, the platform would like to avoid incurring the costs ω and thus refinance only when $C = \underline{C} = 0$. As the costs are proportional to the amount of financing raised when $C = 0$, the platform refinances just enough to avoid liquidation when $C = \underline{C} = 0$. In that case, $C = \underline{C}$ becomes a reflecting boundary with boundary condition $V'(0) = 1 + \omega$.

Note that to prevent liquidation) as C approaches zero, the platform has now two options: i) debasement of token price and setting $\lim_{C \rightarrow 0^+} \sigma^P(C) = \sigma$ or ii) refinancing. When

$$\lim_{C \rightarrow 0^+} V'(C) = \lim_{C \rightarrow 0^+} V'(C) \left(\frac{1}{\rho} \left\{ \underline{N}^\xi A^{1-\xi} - \eta \underline{N} \sigma \right\} \right)^{-1}, \quad (\text{B.35})$$

then debasement is optimal (i.e., $\lim_{C \rightarrow 0^+} \sigma^P(C) = \sigma$). Note that (B.35) follows after rearranging (24). If (B.35) holds, the platform never refinances and the model solution becomes the one of the baseline.

On the other hand, when $V'(0) = 1 + \omega$, the platform refinances at $C = 0$ while $\sigma^P(0) < \sigma$, so refinancing prevents that C falls below zero. In summary, the platform value function solves the ODE (22) subject to the boundary condition

$$\lim_{C \rightarrow 0^+} V'(C) = \lim_{C \rightarrow 0^+} \min \left\{ 1 + \omega, V'(C) \left(\frac{1}{\rho} \left\{ \underline{N}^\xi A^{1-\xi} - \eta \underline{N} \sigma \right\} \right)^{-1} \right\}, \quad (\text{B.36})$$

which contains the above two cases of i) debasement as $C_t \rightarrow 0$ and ii) recapitalization.

Consider that case ii) prevails, i.e., $V'(0) = 1 + \omega$ and the platform recapitalizes at $C = 0$. Overall, the total amount of funds raised F_t after $t = 0$ follows

$$dF_t = \max\{0 - C_t, 0\},$$

so $dF_t \geq 0$. The HJB equation determines the optimal choice of $\sigma^P(C)$ and $N(C)$ for all $C \geq 0$. When $\sigma^P(0) = 0$ and $V'(0) = 1 + \omega$, the token price is constant around $C = 0$, so there is no arbitrage around the recapitalization event. Suppose that $1 > \sigma^P(0) > 0$ and $V'(0) = 1 + \omega$, so

the platform uses both debasement of token price and refinancing to avert liquidation and $C = 0$ is reached with positive probability. As $\sigma^P(0) > 0$, the token price increases upon a positive shock to liquidity reserves, $dZ_t > 0$. In addition, to preclude arbitrage at the recapitalization event, it must be that the token price adjusts downward upon a negative shock to liquidity reserves, $dZ_t < 0$, triggering a refinancing event. Thus, the token price can be written as

$$P_t = \hat{P}_t + L_t,$$

where $dL_t \leq 0$ (i.e., L_t is decreasing) and $\hat{P}_t = \hat{P}(C)$ solves the ODE

$$\sigma^P(C) = \frac{\hat{P}'(C)}{\hat{P}(C)} N(C) (\sigma - \sigma^P(C)),$$

subject to $\hat{P}(\bar{C}) = 1$. That is, after each refinancing event, there is repegging and the price is adjusted downward. This mechanism is analogous to the one presented in Section 4.2. Note that

$$L_t = -\sigma^P(0)F_t$$

so that $dL_t \leq 0$ and at time t with $C_t = 0$,

$$vol(dP_t) = \sigma^P(0).$$

B.4 Details on the Model with User Collateral

In this section, we provide the solution details under the model specification with user collateral requirements. To start with, take users' problem (36) (facing collateral requirements m_t):

$$\max_{u_{i,t}} \left\{ \frac{1}{\beta} N_t^\alpha u_{i,t}^\beta A^{(1-\alpha-\beta)} dt + u_{i,t} (\mu_t^P - \eta |\sigma_t^P| - f_t) dt + u_{i,t} m_t (\tilde{\mu} - \delta - r) dt \right\}.$$

All users act the same so that $u_{i,t} = N_t$. Analogous to the baseline, we then calculate optimal platform transaction volume (after solving users' optimization and invoking $u_{i,t} = N_t$):

$$N_t = \frac{A}{(r + f_t - \mu_t^P + \eta |\sigma_t^P| + m_t(\tilde{\mu} - \delta - r))^{\frac{1}{1-\xi}}},$$

when $N_t < \bar{N}$. We can solve the above for f_t , yielding (37), i.e.,

$$f_t = \left(\frac{A}{N_t} \right)^{1-\xi} - m_t(r + \delta - \tilde{\mu}) + \mu_t^P - \eta |\sigma_t^P|.$$

As a next step in the solution, we calculate

$$\begin{aligned}
\int_{1-\frac{1}{m_t}}^1 (1 - m_t(1 - \theta_a))d\theta_a &= [\theta - m_t\theta + 0.5m_t\theta^2]_{1-\frac{1}{m_t}}^1 \\
&= 1 - 0.5m_t - \left(1 - \frac{1}{m_t} - m_t + 1 + 0.5m_t \left[1 + \frac{1}{m_t^2} - \frac{2}{m_t}\right]\right) \\
&= \frac{1}{2m_t},
\end{aligned}$$

so

$$\begin{aligned}
&2(\delta dt - \sigma dZ_t) \times \mathbb{P}(\{m_t(1 - \theta_a) < 1\}) \mathbb{E}[1 - m_t(1 - \theta_a) | m_t(1 - \theta_a) < 1] \\
&= 2(\delta dt - \sigma dZ_t) \times \left(\int_{1-\frac{1}{m_t}}^1 (1 - m_t(1 - \theta_a))d\theta_a\right) = \frac{1}{m_t}(\delta dt - \sigma dZ_t), \tag{B.37}
\end{aligned}$$

which was to show.

Under this alternative specification, platform reserves follow

$$dM_t = rM_t dt + (P_t + dP_t)dS_t + N_t f_t dt - \frac{\delta N_t}{m_t} dt + \frac{N_t \sigma}{m_t} dZ_t - dDiv_t.$$

Inserting (37), we obtain

$$dM_t - (P_t + dP_t)dS_t = rM_t dt + N_t^\xi A^{1-\xi} dt - \frac{\delta N_t}{m_t} dt - m_t(r + \delta - \tilde{\mu})N_t dt \tag{B.38}$$

$$+ N_t (\mu_t^P - \eta|\sigma_t^P|) dt - \frac{N_t \sigma}{m_t} dZ_t - dDiv_t. \tag{B.39}$$

By Ito's Lemma, $d(S_t P_t) = dS_t P_t + S_t dP_t + dS_t dP_t$. As a result, we can calculate that C_t follows

$$dC_t = \mu_C(C_t)dt + \sigma_C(C_t)dZ_t - dDiv_t,$$

with

$$\begin{aligned}
\mu_C(C) &= rC - r(m-1)N(C) + m(\tilde{\mu} - \delta)N(C) + N(C)^\xi A^{1-\xi} - N(C)\eta|\sigma^P(C)| - \frac{N(C)\delta}{m} \\
\sigma_C(C) &= N(C) \left(\frac{\sigma}{m} - \sigma^P(C)\right)
\end{aligned}$$

and $\sigma_t^P = \sigma^P(C_t)$ and $N_t = N(C_t)$.

As in the baseline, dividend payouts occur at the upper reflecting boundary \bar{C} , satisfying $V'(\bar{C}) - 1 = V''(\bar{C}) = 0$. Then, the dynamic programming principle, the HJB equation for $C \in (0, \bar{C})$ can be written as

$$\rho V(C) = \max_{N \in [0, \bar{N}], m, \sigma^P} V'(C)\mu_C(C) + \frac{\sigma_C(C)^2 V''(C)}{2}.$$

To solve for the optimal controls, we distinguish between the cases 1) $\sigma^P(C) > 0$ and 2) $\sigma^P(C) = 0$:

1. Suppose that $\sigma^P(C) > 0$. Then, the first order condition with respect to σ^P yields

$$\frac{\partial V(C)}{\partial \sigma^P} = 0 \iff -\eta V'(C) - V''(C) \left(\frac{N\sigma}{m} - N\sigma^P \right) = 0$$

so that

$$N\sigma^P = \frac{-\eta V'(C) - V''(C) \frac{N\sigma}{m}}{-V''(C)}.$$

Overall,

$$N\sigma^P = \max \left\{ 0, \frac{-\eta V'(C) - V''(C) \frac{N\sigma}{m}}{-V''(C)} \right\} = \max \left\{ 0, -\frac{\eta V'(C)}{-V''(C)} + \frac{N\sigma}{m} \right\}.$$

We can insert this expression for σ^P into (22) to get

$$\begin{aligned} \rho V(C) = \max_{N \in [0, \bar{N}], m} & \left\{ V'(C) \left[rC + N^\xi A^{1-\xi} - \frac{\eta N\sigma}{m} - r(m-1)N + m(\tilde{\mu} - \delta)N \right. \right. \\ & \left. \left. - \frac{N\delta}{m} - \frac{\eta^2 V'(C)}{V''(C)} \right] + \frac{1}{V''(C)} \left[\frac{(\eta V'(C))^2}{2} \right] \right\}. \end{aligned}$$

The choice of m is independent of N . One can calculate that optimal m solves the first-order condition

$$\tilde{\mu} - \delta - r + \frac{\delta}{m^2} + \frac{\eta\sigma}{m^2} = 0,$$

so that

$$\frac{1}{m^2} = \frac{r + \delta - \tilde{\mu}}{\delta + \eta\sigma} \iff m = \bar{m} \equiv \sqrt{\frac{\delta + \eta\sigma}{r + \delta - \tilde{\mu}}}.$$

Next, we can take the first-order condition with respect to N to obtain

$$\xi N^{\xi-1} A^{1-\xi} - \frac{\eta\sigma}{m} - r(m-1) + m(\tilde{\mu} - \delta) - \frac{\delta}{m} = 0.$$

Thus,

$$N(C) = \underline{N} = A \left(\frac{\xi}{\frac{\eta\sigma}{\bar{m}} + r(\bar{m}-1) - \bar{m}(\tilde{\mu} - \delta) + \frac{\delta}{\bar{m}}} \right)^{\frac{1}{1-\xi}} \wedge \bar{N} \quad (\text{B.40})$$

2. Suppose that $\sigma^P = 0$. Then, taking the derivative with respect to N yields

$$\frac{\partial V(C)}{\partial N} = \frac{1}{\rho} \left(V'(C) \left[\xi N^{\xi-1} A^{1-\xi} - r(m-1) + m(\tilde{\mu} - \delta) - \frac{\delta}{m} \right] + N \left(\frac{\sigma}{m} \right)^2 V''(C) \right).$$

Taking the first-order condition with respect to m yields

$$\frac{\partial V(C)}{\partial m} = 0 \iff V'(C)N\left[\tilde{\mu} - \delta - r + \frac{\delta}{m^2}\right] - N^2V''(C)\frac{\sigma^2}{m^3} = 0. \quad (\text{B.41})$$

Thus,

$$N = N(C) = \frac{-V'(C)}{V''(C)} \left(\frac{r + \delta - \delta/m^2 - \tilde{\mu}}{\sigma^2/m^3} \right) = \frac{-V'(C)}{V''(C)} \left(\frac{(r + \delta - \tilde{\mu})m^3 - \delta m}{\sigma^2} \right)$$

Finally, we discuss the value function at the payout boundary \bar{C} where $V'(\bar{C}) - 1 = V''(\bar{C}) = 0$. At $C = \bar{C}$, we have — as in the baseline — $\gamma(\bar{C}) = V''(\bar{C}) = 0$. As such,

$$\sigma^P(\bar{C}) = 0$$

and

$$N(\bar{C}) = \bar{N}.$$

Using (B.41), we obtain

$$m(\bar{C}) = \sqrt{\frac{\delta}{r + \delta - \tilde{\mu}}}$$

as the margin requirement at $C = \bar{C}$. Analogous to the baseline, there exist three regions and two thresholds \tilde{C} and \tilde{C}' such that i) $\sigma^P(C) > 0$ if and only if $C < \tilde{C}$ (otherwise, $\sigma^P(C) = 0$) and ii) $N(C) = \bar{N}$ if and only if $C \geq \tilde{C}'$ (otherwise, $N(C) < \bar{N}$). The platform optimally prevents liquidation as C approaches zero, leading to the boundary condition

$$\lim_{C \rightarrow 0^+} \sigma^P(C) = 0 \iff \lim_{C \rightarrow 0^+} \sigma^P(C) = \frac{\sigma}{\bar{m}}.$$

This boundary condition can be manipulated to obtain a condition analogous to (B.35). Using that

$$\lim_{C \rightarrow 0^+} N(C) = \underline{N}, \quad \lim_{C \rightarrow 0^+} m(C) = \bar{m} \quad \text{and} \quad \lim_{C \rightarrow 0^+} \sigma_C(C) = 0,$$

we obtain

$$\lim_{C \rightarrow 0^+} \frac{V(C)}{V'(C)} = \frac{1}{\rho} \left\{ -r(\bar{m} - 1)\underline{N} + m(\tilde{\mu} - \delta)\underline{N} + \underline{N}^\xi A^{1-\xi} - \underline{N}\eta \frac{\sigma}{\bar{m}} - \frac{\underline{N}\delta}{\bar{m}} \right\}.$$